Thursday, June 2nd: 9.00 am – 6.00 pm Berlin Time

Skin Imaging

Friday, June 3rd: 9.00 am – 6.00 pm Berlin Time

Skin Biophysics

Thank you!

I would like to thank all participants from 23 countries including the sponsors, the ten exhibitors, and the players behind the scenes for the successful ISBS2022 World Congress in Berlin.
The *International Society of Biophysics and Imaging of the Skin (ISBS)* invites you to join our next ISBS World Congress in the USA in 2024.

June 4, 2022

Prof. Karsten König
Congress President

Scientific Committee

Bernard Querleux, L'Oréal, France

Karsten König, Saarland University and JenLab GmbH, Germany

Joachim Fluhr, Charité and Fraunhofer ITMP, Germany

Stacy Hawkins, Unilever R&D, USA

Neelam Muizzuddin, SCR Consultants, USA

Martha Tate, Tate Science, USA

Tim Lee, BC Cancer Research Center, Vancouver, Canada

Silvia H. Pérez Damonte, CLAIM, Argentina

Sponsors

www.dermicolab.com

www.jenlab.de

www.loreal.com

www.uni-saarland.de

www.blt.uni-saarland.de

Exhibitors

www.ithera-medical.com

www.jenlab.de

www.damae-medical.com

www.courage-khazaka.de

www.eotech.fr

www.riverd.com

www.topag.eu

www.ekspla.com

www.tpm.eu

www.CanfieldSci.com

Thursday, June 2

TOPIC 1 Emerging Trends in Skin Science Chairs: König, Muizzuddin

09:00-09:15 Live Opening (Congress president, ISBS president)

09:15-10:00 Plenary talk #1: Thomas SCHNALKE
Cells, sera, and microbes: Berlin and the rise of modern medicine

10:00-11:00 Oral presentations (12min + 3min QA)

10:00-10:15	Schleusener:	Far-UVC-irradiation at 233 nm for eradication of microbes
10:15-10:30	Darvin:	Label-free in vivo imaging of mast cells and macrophages in the dermis
10:30-10:45	Alsamad:	Effect of hormonal status on skin physiology in postmenopausal women

10:45-11:30 Coffee break and exhibition

TOPIC 2 Skin in its environment Chairs: Meinke, El Gammal

11:30-12:00 Plenary talk #2: Tracy WANG:
Understanding the skin response to environmental and climate changes

12:00-12:30 Oral presentations (12min + 3min QA)

12:00-12:15	Muizzuddin:	Effect of seasonal and geographical variations on skin barrier
12:15-12:30	Tran:	Two methods to measure the effect of air pollution in the skin

12:30-13:00 Poster flash presentation #1
13:00-14:00 Lunch break and exhibition/board meeting #1

TOPIC 3 Skin Imaging #1 Chairs: Dubois, Tate

14:00-14:45 Plenary talk #3: Karsten KÖNIG
State-of-the-Art Optical Skin Biopsies

14:45-15:30 Oral presentations (12min + 3min QA)

14:45-15:00	Breunig:	Multiphoton Fluorescence Lifetime Imaging for in vivo Skin Investigations
15:00-15:15	Becker:	Ultra-Fast Fluorescence Decay in Malignant Melanoma
15:15-15:30	Puppels:	Quantitative analysis of in vivo skin penetration by confocal Raman

15:30-16:00 Coffee break and exhibition

TOPIC 4 Skin Imaging #2 Chairs: Fluhr, Lee

16:00-16:45 Plenary talk #4: Arnaud DUBOIS
Line-field confocal optical coherence tomography of the human skin

16:45-17:30 Oral presentations (12min + 3min QA)

16:45-17:00	Folgosa:	Optoacoustic 3D functional imaging of skin microvasculature
17:00-17:15	Lboukili:	Automated identification of keratinocytes by in vivo RCM
17:15-17:30	König, A:	Reflectance microscopy with femtosecond laser pulses

18:00-19:00 General Assembly
19:30-23:30 Boat Tour with Dinner

Friday, June 3

TOPIC 5 Skin Biophysics : Methods&Models Chairs: Querleux, Houser

09:00-09:45 Plenary talk #5: Edoardo MAZZA
Multiscale Analysis of Skin Biomechanics

09:45-10:30 Oral presentations (12min + 3min QA)

09:45-10:00	Évora:	Biomechanics and topography of corneocytes using AFM
10:00-10:15	Qiao:	Effects of Mechanotransduction on Skin and Fascia
10:15-10:30	Serup:	Ultrasound Treatment (HIFU) of dermatological diseases

10:30-11:00 Coffee break and exhibition

TOPIC 6 Biophysics: Methods & Clinics Chairs: Mazza, Fluhr

11:00-11:45 Plenary talk #6: M.C. MEINKE & J.W. FLUHR
From molecular mechanisms to clinical Signs of Aging

11:45-12:45 Oral presentations (12min + 3min QA)

11:45-12:00	Darlenski:	Multi-sensor device for Antarctica expedition
12:00-12:15	Andrade:	Associating skin variables to dietary patterns
12:15-12:30	Busch:	UVA-induced drug release from nanocapsules in hair follicles
12:30-12:45	Maia Campos:	RCM for quantification of the skin photoaging and melasma

12:45-13:00 Poster flash presentation #2
13:00-14:00 Lunch break and exhibition

TOPIC 7 Skin Sensory Responses & Treatments Chairs: McGlone, Hawkins

14:00-14:45 Plenary talk #7: Laurent MISERY
Touch, Skin and Nerve Endings

14:45-15:45 Oral presentations (12min + 3min QA)

14:45-15:00	Infante:	The Meissner Corpuscles create protrusions in the epidermis
15:00-15:15	Zahouani:	Novel finger engineering technology to study human touch
15:15-15:30	Mohammed:	Sensory profiling of topical semisolid products
15:30-15:45	Kröger:	In vivo localization of carbon black tattoo inks by two-photon FLIM

15:45-16:15 Coffee break and exhibition

TOPIC 8 Skin, Brain & Perception Chairs: Misery, Perez Damonte

16:15-17:00 Plenary talk #8: Francis McGLONE
How about C-Fibres: A Protection Racket from Skin to Brain

17:00-18:00 Oral presentations (12min + 3min QA)

17:00-17:15	Wang:	Quantifying facial skin aging signs by deep learning-based algorithm
17:15-17:30	Reble:	Estimates of SPF and UVA-PF with simplified diffuse reflectance
17:30-17:45	Nappez:	Taking pictures for at-home studies in cosmetics
17:45-18:00	Jiang:	Human Perception of Wrinkle Depth

18:00-18:15 Closing Remarks

CV and abstract of the invited speakers

In alphabetical order

Arnaud DUBOIS

Arnaud Dubois received his Ph.D. in physics in 1997 from Paris-Saclay University. Since 2006, he is a professor of optics at Institut d'Optique Graduate School in Palaiseau, France. A pioneer of full-field optical coherence tomography (OCT) in the early 2000s, A. Dubois has since contributed greatly to the development of this biological tissue imaging technique. He has published 140 research articles in scientific journals and conference proceedings and 12 book chapters. In particular, he was the scientific editor in 2016 of the first and only textbook entirely dedicated to full-field OCT. He has 5 patents to his credit. In 2014, he co-founded DAMAE Medical, a startup company working on an innovative OCT technique for high-resolution skin imaging.

Line-field confocal optical coherence tomography of the human skin

A. Dubois[1,2]

[1]*Université Paris-Saclay, Institut d'Optique Graduate School, CNRS, Laboratoire Charles Fabry, 91127 Palaiseau, France*
[2]*DAMAE Medical, 14 rue Sthrau, 75013 Paris, France*
Corresponding author e-mail address: arnaud.dubois@institutoptique.fr

KEY WORDS: Optical coherence tomography, confocal microscopy, skin

Line-field confocal optical coherence tomography (LC-OCT) is an imaging technique based on a combination of confocal microscopy and OCT, allowing three-dimensional (3D) cellular-resolution ($\sim 1\mu m$) imaging of the skin *in vivo*[1,2].

We present the latest advances in LC-OCT to facilitate the use of the technique in cosmetology[3] and dermatology and to improve the diagnosis and analysis of various skin lesions, including cancers[4].

A video camera was incorporated into a handheld probe to acquire dermoscopic images in parallel with LC-OCT images. A confocal Raman spectrometer was associated with a LC-OCT device to record morphological images of the skin in which points of interest can be subjected to molecular characterization. Artificial intelligence was used to automate the computation of metrics for the quantification of the epidermis and for diagnostic support by identifying suspect regions within a 3D image.

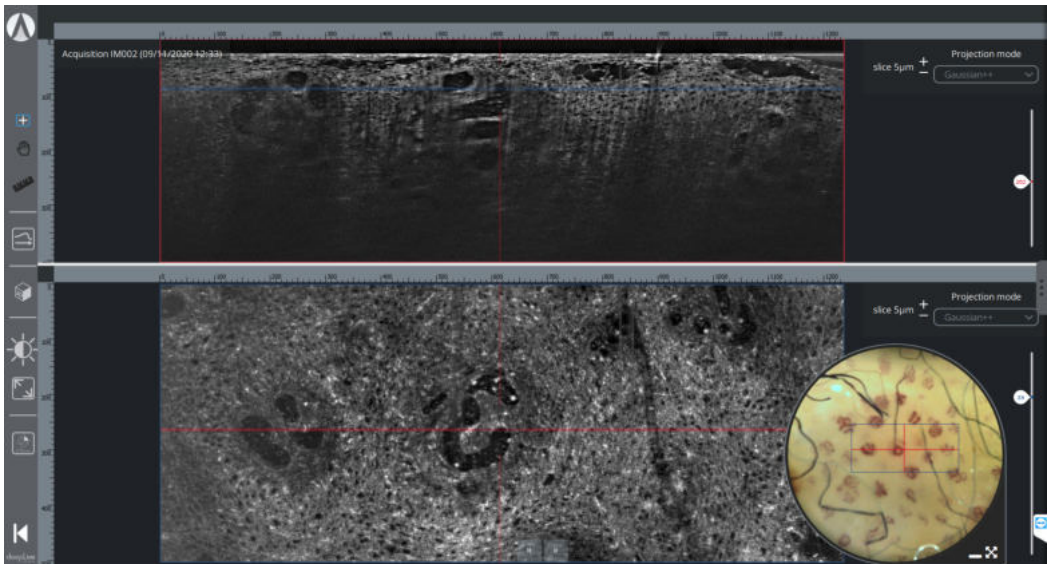

Fig. 1. Vertical (top) and horizontal (bottom) sectional LC-OCT images of a Squamous Cell Carcinoma (SCC) with its associated dermoscopic image (in the lower right circle). The blue rectangle superimposed on the dermoscopic image delineates the location of the horizontal sectional LC-OCT image, while the red line indicates the position of the vertical sectional LC-OCT image.
Image courtesy of Prof. M. Suppa, Erasme hospital, Brussels, Belgium.

[1] J. Ogien et al., Front. Optoelectron., 13(2020)381-392.
[2] J. Monnier et al., J. Eur. Acad. Dermatol. Venereol. 34(2020)2914-2921.
[3] M. Pedrazzani et al., Skin Res. Technol., 26(2020)398-404.
[4] C. Ruini et al., Skin Res. Technol., 27(2021), 340-352.

Joachim FLUHR

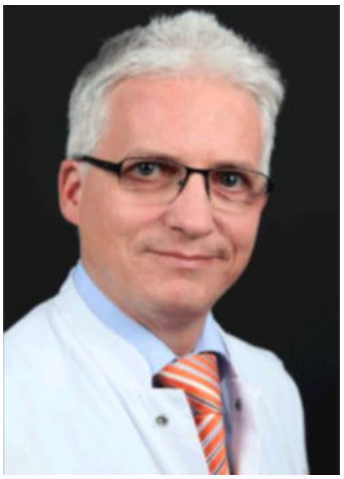

Joachim Fluhr is professor and lecturer at the Institute of Allergology, Charité – Universitätsmedizin Berlin. He is involved in patient care, clinical teaching of dermatology, allergology and immunology of the MD program and an active researcher. He has longstanding experience in epidermal barrier and associated function implicated in a variety of dermatological conditions. Furthermore, he is interested in non-invasive assessment of skin functions. His current research activities focus on understanding the regulatory role of the mast cells in epidermal barrier function as well as sensitive skin.

He received his doctor of medicine degree from Johannes Gutenberg University Mainz. He worked as a Postdoctoral Research Fellow at the University of California in San Francisco. He earned his degree as lecturer (habilitation) at the Department of dermatology at Friedrich Schiller University Jena, where he was the head of the skin physiology laboratory for 5 years. He served three years as the Medical Director of BioSkin, clinical trials specialists, before he joined Charité in Berlin as senior physician. He was a visiting senior scientist at San Gallicano, Rome, Italy and Univ. of Brest, France. He is the author of more than 200 Medline-listed publications (h-index 68) and currently serves as editor in chief of the Journal of Skin Pharmacology and Physiology.

From molecular mechanisms to clinical signs of aging

Presented by Martina C. Meinke and Joachim W. Fluhr

Charité – Universitätsmedizin Berlin
Department of Dermatology and Institute of Allergology

Skin as the outermost compartment of the human body, is affected by the universal process of aging. The characteristic for the skin of elderly are traditionally attributed to changes in the dermal connective tissue constituents. In the past decades specific age-related alterations in the epidermis and dermis have been revealed. The morphological characteristics of the intrinsically and extrinsically aging are the basis for the complex changes of the skin physiology with age.

Our presentation will give insights into the mechanism of aging and changes of the skin biology at different ages. This will include changes on the molecular and cellular level (e.g. in collagen and elastin composition) as well as the consequences in terms of clinical signs. We will present non-invasive methods to determine different degrees of skin aging by multiphoton and Raman microspectroscopy compared to classical standard techniques. Current trends of anti-aging strategies will be presented.

Karsten KÖNIG

Karsten König (Koenig) received his PhD degree in physics and the habilitation degree in cell biology from the Friedrich Schiller University Jena. Since 2003, he is Full professor and Head of the *Department of Biophotonics and Laser Technology* of the Saarland University at Saarbrücken. He is also Founder/CEO of JenLab GmbH and Fellow of SPIE. Prof. König published about 500 scientific papers in the field of biophotonics and femtosecond laser material processing. He pioneered fluorescence lifetime imaging (FLIM) in life sciences in 1988/89, femtosecond laser nanoprocessing in 1999, femtosecond laser transfection in 2002, clinical two-photon microendoscopy and clinical multiphoton tomography MPT (2001-2004).

Awards include the Research Award of the State of Thuringia, the Feulgen Award, the Technology Award of the Fraunhofer Society, the Leibinger Innovation Award, the SPIE-Prism-Award, the IAIR award Man of the Year, the IAIR award Best Company for Innovation & Leadership Biomedicine, the CFI Award, and the AI Award Most Innovative Femtosecond Laser Technology Provider.

Professor König organized the *3rd World Conference and Cellular and Molecular Biology* with eight Nobel Prize winners, the *Focus on Microscopy* conference in Jena, international FLIM workshops in Saarbrücken, the annual SPIE Multiphoton Microscopy Conferences in San Francisco, and the on-line ISBS2021 conference.

He climbed two times the *Shisha Pangma* (8033m) in Tibet.

State-of-the-Art Optical Skin Biopsies

K.König[1,2]

Saarland University, Department of Biophotonics and Laser Technology, Saarbrücken
JenLab GmbH, Berlin, www.jenlab.de
Corresponding Author: k.koenig@blt.uni-saarland.de, www.blt.uni-saarland

KEY WORDS: OCT, reflectance, multiphoton

The most common human diseases are skin diseases. The diagnosis is typically based on conventional histology of physically taken biopsies. However, modern non-invasive and label-free in-vivo skin imaging with laser beams can provide optical sections from the epidermis and upper dermis with a spatial resolution better than 10 micrometer. These virtual optical skin biopsies reflect in nearly real-time the tissue and cell structure as well as the function such as the cellular metabolism of in vivo skin in its natural environment. These optical skin biopsies have the potential to reduce the number of "real" tissue biopsies in hospitals, to reduce animal studies in the pharmaceutic industry, and to test the efficacy of cosmetic products over long time periods.

Optical coherence tomography (OCT), confocal reflectance confocal microscopy (RCM), laser Doppler, multiphoton tomography (MPT), RAMAN and CARS imaging as well as photoacoustic tomography (PAT) have so far been used to image optically in vivo the skin of patients.

OCT, RCM and laser Doppler are based on modifications of the refractive index. MPT signals include autofluorescence (NADH, flavins, keratin, melanin, porphyrin, elastin) and second harmonic generation (SHG of collagen). Raman and CARS provide "chemical" signals from lipids, water, proteins, and "fingerprint chemicals". In PAT, absorbers such as hemoglobin and melanin transfer the absorbed light into pressure waves that can be imaged. In PAT, pulsed laser radiation from the green to the near infrared (NIR) is used whereas CRM and Raman are based on continuous wave (CW) laser radiation. Clinical MPT and CARS employ NIR femtosecond laser pulses. OCT sources include femtosecond laser, superluminescent diodes, and supercontinuum laser s in the case of line-field confocal OCT (LC-OCT). The novel high-resolution imaging method LC-OCT combines the principles of confocal microscopy with line illumination and time-domain OCT. The highest resolution is obtained by MPT (300 nm lateral resolution) based on NA1.3 focusing optics. The two very first medical MPT devices DermaInspect (CE0118 mark obtained in 2004) were employed in the cosmetic industry and for malignant melanoma detection. Modern compact multimodal multiphoton tomographs such as the MPTcompact provide autofluorescence FLIM images with high spatial and picosecond temporal resolution (FLIM: fluorescence lifetime imaging), SHG images, and CRM images. In that case, the confocal reflectance signals are backscattered femtosecond NIR laser pulses.

RCM, LC-OCT, MPT, and PAT will become the modern imaging tools for dermatologists and researchers of the cosmetic industry.

Edoardo MAZZA

Edoardo Mazza has been Full Professor of Mechanics at the Institute of Mechanical Systems in the Department of Mechanical and Process Engineering (D-MAVT) since 2010. He currently serves as the Head of Department of D-MAVT. Edoardo Mazza studied mechanical engineering at ETH Zurich and received his Dr. sc. techn. degree at ETH in 1997. For his dissertation he was awarded the ETH medal. He has been working in industry from 1997 to 2001. In 2002 he was appointed as Assistant Professor, in 2006 as Associate Professor of Mechanics at ETH Zurich. Since 2006 he also leads the laboratory "Experimental Continuum Mechanics" of Empa, the Swiss Federal Laboratories for Materials Science and Technology.

Professor Mazza's research deals with experimental continuum mechanics, applied for the solution of challenging engineering problems. Novel experimental techniques are developed for the characterization of soft biological tissues in human organs, with a particular focus on skin. The deformation behavior is analyzed at each relevant length scale, and described with appropriate mathematical models. Applications in mechanobiology address the chemo-physical factors of the extracellular environment influencing cell behavior. Tissue engineered and synthetic materials, mesh implants and stents are evaluated in terms of "mechanical biocompatibility".

Multiscale Analysis of Skin Biomechanics

E. Mazza[1,2], A. Wahlsten[1], D. Sachs[1] , A. Ehret[1,2] (Author name(s) [10-point type, centered, bolded])

1: D. Mechanical and Process Engineering, ETH Zurich, Switzerland
2: Swiss federal Laboratories for Materials Research and Technology, Empa Düberndorf, Switzerland

KEY WORDS: Multilayer, biphasic, discrete

Combination of mechanical experiments on human skin *in vivo* and multiscale measurements *ex vivo* provided a wide range of data which were used to inform advanced constitutive models for simulation of skin biomechanics. As for other soft collagenous tissues, at macroscopic length scale, the interplay between collagen fibers and ground matrix determines the resistance to deformation and explains the difference between uniaxial and equibiaxial tension [1], [2].

The motion of interstitial fluid and dissipative processes in the fibers' network influence the viscoelastic behavior of the tissue. Suction experiments and in situ measurements in a multiphoton microscope helped distinguishing between the properties of the superficial epidermis and those of reticular and papillary dermis [3].

Surface elstography was applied to characterize the mechanical response of healing incisional wounds in mice [4], [5]. The wound core was shown to be less deformable compared with the healthy tissue in the far field. Progression in wound core strain was quantified and correlated with the development of the matrix, providing a non-invasive functional read-out to monitor the repair processes.

As a complement to tissue level characterization, indentation using an atomic force microscope delivered information on the mechanical properties of skin at μm length scale. Combination of measurements and corresponding simulations, based on a discrete fiber network model, demonstrated that local indentation does not engage collagen fibers. Thus, the corresponding apparent modulus depends solely on the properties of the ground matrix, and this has also implications on the mechanobiology of dermal cells.

Finally, knowledge of skin biomechanics at macroscopic and cell length scales is combined for the improvement of skin tissue engineering. Using a dedicated bioreactor, it was possible to demonstrate that optimized mechanical environment and stimulation strongly accelerates the *in vitro* maturation of skin substitutes [6].

[1] Ehret A.E. et al., 2017, Nat. Commun., 8, 1002
[2] Wahlsten A. et al., 2021, Biomechanics and Modeling in Mechanobiology, 18.
[3] Sachs D., et al., 2021, Biomechanics and Modeling in Mechanobiology, 20
[4] Pensalfini M. et al., 2018, Acta Biomaterialia 65, 226–236
[5] Wietecha M.S. et al., 2020, Nat Commun 11, 2604
[6] Wahlsten A. et al., 2021, Biomaterials, 273

Francis McCLONE

Francis McGlone is Professor in Neuroscience at Liverpool John Moores University, Visiting Professor, Liverpool University, UK and Aalto University, Finland. He is Co-Director of the Somatosensory & Affective Neuroscience Lab at the School of Natural Sciences & Psychology. He has a long-term interest in the function of the different classes of afferent c-fibres innervating human skin - those that code for pain, itch (for which an Ig Nobel prize was awarded) and 'pleasure' - at both peripheral and central levels. Techniques used in this research span single-unit recordings with microneurography, psychophysical measurements, functional neuroimaging, behavioural measures, and psychopharmacological approaches to investigate the role of the brain transmitter serotonin in affiliative and social touch. He is President of the International Association for the Study of Affective Touch (IASAT) https://iasat.org/

How About C-Fibers? A protection Racket from Skin to Brain

F. McGlone

Research Centre Brain & Behavior, Liverpool John Moores University, L3 3AF, UK

KEY WORDS: Itch, Pain, Pleasure, Touch

Research into the sense of touch – somatosensation - has focused mainly on the fingertips, which have been described, in an analogy with vision, as the 'fovea' of this sensory modality. We therefore have a reasonably good understanding of the specialized receptors in the fingers that code for touch, and how their exquisite sensitivity enables us to detect the microscopic physical surface properties of handled objects, such as their roughness, smoothness, or softness. Information from these receptors is conveyed to discriminative processing sensory areas of the brain by fast-conducting myelinated A-β nerve fibers, enabling this information to be processed in 'real-time' – an important factor when handling tools, or detecting the presence of an insect on your skin. A more finely myelinated class of sensory afferents called A-δ nerves have a role in temperature and as an early warning pain system.

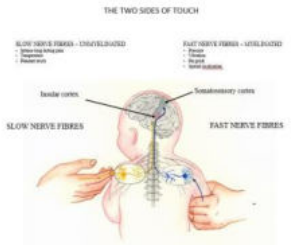

The skin senses have another class of sensory nerves that are unmyelinated - nociceptors or pruriceptors - excitation of which leads to the experience of pain or itch (negative emotional states), and as such provide vital protective role over the lifespan. However, more recently (~1990), another class of c-fiber was discovered innervating human hairy skin the optimal stimulus for which was a gentle caressing touch, called c-tactile afferents (CT). Over the past ~20 years we and others have used a converging methodologies approach to characterize their functional properties. Each technique has provided one further piece of the jigsaw puzzle – microneurography, psychophysics, neuroimaging, behavioral studies, rating scales, psychopharmacology, epigenetics, clinical models, and data from animal research. The emerging picture is still blurred, but some pieces of the puzzle a becoming clearer in terms of the role CTs might be playing in the neurodevelopment of the social brain. As with itch and pain CTs also protect, but here the behaviors provoked by stimulation are not of withdrawal, but one of approach. Here we see the power of social touch - from the cradle to the grave – and the protective role over evolutionary time of c-fibers.

Martina MEINKE

Martina C. Meinke is Professor and Head of the Center of Experimental and Applied Cutaneous Physiology of the Dept. of Dermatology, Venerology and Allergology, Charité - Universitätsmedizin Berlin since April 2016 and 2020, respectively. She studied chemistry at the Free University of Berlin and did her PhD in 1994 with a research stay at the University of Sherbrooke, Québec, Canada. Afterwards she managed a laboratory for environmental analysis but 1999 she switched to the medical diagnostics field and was awarded the title medical physicist in 2006. Her research fields are sophisticated optical and spectroscopic mostly non-invasive methods to determine changes skin physiological parameters.

From molecular mechanisms to clinical signs of aging

Presented by Martina C. Meinke and Joachim W. Fluhr

Charité – Universitätsmedizin Berlin
Department of Dermatology and Institute of Allergology

Skin as the outermost compartment of the human body, is affected by the universal process of aging. The characteristic for the skin of elderly are traditionally attributed to changes in the dermal connective tissue constituents. In the past decades specific age-related alterations in the epidermis and dermis have been revealed. The morphological characteristics of the intrinsically and extrinsically aging are the basis for the complex changes of the skin physiology with age.

Our presentation will give insights into the mechanism of aging and changes of the skin biology at different ages. This will include changes on the molecular and cellular level (e.g. in collagen and elastin composition) as well as the consequences in terms of clinical signs. We will present non-invasive methods to determine different degrees of skin aging by multiphoton and Raman microspectroscopy compared to classical standard techniques. Current trends of anti-aging strategies will be presented.

Laurent MISERY

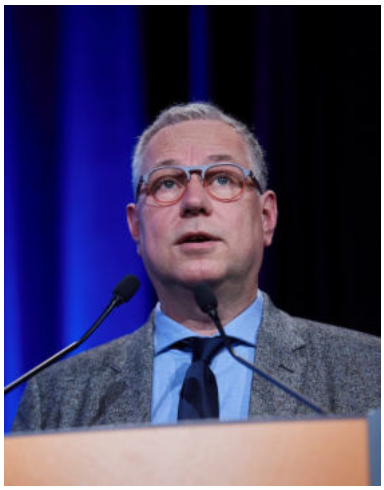

Professor Laurent Misery is the head of the department of dermatology at the University Hospital of Brest and the French Expert Center on Pruritus. He is professor of dermatology and founder of the partnership chair of neuro-sensory dermatology and the master of clinical neurosciences. He is the director and founder of the laboratory of neurosciences at the University of Western Brittany, which is named « Laboratory on Interactions Neurons-Keratinocytes » (LINK).

Touch, Skin and Nerve Endings

L.Misery[1,2]

[1] *Laboratory Interactions Neurons-Keratinocytes (LINK), University of Western Brittany, Brest, France*

[2] *Department of Dermatology, University Hospital of Brest, Brest, France*

laurent.misery@chu-brest.fr

KEY WORDS: touch, nerve endings, neuro-immuno-cutaneous system

The skin is the organ of touch, a sense as important as vision, although we are less aware of it. As a result, the cutaneous sensory innervation is very dense and extends to the most superficial layers of the epidermis, excluding the horny layer. Instead of the classical morphological classification, it is preferable to use the functional classification. We have four types of sensory receptors in the skin:

- mechanoreceptors
- thermoreceptors
- nociceptors
- pruriceptors.

The transformation of mechanical, thermal or other signals into electrical and biochemical signals is possible thanks to the presence of sensory molecules on the surface of the nerve endings, mainly from the TRPs family. The discovery of these molecules earned David Julius and Ardem Patapoutian the Nobel Prize in Medicine and Physiology in 2021.

It is becoming increasingly clear that cutaneous nerve endings, and especially epidermal nerve endings, form synapses with the cells in their environment, not only Merkel cells, but also keratinocytes, Langerhans cells, melanocytes or immune cells. These synapses allow interactions in both directions. On the one hand, they are used for sensory perception. On the other hand, they allow the nervous system to send information to the skin cells and thus to modulate their functions.

In the laboratory, we are able to reproduce this in vitro because we have developed co-cultures of neurons and skin, epidermis or keratinocytes or Merkel cells. We can then measure the interactions by electrophysiological studies or by measuring the release of neurotransmitters.

Keratinocytes Communicate with Sensory Neurons via Synaptic-like Contacts.
Talagas M, Lebonvallet N, Leschiera R, Sinquin G, Elies P, Haftek M, Pennec JP, Ressnikoff D, La Padula V, Le Garrec R, L'herondelle K, Mignen O, Le Pottier L, Kerfant N, Reux A, Marcorelles P, Misery L
Ann Neurol. 2020;88:1205-1219

Thomas SCHNALKE

Thomas Schnalke is a professor of medical history and medical museology and director of the Berlin Museum of Medical History at the Charité. He has studied medicine in Germany (Würzburg and Marburg/Lahn) and received his MD in 1987. In this thesis he dealt with the history and technology of dermatological moulages. From 1988 onward, he worked as assistant professor at the Institute for the History of Medicine at the University of Erlangen-Nuremberg, where he got his habilitation for medical history in 1993 with an analysis of German urban medicine in the 18th century. Since 2000 he acts as director of the Charité museum. His research focuses on different museological aspects in medical history (museum's studies), methods and approaches in the material cultures of the history of medicine and the sciences, history of medical teaching objects and collections, especially specimens and moulages.

Tracy WANG

Dr. Tracy (Hequn) Wang is a senior manager in Evaluation Intelligence department at L'Oréal China Research and Innovation Center. In this role, Tracy is responsible for designing and conducting clinical and instrumental studies to evaluate formula efficacies across product categories of skincare, haircare and makeup. She is also leading new evaluation method development and validation. Prior joining L'Oréal, Tracy was with Johnson & Johnson Consumer Inc. Translational Science in the United States, working on skincare ingredient innovation and validation. Tracy earned her Ph.D. degree in Interdisciplinary Oncology, specializing in biomedical optics at the University of British Columbia. She also completed two postdoctoral research fellowships around skin diagnosis and characterization at the University of Washington and Harvard Medical School. Tracy has published more than 20 peer reviewed journal articles and book chapters and is the owner of several patents.

Understanding the skin response to environmental and climate changes

T. Wang
L'Oréal, China

The skin structure and function are dynamic and undergoes many changes throughout development and maturation. In each stage of life from infants to teenagers, adults to post-menopause, skin exhibits distinct characteristics. As skin intrinsically ages it undergoes many physiological changes, which can alter the gene expression levels that are possibly linked with cellular metabolic activity. These cellular changes can manifest as changes in the appearance of skin tone, texture, fine lines, hydration, and oiliness. In addition to intrinsic aging, external factors, such as solar exposure, hormones, life style can also change the skin homeostasis, which may influence cellular mechanisms and contribute to a disruption in the status of skin health. The skin is also directly affected by environmental and climate changes, such as pollution, extreme or fluctuating temperature and humidity, causing skin to react and become unstable, and even go through accelerated aging. This talk will mainly focus on revealing the skin response to environmental and climate changes, and discuss the clinical design, as well as key methods and attributes used in the studies to holistically evaluate the skin.

Abstracts

Oral Presentations

In alphabetical order of the corresponding author

Effect of hormonal status on skin physiology in postmenopausal women

F. Alsamad[1], I. Lboukili[1], G. Stamatas[1]

Research & Development, Johnson &Johnson Santé Beauté France, Issy-Les-Moulineaux, France
Corresponding Author e-mail address: falsamad@its.jnj.com

KEY WORDS: Postmenopausal women, skin physiology, clinical study

Skin responds to sex hormones through numerous receptors. A change in hormonal status such as menopause therefore influences the state of skin. In this work, a clinical study was conducted to investigate skin changes in postmenopausal women. Biochemical, biophysical, spectral, and imaging techniques were used to collect information markers on skin surface at 3 sites (face and arm) in pre (n=15) and postmenopausal (n=33) women aged 40 to 80 with skin phototype I-III (Fitzpatrick Scale). Our results showed that postmenopausal women had significantly less sebum (42%) on cheek, highlighting reduced sebaceous glands activity due to sex hormones decline. Moreover, a significant decrease in TEWL was observed on cheek (21%) and upper inner arm (11%) of the same group. TEWL is informative about skin barrier which is likely modified in postmenopausal women due to slower cell turnover in the epidermis. Furthermore, an increase in IL-1A, an inflammatory marker, and a significant decrease in its antagonist receptors, IL-1RA, as well as certain anti-inflammatory markers, namely TIMP-2 and trappin-2, were shown on the cheek. Hence, the study of inflammatory markers shows an increase in the micro-inflammatory state of skin in postmenopausal women. This was also manifested by diminished MMP-9, reflecting decreased extracellular matrix (ECM) turnover and skin tissue remodeling in the same group. This change in metalloproteinase was significant on dorsal forearm but not on cheek where data was variable. Additionally, a significant decrease in skin elasticity (24%) was observed on the dorsal forearm and upper inner arm of postmenopausal women. The balance of degradation and synthesis of collagen and other ECM components is therefore thought to be disturbed. To obtain maximum insights on collagen, i*n vivo* Raman analysis was also performed. Finally, visual inspection of facial and scalp images revealed paler skin color, thinner hair fibers, and lower hair density in postmenopausal women. In conclusion, our work identifies some physiological modifications in skin of postmenopausal women and enables us to reflect on new solutions to offer our consumers to take care of their skin and feel good about it.

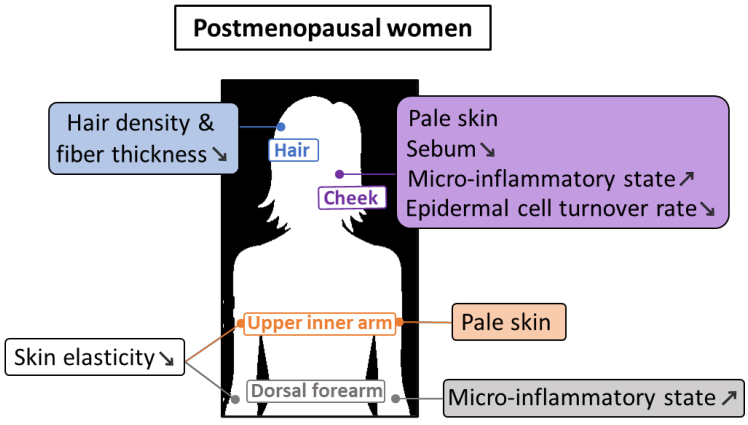

Skin physiology of postmenopausal women compared to premenopausal women

Associating skin variables to dietary patterns

Sérgio Faloni de Andrade, Tatiana Matos Ferreira, Tatiana Fontes, Sofia Lopes, Regina Menezes, Cíntia Ferreira-Pêgo, Luis Monteiro Rodrigues

CBIOS - Research Center for Biosciences and Health Technologies, Universidade Lusófona Lisboa, Portugal.
Corresponding Author e-mail address: sergio.andrade@ulusofona.pt

KEY WORDS: Dietary patterns, Skin physiology, Vegan-vegetarian

The link between nutrition and skin physiology has been explored in the last few years. However, the effect of dietary patterns on skin health is still unclear. Here we investigate potential differences in the cutaneous physiology related to omnivorous and vegan-vegetarian regimens and relate with the relevant food groups. Eighty seven healthy volunteers both sexes were recruited after informed written consent. These included 63 omnivores (OM) (28.60±11.35 y.o.) and 24 vegetarian-vegan (VG) (39.80±7.48 y.o.) with similar Body Mass Index (23.20Kg/m^2±4,16 and 23.20 Kg/m^2±3.22, respectively). Representative variables were transepidermal water loss (Tewameter® CK electronics), epidermal hydration (Moisturemeter® DTec), and biomechanics (Cutometer® CK electronics) measured in five anatomical sites (forehead, cheek, neck, hand, and leg). Skin carotenes were also measured by the Multiple Spatially Resolved Reflection Spectroscopy (MSRRS) (Biozoom® GmbH). Food group intake was assessed using a validated Food Frequency Questionnaire. The statistical analysis was done by Jamovi® Software. The dietary patterns and their impact on the skin were compared using Mann–Whitney test and correlations were investigated by the Spearman rank correlation coefficient ($p<0.05$). Vegetable based diets are believed to bring multiple health benefits. Regarding skin physiology we could not find significant differences between the two groups, including the carotenoid content. TEWL was consistently higher in the VG group but significant differences could only be detected in the neck and leg. Looking for a potential relationship between the most frequent foods consumed by these two groups of participants and skin physiology we found that vegetables, vegetable drinks, milk, yogurt, and cheese showed a significant positive relationship with epidermal water balance. By opposition, alcoholic beverages and fast food showed a significant negative relationship with those variables. The VG group depicted a positive correlation with the carotenoid content, while red meat, viscera, alcoholic beverages, and sugar-sweetened beverages consumption typical of the OM group depicted a negative correlation. Our results are still exploratory being obvious that larger samples are needed for consistency. Nevertheless it is clear that dietary patterns might influence skin physiology and that this theme should be further explored.

Acknowledgments: This work is funded by national funds through FCT - Foundation for Science and Technology, I.P., under the UIDB/04567/2020 and UIDP/ 04567/2020 projects. Cíntia Ferreira Pêgo is funded by Foundation for Science and Technology (FCT) Scientific Employment Stimulus contract with the reference number CEEC/CBIOS/NUT/2018.

---

1 Hai, J., Nguyen, M., Hasan, A., Pan, A., Engel, T., & Sivamani, R. (2021). https://doi.org/10.5070/d3271052020
2 Greenberg, S. A. (2020). https://doi.org/10.12788/cutis.0143
3 Michalak, M., Pierzak, M., Kręcisz, B., & Suliga, E. (2021). https://doi.org/10.3390/nu13010203
4 Zerres, S., & Stahl, W. (2020). https://doi.org/10.1016/j.bbalip.2019.158588

Ultra-Fast Fluorescence Decay in Malignant Melanoma

Wolfgang Becker, Vladislav Shcheslavskiy, Marina Shirmanova, Oksana Garanina, Vadim Elagin

Wolfgang Becker
Becker & Hickl GmbH, Nunsdorfer Ring 6-9, 12277 Berlin, Germany
Vladislav Shcheslavskiy, Marina Shirmanova, Oksana Garanina, Vadim Elagin
Privolzhskiy Research Medical University, Nizhni Novgorod, Russia
Corresponding Author: Wolfgang Becker, becker@becker-hickl.com, https://www.becker-hickl.com

KEY WORDS: Malignant Melanoma, FLIM

Using a multiphoton TCSPC-FLIM system with ultra-fast detectors, we found extremely fast fluorescence-decay components in malignant melanoma. We found decay components with lifetimes, τ_1, from 10 ps to 20 ps, with amplitudes, a_1, as large as 98%. The data are in sharp contrast to the decay parameters in healthy tissue (τ_1 = 185 ps, a_1 = 55%) and in material from benign basal cell papilloma (τ_1 = 96 ps, a_1 = 45%). We believe that the ultra-fast decay component not only can be used to identify malignant-melanoma tissue and malignant-melanoma cells but also to gain information on mechanisms of tumor development.

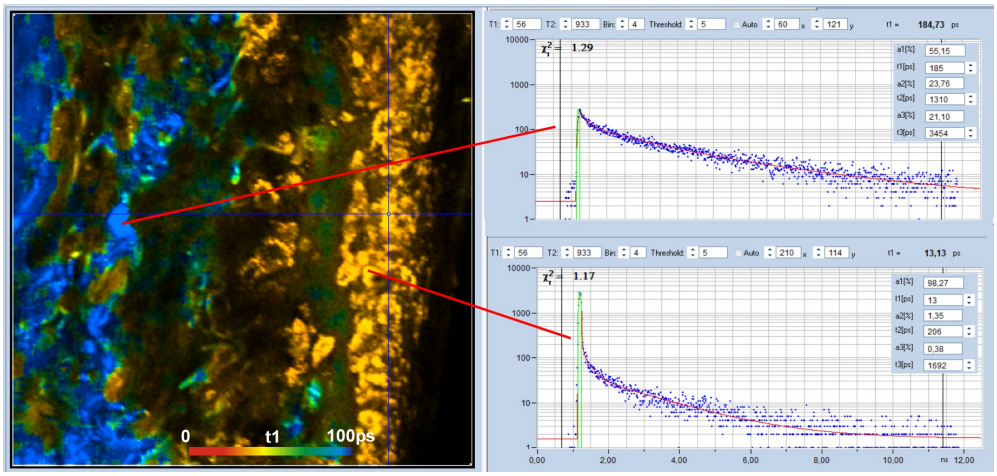

Fig. 1: FLIM of malignant-melanoma tissue. Vertical section through tissue sample, healthy tissue left, melanoma tissue right. Colour-coded image of the lifetime of the fast component, t1, of a triple-exponential fit of the data. Red to blue corresponds to 0 to 100 ps. Decay curves in characteristic spots of the image shown on the right.

Multiphoton Fluorescence Lifetime Imaging for *in vivo* Skin Investigations

H. G. Breunig, K. König

JenLab GmbH, Johann-Hittorf-Str. 8, 12489 Berlin, Germany
Corresponding Author e-mail address and URL: breunig@jenlab.de, jenlab.de

KEY WORDS: Multiphoton imaging, FLIM, skin imaging

Multiphoton imaging offers unique, high-resolution insights into the composition of the epidermal and upper dermal skin. The noninvasive technique can be readily performed *in vivo* since it relies on endogenous fluorophores which are excited by harmless NIR-laser pulses[1]. The fluorescence lifetime can provide, in addition to the signal intensity, information on the molecular signal origin and local metabolic activity. Its spatial distribution, depicted in pseudo-colors, is represented in so-called FLIM images[2]. These images are used for identification of the skin composition, to evaluate healthy and diseased skin and to follow the penetration of substances and particles into tissues. In particular, the equipment of clinical multiphoton tomographs with FLIM capability enhances their application capabilities. It enables dermatological FLIM imaging which gives insight into skin conditions like inflammations as well as the state of skin cancer and is used in cosmetic research to evaluate the effect of anti-ageing products[3]. We give an overview of the technical possibilities and limitations of clinical *in vivo* multiphoton FLIM imaging for dermatological applications based on our own data as well as literature examples.

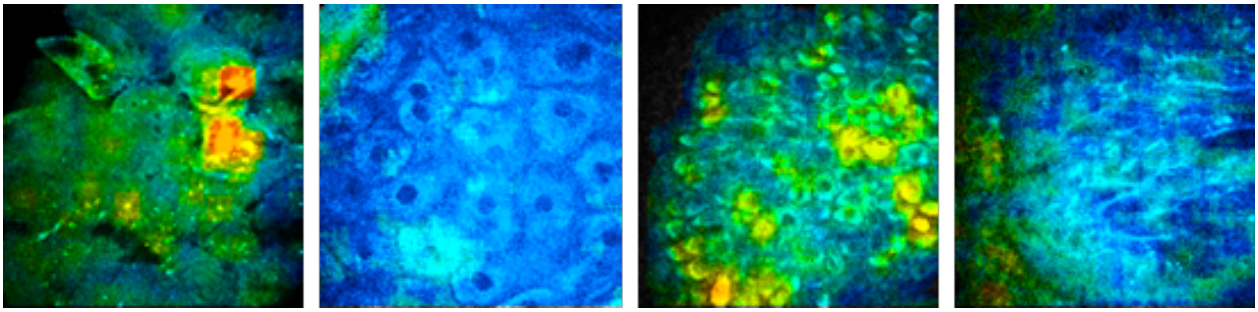

Multiphoton FLIM imaging of healthy human skin *in vivo*. The images depict horizontal sections from the stratum corneum, stratum spinosum, stratum basale and the elastin-collagen network of the upper dermis (left to right). The colors represent the long decay-time parameter (t_2) of endogenous autofluoroscence (here mainly from keratin, NAD(P)H, melanin, elastin, and collagen). The decay time was obtained by pixelwise fitting a two-exponetial decay function to time dependent autofluorescence data (red :< 1 ns, green : 1.5 ns, blue : >2 ns). The autofluorescence was generated by two-photon excitation with 780 nm femtosecond-laser pulses and its time dependence recorded using the technique of time correlated signal counting. Image regions : 135 µm x 135 µm.

[1]K. König, J Biophotonics, 1;1(2008)13-23.
[2]K. König (ed.), "Multiphoton Microscopy and Fluorescence Lifetime Imaging" (De Gruyter, Berlin, 2018).
[3]K. König, Methods Appl Fluoresc., 22;8(3) (2020)034002.

A new, multi-sensor open chamber water evaporation device: TEWA-Hex in a controlled study and in an Antarctica expedition

Razvigor Darlenski[3,4], MD, PhD, Georg Wiora[5] PhD, Dessyslava G. Nikolaeva[3], Joachim W. Fluhr[1,2] MD

1- Charité – Universitätsmedizin Berlin, Institute of Allergology, Berlin, Germany
2- Fraunhofer Institute for Translational Medicine and Pharmacology ITMP, Allergology and Immunology
3- Department of Dermatology and Venereology, Acibadem City Clinic Tokuda Hospital – Sofia, Bulgaria
4- Department of Dermatology and Venereology, Medical Faculty, Trakia University- Stara Zagora, Bulgaria
5- Courage & Khazaka GmbH, Cologne German

Background and aims of the study
Instrumentation technology for transepidermal water loss (TEWL) measurements has not been substantially modified since its introduction by Nilsson in 1977. Recent progresses in sensor development allow new designs in sensor arrangement and innovative data evaluation techniques make new skin parameters accessible. A new generation of probes for TEWL measurements using a matrix of 30 sensors instead of the typical two has been developed. It uses spatial statistical analysis of raw measurement values.
The objective of an in vivo study was to compare the new, multi-sensor open chamber water evaporation probe (TM-Hex) for epidermal barrier assessment with the established TM300 probe. The primary endpoint was to test the equivalence or comparability of the established tewameter measurement probe TM300 with the new TM-Hex.

Material and methods:
Baseline measurements on the volar forearam, repeated measurements and assessement on eight different anatomical locations were performed in 24 healthy volunteers of both gender with the TEWA Hex and the TM300. Real life data were assessed in a very recent study for the TEWA Hex in an Antarctica expedition.

Results:
We could show an excellent correlation $p<0.001$; R-coefficient=0.9) between TEWA Hex and the TM300. The coefficient of variance (CV)was 11% for TEWA Hex and 19% for TM300. At the different anatomical locations the CV ranked between 7% (right inner upper arm) and 14% (palms).
The real life data showed robust results under harsh external conditions.

Conclusion:
The correlation between TEWA Hex and TM300 along with the robustness of the measurements with TEWA Hex provide evidence that the new probe for assessement of epidermal barrier function is comparable to the TM 300. In most conditions TEWA Hex shows even more accurate measurements than the TM300 probe.

Label-free *in vivo* imaging of mast cells and macrophages in the human papillary dermis using two-photon fluorescence lifetime imaging

M.E. Darvin[1,2], M. Kröger[1], J. Scheffel[1], J. Schleusener[1], M. Maurer[1], J. Lademann[1], M.C. Meinke[1]

[1] *Department of Dermatology, Venerology and Allergology, Charité – Universitätsmedizin Berlin, corporate member of Freie Universität Berlin and Humboldt-Universität zu Berlin, Berlin, Germany*
[2] *Institute for Organic Chemistry and Biochemistry, Technical University of Darmstadt, Germany*

Corresponding Author e-mail address: maxim.darvin@protonmail.com

KEY WORDS: Intravital imaging, Immune cells, Skin

Mast cells and macrophages are critical immune effector cells, which are present in most of the tissue and organs in the human body and play a crucial role in disease response. Assessment of their number and activation state is limited to histomorphometric analysis of biopsies. We showed label-free, *in vivo* and non-invasive visualization of mast cells[1] and macrophages[2] in human skin using two-photon excited fluorescence lifetime imaging (TPE-FLIM). A titanium sapphire laser at 760 nm, generating 100 fs pulses at 80 MHz (Fig. 1a) was applied and provide an imaging depth of ≈150 µm in the skin at high resolution. We have identified TPE-FLIM parameters (fluorescence lifetime and intensity) of resting/activated mast cells and M1/M2 macrophages *in vitro* in the cell culture and confirm it in skin biopsies using cell-specific staining. Then, based on determined TPE-FLIM parameters, we have visualized and quantified resting/activated mast cells (Fig. 1b, 1c) and M1/M2 macrophages (Fig. 1d, 1e) in the papillary dermis of healthy volunteers for the first time *in vivo*. TPE-FLIM parameters of resting/activated mast cells and M1/M2 macrophages are distinct and can be differentiated between each other, other cells and extracellular matrix at high sensitivity and specificity by the use of a developed machine learning model. The developed technique could be useful in clinical practice for managing patients with mast cell- and/or macrophage-related diseases including diagnostics, disease development and treatment control on the cellular level.

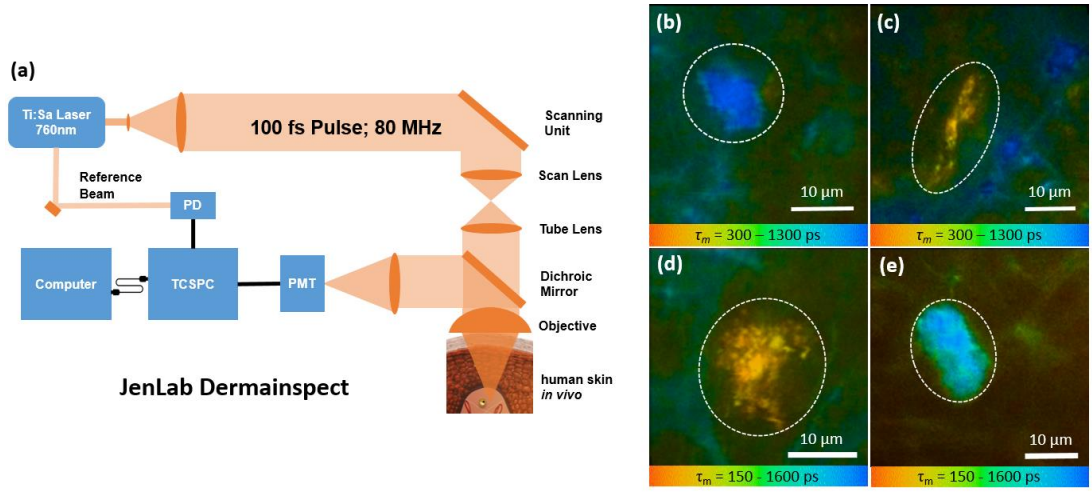

Figure 1: Schematic of the two-photon excited fluorescence lifetime imaging microscope (a), resting (b) and activated (c) mast cells and M1 (d) and M2 (e) macrophages in healthy human dermis *in vivo*.

[1] M. Kröger., J. Scheffel, V.V. Nikolaev, *et al*. Sci Rep 10, 14930 (2020).
[2] M. Kröger., J. Scheffel, E.A Shirshin, *et al*. Biorxiv, 2021.11.29.470361 (2021).

Biomechanical and topographical properties of corneocytes using AFM

A. S. Évora[1], N. Piasentin[2,3], S. A. Johnson[1], G. Lian[2,3], Q. Cai[2], Z. Zhang[1], M. J. Adams[1]

[1]School of Chemical Engineering, University of Birmingham, Birmingham, United Kingdom
[2]Department of Chemical and Process Engineering, University of Surrey, Guildford, United Kingdom
[3]Unilever R&D Colworth, Unilever, Sharnbrook, United Kingdom

KEY WORDS: AFM, corneocytes, biomechanics

The Stratum Corneum (SC) is the first barrier of the skin[1]. When the integrity of the skin is compromised by constant high normal and shear stresses, pressure injuries may occur[2]. Therefore, investigating the mechanical properties of corneocytes, the SC main cells, can reveal important hints as to how skin at different anatomical locations bears load. Although dead, these cells undergo an active maturation process as they migrate upward, which includes the loss of corneodesmosomes and the stiffening of the cornified envelope (CE)[1,3,4]. The aim of this project was to characterize the mechanical and topographical characteristics of corneocytes using Atomic Force microscopy (AFM). Tapping mode and force spectroscopy were used for imaging and to assess changes in mechanical properties, respectively. A critical experimental review of the state-of-the-art served as the basis for the characterization of the viscoplastic properties of these cells, which highlighted the main issues of deconvoluting AFM mechanical data. Corneocytes from different body sites (forearm, cheek, neck, sacrum, and medial heel) were analysed, and their surface properties (i.e., distribution of corneodesmosomes and CE maturity) revealed differences across anatomical regions. Finally, the influence of hydration and certain dermatologically relevant compounds (glycerol, ethanol, urea) on the mechanical and surface properties of corneocytes was investigated.

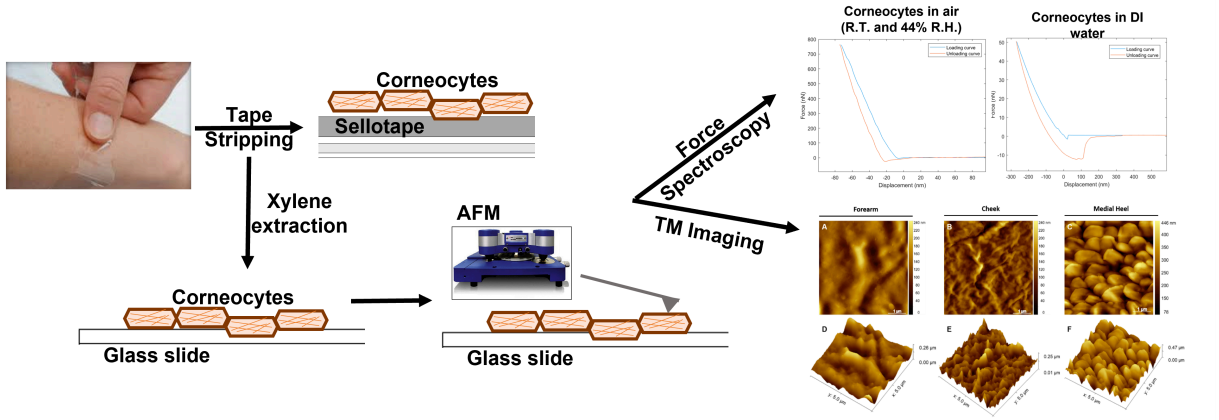

Protocol for AFM measurements of corneocytes. Tape stripping was used to collect cells from the skin of healthy volunteers and corneocytes were extracted from the tape onto a glass slide by overnight incubation in xylene. AFM tapping mode and force spectroscopy were used to explore differences between anatomical sites and test conditions.

Acknowledgement: this research has received funding from the European Union's Horizon 2020 research and innovation programme under the Marie Skłodowska Curie grant agreement No 811965; project STINTS (Skin Tissue Integrity under Shear).

[1] Évora AS, Adams MJ, Johnson SA, Zhang Z. Skin Pharmacol Physiol 2021;34:146–161.
[2] Hanson D, Langemo DK, Anderson J, Thompson P, Hunter S. Adv. Skin Wound Care 2010; 23:21-24
[3] Menon GK, Cleary GW, Lane ME. Int J Pharm 2012;435(1):3–9.
[4] Lin TK, Crumrine D, Ackerman LD, et al. J Invest Dermatol 2012;132(10):2430–2439.

Optoacoustic 3D functional imaging of skin microvasculature

Tiago Granja, Sergio Andrade, Luis Monteiro Rodrigues

CBIOS – Universidade Lusófona's Research Center for Biosciences & Health Technologies, Corresponding Author
tiago.granja@ulusofona.pt; https://cbios.ulusofona.pt/

KEY WORDS: optoacoustic tomography; functional imaging, skin microcirculation; vascular research

Skin microcirculatory research is in the center of multiple issues in health and disease, motivating the development of new technologies[1]. To generate functional imaging for fundamental purposes, including diagnostic is the ultimate trend justifying this current interest for the multiscan optoacoustic tomography. Our group has been specially interested in this multiple spectra optoacoustic tomography (MSOT). This system allows 3D visualization of reconstructed videos holding image signals from multiple wavelengths simultaneous[2]. In the present study we provide skin functional imaging after a challenge with Post-Occlusive Reactive Hyperemia (PORH) a classical exploratory maneuver often used in experimental physiology.

Over a time window of 5minuts, the ventral forearm skin microvasculature of 6 healthy participants recruited after written consent was evaluated by MSOT during a PORH maneuver using a pressure cuff inflated up to 200mmHg. The interest wavelengths – chromophores were 900nm for oxygenated hemoglobin-HbO_2, 760nm for deoxygenated hemoglobin-Hb and 700nm for melanin. Microvasculature performance during this phases - rest (1min), cuff inflation to 200mmHg compressing the brachial artery (1min), and deflation - recovery (3min) was continuously recorded during the process. Analysis of imaging reconstruction and unmixing provided quantification of HbO_2, Hb, mean saturation of oxygen (mSO2) and total Hb (HbT) in selected video regions of interest (ROI)[3]. Acquisitions allowed the evaluation of microvasculature performance in 15mm volume within the skin. The time lapse analysis focused both skin plexus interconnectivity and distribution time, of microvascular units count (µVu – vascular density), inter unit average distance (Ad), and capillary blood volume (mm^3).

This approach offers a functional approach over PORH, that appeals to an increasing community, in contrast to the single point measurements normally provided by laser Doppler flowmetry or by photopletysmography.

1 Guerraty, M., Bhargava, A., Senarathna, J., Mendelson, A. A. & Pathak, A. P. Advances in translational imaging of the microcirculation. Microcirculation. 28 (3), e12683, doi:10.1111/micc.12683, (2021).

2 Wang, L. V. & Yao, J. A practical guide to photoacoustic tomography in the life sciences. Nat Methods. 13 (8), 627-638, doi:10.1038/nmeth.3925, (2016).

3 Granja, T., Andrade, S. & Rodrigues, L. Optoaccoustic Tomography – good news for microcirculatory research: Tomografia Optoacústica – boas notícias para a investigação microcirculatória. Journal Biomedical and Biopharmaceutical Research. 18 1-13, doi:10.19277/bbr.18.269, (2022).

Acknowledgments: This work is funded by national funds through FCT - Foundation for Science and Technology, I.P., under the UIDB/04567/2020 and UIDP/ 04567/2020 projects. Sergio Andrade and Cíntia Ferreira Pêgo are funded by Foundation for Science and Technology (FCT) Scientific Employment Stimulus contract with the reference number CEEC/CBIOS/NUT/2018.

The Meissner Corpuscles create protrusions in the epidermis of glabrous skin

Victor Hugo Pacagnelli Infante[1,2], Roland Bennewitz[1,3], Maxim E. Darvin[2], Martina C. Meinke[2]

[1]INM - Leibniz Institute for New Materials, 66123 Saarbrücken, Germany
[2]Charité – Universitätsmedizin Berlin, corporate member of Freie Universität Berlin and Humboldt-Universität zu Berlin, Department of Dermatology, Venerology and Allergology, Center of Experimental and Applied Cutaneous Physiology (CCP), Charitéplatz 1, 10117 Berlin, Germany
[3]Department of Physics, Saarland University, 66123 Saarbrücken, Germany
Corresponding author: victor.infante@leibniz-inm.de

KEY WORDS: Glabrous skin, Meissner Corpuscles, Confocal Laser Scanning Microscopy

Glabrous skin (GS) is a hair-free skin found on the palms and soles. It is innervated by specialized nerves, such as Meissner Corpuscles (MCs) that help to decodify tactile details. The aim of this study was to investigate the morphology of MCs in the hand using confocal laser scanning microscopy (LSM). Eighteen points on the hand of one volunteer (male, 30 years old) were analyzed with LSM. The number of MCs per mm² was determined. Later, eight participants (aged 26 to 62 years) had their index and little fingers and tenar palm regions analyzed for the number of MCs, morphology, and thickness of the *stratum corneum* (SC). We discovered that the intensity of the reflectance differed between regions with and without receptors. MCs may be present alone, in duet or triplet in the same papillae and in proximity to the ridges. The distal phalanx presents a higher number of MCs per mm² (9 to 11) compared to medial and proximal phalanx (4 to 6) and to the palm (1 to 4). Regions with MCs could be identified by a higher reflectance (p<0.001) above the corpuscles which was related to a protrusion of the epidermis. We found a difference of 17±10 µm in the depth at which the epidermis starts (red circles in Fig. 1A) between areas with and without MCs (Fig. 1). The SC thickness depends on the anatomic position, being thicker for the index finger. This peculiar local morphology of epidermis and SC above MCs may have a function in the transmission of mechanical stimuli towards tactile perception, reminiscent of a remote control where the SC is the button with increased area of contact and the MCs are the underlying electric switches.

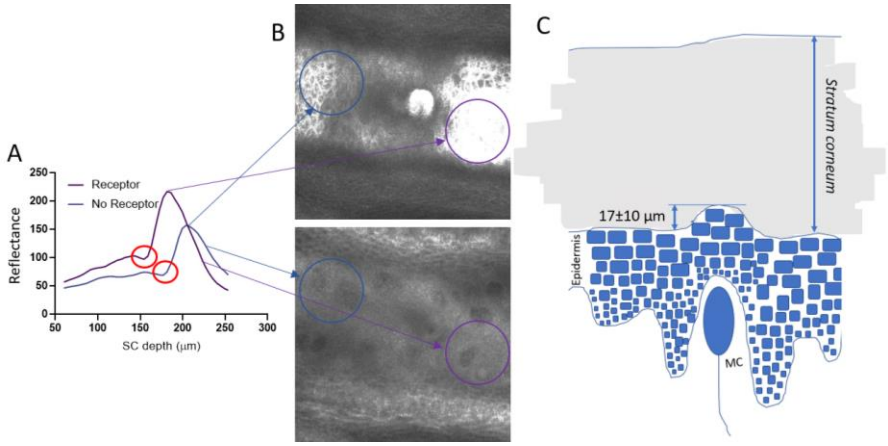

Fig. 1 – Regions with receptors exhibit a protrusion of the epidermis into the SC appearing first in the stacks (red circles) and presenting a higher reflectance in the epidermis (A), evidenced by the purple circles (B), which are the highest points for the reflectance curves in A. The blue and purple curves evidence this differences in the LSM images, representing areas without and with MCs respectively (B). A schematic representation of the epidermal protusion caused by the MCs (C).

Human Perception of Wrinkle Depth

Lily Jiang, PhD

SGS
Corresponding Author e-mail address: Li.Jiang@sgs.com

KEY WORDS: wrinkle depth, primos, human perception

Facial wrinkle is an important hallmark for photoaging and a key evaluation parameter for testing the anti-aging benefit of a cosmetic product. In the cosmetic clinical testing field, wrinkle assessment is typically done by expert grading, 2D imaging with image analysis, silicone replica impression, and/or 3D imaging. One central question is that what is the minimal change in wrinkle depth that can be detected by trained human eyes. As cosmetic products focus on addressing the appearance of facial features, it is important to understand how much change is perceptible so we can further correlate with products effect and feedback into products formulation and innovation. Coupling the 3D imaging system and expert grader evaluation allowed us to address such a question. We asked several expert graders to score the wrinkle depth using a set of 2D photos captured with Primos device and analyzed the 3D capture using Primos software in parallel. Wrinkle depth at specific locations were marked. The expert grading was done following a 0-9 scale with half point allowed. Grading scores from multiple graders were well aligned. When compared to the actual wrinkle depth measured with Primos device and software, good alignment was also achieved. Linear regression analysis indicates that 1 point grade in expert grading is about 90-110 μm in depth difference with an R value > 0.8. Therefore, we believe the minimal change in wrinkle depth that can be detected by trained human eyes, typically half a point in grading, is about 50 μm.

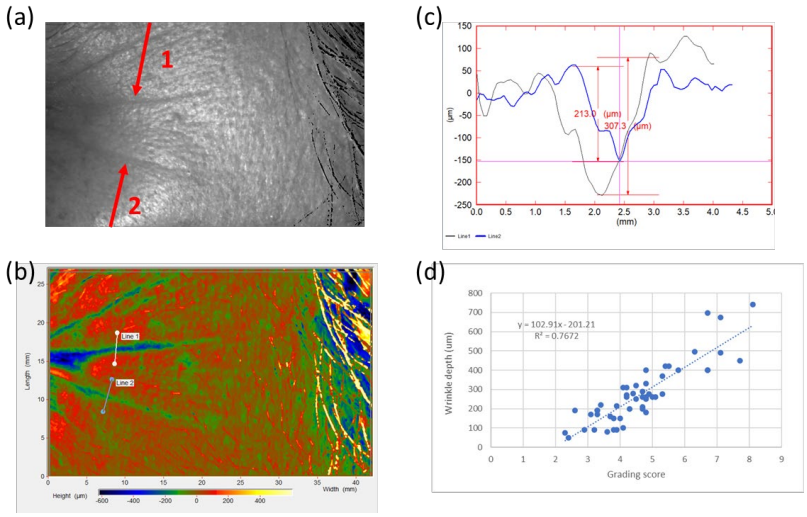

Figure 1. Wrinkle depth perception and measurement. (a). 2D image capture used for expert grading of wrinkle depth; (b). 3D image used for wrinkle depth analysis; (c). Wrinkle depth measurement performed using Primos software; (d). Correlation graph between measured wrinkle depth and expert grading data.

Multimode Multiphoton and Reflectance Microscopy of Skin Using Femtosecond Laser Pulses

Aisada König[a,b] and Karsten König[a,b]

[a]JenLab GmbH, Johann-Hittorf-Strasse 8, 12489 Berlin, Germany
[b]Saarland University, Department of Biophotonics and Laser Technology, 66123 Saarbruecken, Germany
Corresponding Author: a.koenig@uni-saarland.de, www.blt.uni-saarland.de

KEY WORDS: reflectance, femtosecond laser, near-infrared, skin, two-photon imaging, confocal microscopy, multiphoton tomography

Multiphoton tomography based on near-infrared (NIR) femtosecond (fs) lasers provide non-invasive 3D-optical biopsies with high-resolution (~300 nm) and has already been successfully used as a diagnostic tool in clinics[1].

So far, imaging is based on two-photon excitation of endogenous fluorophores e.g., elastin and metabolic coenzymes NAD(P)H and FAD as well as second harmonic generation of extracellular matrix protein collagen. Additionally, reflectance confocal microscopy (RCM) yields non-invasive cellular imaging of the skin *in vivo* based on modifications of intradermal refraction values[2,3]. The commercial system *VivaScope* employs a continuous wave (cw) NIR laser diode operating at 830 nm.

The novel MPT*compact* is a multimodal high-resolution optical imaging tomograph with a reflectance confocal microscopy (RCM) module. The tomograph employs 80 MHz NIR femtosecond laser pulses for reflectance imaging in contrast to conventional RCM with a cw NIR laser. The use of fs NIR laser pulses has the advantage of complementary multiphoton and reflectance microscopy of skin.

We demonstrate simultaneously recorded high-resolution multiphoton and reflectance confocal in vivo skin images of volunteers, patients with dermatological disorders, and of skin appendages.

[1] K. König (Ed.) Multiphoton Microscopy and Fluorescence Lifetime Imaging. De Gruyter, Berlin, 2018
[2] M. Rajadhyaksha et al., J Invest Dermatol. 104, 946-952 (1995)
[3] S. Gonzales et al., J Invest Dermatol. 111, 538-539 (1998)

In vivo localization of carbon black tattoo inks in tattooed human skin using two-photon excited fluorescence lifetime imaging

M. Kröger, J. Schleusener, S. Jung, M.C. Meinke, M.E. Darvin

Department of Dermatology, Venerology and Allergology, Charité – Universitätsmedizin Berlin, corporate member of Freie Universität Berlin and Humboldt-Universität zu Berlin, Berlin, Germany

KEY WORDS: Tattoo, Fibroblasts, Intravital imaging, Immune cells, Epidermis, Dermis

Tattoos and body art are increasingly common, yet the influence of tattoo ink pigments on the skin is not well established, partly due to missing of imaging non-invasive methods.[1] Following the recent development of label-free non-invasive visualization of resting/activated mast cells[2] and M1/M2 macrophage[3] using two-photon excited autofluorescence (TPE-AF) and fluorescence lifetime imaging (TPE-FLIM), we investigate the localization of carbon black ink pigment in tattooed human skin *in vivo*. A tunable titanium sapphire laser at 760 nm, generating 100 fs pulses at 80 MHz (Fig. 1a) was applied and provide an imaging depth of ≈150 µm in the skin at high spatial and axial resolution. The cellular intake of carbon black nanoparticles is categorized with TPE-FLIM. Carbon black nanoparticle agglomerates were successfully identified in mast cells, macrophages and fibroblasts in the dermis and in the keratinocytes and Langerhans cells in the epidermis of fresh and old tattooed skin. The extracellular matrix was found to be free of tattoo inks after the initial skin regeneration of 3 weeks. Loading of highly fluorescent carbon black nanoparticles enables *in vivo* imaging of fibroblasts in the dermis by TPE-AF (Fig. 1b) and by TPE-FLIM (Fig. 1c) and Langerhans cells in the epidermis, which cannot be visualized in native conditions. In tattooed skin, cells are able to absorb/phagocytose tattoo inks and keep them for their lifespan, which was measured by the short TPE-FLIM and enhanced TPE-AF intensity. Tattooed skin has increased firmness and decreased elasticity, visible in thicker and less randomly oriented collagen I fibers compared to non-tattooed skin. The TPE-FLIM technique could be useful in clinical dermatological practice for managing patients with tattoo-related complications and to give useful information about cellular pathways of exogenous substances in the skin, their accumulation and understanding the skin regeneration after trauma.

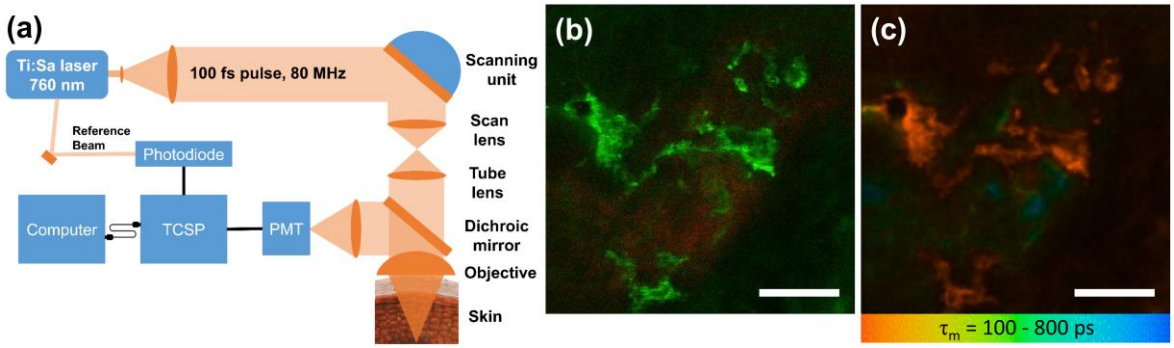

Figure 1: Schematic illustration of the TPE-FLIM tomograph (a). TPE-AF (b) and TPE-FLIM (c) images of carbon black nanoparticles-loaded fibroblasts (green in (b) and red in (c)), located between collagen I matrix (red in (b)) measured *in vivo* in a 24 months old tattoo. Scale bar: 12 µm.

[1] W. Bäumler. Curr Probl Dermatol. 48, 176 (2015).
[2] M. Kröger., J. Scheffel, V.V. Nikolaev, *et al*. Sci Rep 10, 14930 (2020).
[3] M. Kröger., J. Scheffel, E.A Shirshin, *et al*. Biorxiv, 2021.11.29.470361 (2021).

Automated identification of keratinocytes on *in vivo* reflectance confocal microscopy images of the human skin epidermis

Imane Lboukili[1,2], Georgios Stamatas [1], Xavier Descombes[2]

[1]*Johnson & Johnson Santé Beauté France, [2] UCA – INRIA – I3S/CNRS, Antibes, France*

Ilbouki1@its.jnj.com

KEY WORDS: confocal microscopy, epidermis, image segmentation

Reflectance confocal microscopy (RCM) is an *in vivo*, non-invasive method that allows real-time visualization of the epidermis at the cellular level. Thus, it allows the visualization of individual keratinocytes, providing topological and geometrical information which change with age during childhood and from one epidermal layer to another. To be able to calculate these properties, the first step is to identify the location of individual cells. Unfortunately, manual analysis of RCM images is hindered by image noise, graininess, and non-uniformity and thus is time-consuming, intensive, and subject to human error and inter-expert variability.

We propose a method to automatically identify keratinocytes on RCM images of the *stratum granulosum* (SG) and *stratum spinosum* (SS) aiming to understand how skin architecture and cellular topology change with age during childhood. Our objective is to match the accuracy of manual identification of cells by experts.

The proposed method is based on image analysis methods and is a three-step approach: (1) identification of the region of interest (ROI) containing the cells, (2) identification of the keratinocytes within the ROI, and (3) post processing to improve detection and correct it by removing detected cells too small to be correct and locally reapplying the first two steps to detected cells that were too large to be correct.

RCM images of the volar forearm were collected from children, aged 3 months to 10 years old, and adults (as control group), aged 25 to 40 years old, preferably mothers of enrolled children. All participants were healthy and with Fitzpatrick types between I and III. In total, 1705 RCM images of the SG and SS were analyzed.

To date attempts at automating the identification of cells on RCM images have been reported in the literature[1] [2] but on a limited number of images. This is the first "large-scale" analysis of RCM images of the epidermis that the authors are aware of.

For all age groups and layers, we calculate cell area, cell perimeter, cell density and average distance to the nearest neighbor.

Our results validate that keratinocytes are significantly larger in the granular layer than in the spinous layer, and that they get progressively larger with age. Accordingly, cell density decreases with age, while cell perimeters increase. Additionally, the differences are more pronounced in the SG than in the SS.

---

[1] D. Gareau, "Automated identification of epidermal keratinocytes in reflectance confocal microscopy," J. Biomed. Opt. **16**(3), 030502 (2011) [doi:10.1117/1.3552639].

[2] M. A. Harris et al., "A Pulse Coupled Neural Network Segmentation Algorithm for Reflectance Confocal Images of Epithelial Tissue," PLoS [2]ONE **10**(3), e0122368 (2015) [doi:10.1371/journal.pone.0122368].

Reflectance Confocal Microscopy 3D imaging analysis for quantification of the skin photoaging and melasma

Maia Campos, P.M.B.G.[1*], Kakuda, L.[1], Infante, V.H.P.[1]
[1]School of Pharmaceutical Sciences of Ribeirão Preto - University of São Paulo – USP – Av. Do café S/N.Ribeirão Preto – SP, Brazil. Zip: 14040-903
**Corresponding Author: pmcampos@usp.br*

KEY WORDS: skin hyperpigmentation, 3D imaging, RCM

There are different types of skin hyperpigmentation, and the diagnosis of the skin pigmentation pattern alterations is fundamental for the right choice of treatment. Reflectance Confocal Microscopy (RCM) has been applied for the evaluation of morphological and structural characteristics of the skin as a support for the diagnosis and treatment of skin alterations [a]. In this context, the application of 3D imaging analysis for quantification of the skin hyperpigmentation can be useful for identify the extension of hyperpigmented area, which can help the development of more effective dermocosmetic products. Thus, the aim of this study was to quantify the hyperpigmented area of the skin photoaged and with melasma. After approval of Ethnics Committee, 20 females, aged between 45 and 50 years, Fitzpatrick phototype III and IV, with skin photoaged or melasma, were enrolled. The obtained images from RCM were sequentially imported and superimposed. This overlap was made according to the reflectance of the hyperpigmentation. Thus, after the formation of the 3D image, the brightness area was calculated in pixels². The results showed that there are significant differences ($p<0.002$) between extension of hyperpigmented area in the skin photoaged and melasma (Figure 1), where melasma covers almost the entire area of the image. In conclusion, the application of this kind of analysis allowed the evaluation of hyperpigmentation in different skin layers at same time, which is very important to optimize the imaging analysis by RCM. Finally, RCM 3D imaging analysis adds important information for the evaluation of different skin hyperpigmentation types in a quantitative, complete, and quick way.

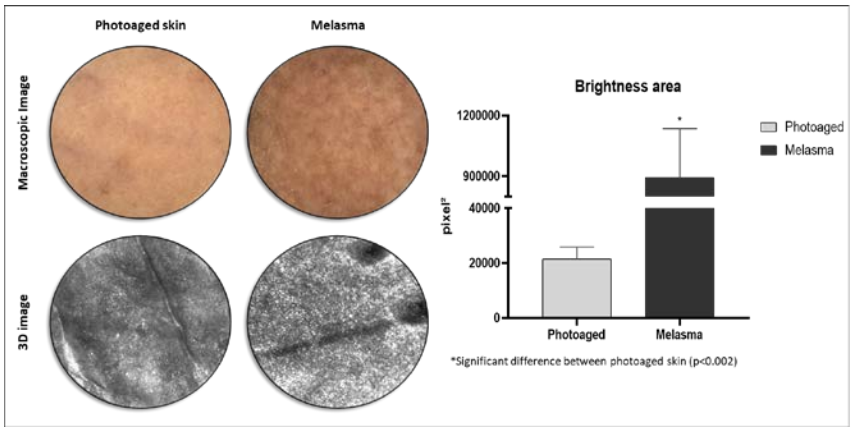

Figure 1: Representative RCM images of photoaged skin and melasma and quantitative analysis.

[a] Maia Campos P.M.B.G., de Melo M.O., Mercurio D.G. ''Assessment of Skin Photoaging with Reflectance Confocal Microscopy''. In: Issa M., Tamura B. (eds) Daily Routine in Cosmetic Dermatology. Clinical Approaches and Procedures in Cosmetic Dermatology. (Springer, Cham., New York, 2016).

Sensory profiling of topical semisolid products: Potential for instrumental tests to assess perception

Yousuf H Mohammed[1], Sarika M Namjoshi[1], Bhaveshkumar Panchal[1], Arianna Dick Zambrano[1],Vania Liete Silva[1,2], Tannaz Ramazanli[3], Sam G. Raney[3], and Michael S Roberts[1]

1University of Queensland Diamantina Institute, The University of Queensland. Woolloongabba, Brisbane, Australia

2 Instituto de Ciências Ambientais Químicas e Farmacêuticas, Universidade Federal de São Paulo, Diadema SP, Brazil

3 Division of Therapeutic Performance, Office of Research and Standards, Office of Generic Drugs, Center for Drug Evaluation and Research, United States Food and Drug Administration, Silver Spring, MD, USA

y.mohammed@uq.edu.au. URL: https://researchers.uq.edu.au/researcher/11844

KEY WORDS: Sensorial evaluation of skin products, Infrared camera, patient perception

A perception of superior quality is key to the success for topical semisolid products. Poor aesthetics (sensory attributes) of the product may adversely affect patient adherence and, in turn, lead to product failure. Furthermore, certain sensory perceptions such as cooling sensation are closely associated with therapeutic performance and hence must be evaluated to capture the full spectrum of therapeutic activity of the product. In this study, sensory comparison of metronidazole products comprising of gels, creams and lotion was conducted to obtain sensory profiles, through evaluations of a skin product panel and descriptive sensory analysis methodology. Parallelly, for laboratory manufactured products, we assessed the potential of instrumental analysis to evaluate sensory perceptions. Infrared camera thermal imagining (IRT) and thermocouples were used to measure and quantify cooling sensation. Rheological, Tribological and textural analysis was conducted to evaluate stickiness, spreadability, smoothness and other sensory perceptions. This work highlights the use of IRT-based technique for in vitro assessment of cooling effect through precise measurement of temperature dynamics.

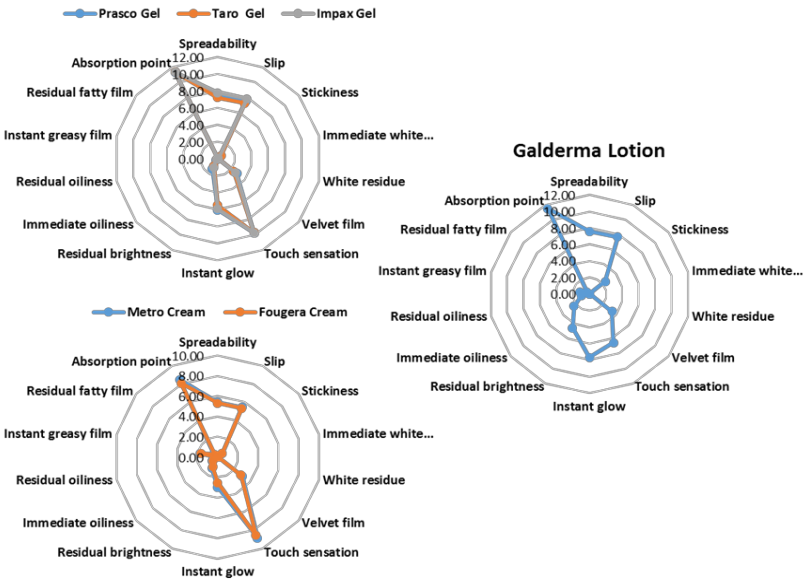

Figure 1. Sensory profile of metronidazole products.

Effect of seasonal and geographical variations on skin barrier

Neelam Muizzuddin, PhD
Skin Clinical Research Consultants, LLC
neelam@skinclinicalresearch.com, https://skinclinicalresearch.com/

KEY WORDS: skin barrier, dry environment, seasonal change,

Human skin maintains an optimal permeability barrier function in a terrestrial environment that varies considerably in humidity. Epidermal keratinocytes experience high osmolality under dry environmental conditions, due to increased transepidermal water loss, and a concomitant drying of the skin. This study was designed to evaluate the effect of a formulation containing topical sorbitol on skin barrier and moisturization of subjects living in arid and humid regions in summer as well as winter. Clinical studies indicated that skin chronically exposed to hot, dry environment appeared to exhibit stronger skin barrier and a lower baseline trans epidermal water loss. In addition, skin barrier was stronger in summer than winter. Sorbitol exhibited significant improvement in both barrier repair and moisturization, especially in individuals subjected to arid environmental conditions.

Taking pictures for at-home studies in cosmetics: can pictures taken directly by the volunteers be used in a clinical study?

T. Nappez[1], A. Bigouret[2], Q. Pré[1], F. Atmani[2], D. Godet[2], H. Lepage[1]

1 Connected Physics SAS - 59, rue de Ponthieu - 75008 Paris - FRANCE
2 Laboratoires CLARINS - 5, rue Ampère - 95300 Pontoise - FRANCE
Corresponding Author e-mail address and URL: Thomas Nappez - thomas.nappez@connectedphysics.com - www.connectedphysics.com

KEY WORDS: Calibrated Pictures, At-home Studies, AI-Face analysis

The setup of studies including physiological measurements directly at the home of the volunteers is a key step for the future of clinical evaluation in cosmetics. These kind of studies will indeed allow to track the efficacy of skincare products in real-time and real-life. However, some challenges need to be overcame. Two of these challenges are to assess the ability of the volunteers to perform correctly the measurements by themselves and to ensure that the reproducibility and the quality of the measurements are good enough to be used in a clinical study.

This study is structured around 3 main aims :

- evaluate the ease of use for the volunteers of the connected mirror
- determine the acceptability of protocols carried out by the volunteers themselves at home
- analyse the quality of the positioning of the face of the volunteers (also including the expression of the faces, the use of the blindfold to clear the face) on the « selfie » pictures taken with the mirror.

In this test, 13 connected mirrors called Pixel have been sent and used during 5 days. These devices are composed by a 12MP wifi camera, a controlled light, a color chart and a magnetic system to set the distance between the mirror and the face. The volunteers took pictures of their entire face themselves directly at home in the evening after removing their make-up. The information on the protocol and the use of connected mirror was provided to the volunteers, thanks to a dedicated App that includes a chat. No face to face explanation was given.

Finally, the connected mirrors appeared rather user-friendly especially after a first use. Indeed, the volunteers said that taking a front face photo was, on average, "a little difficult" on the first day and then "easy" from the second day of use. All of the volunteers did agree to participate again in this kind of study.

For the positioning, 6 of the 13 volunteers were perfectly positioned all the time. For the other volunteers, the face was slightly cut at the top of the forehead or at the color checker located under the chin. This point could be improved by increasing the distance between the face and the mirror. A clinical scoring on these pictures is currently being performed to further validate the reproducibility of scoring.

In conclusion, the Pixel mirror seems to be a promising means of measurement at home and in real condition for the volunteers.

Non-invasive quantitative Analysis of *in vivo* Skin Penetration by Confocal Raman Spectroscopy

G. Puppels[1,2], P. Caspers[1,2], C. Nico[2] , T. Bakker Schut[1,2]

1. *RiverD International B.V., Marconistraat 16, 3029AK Rotterdam, The Netherlands*
2. *Department of Dermatology, Erasmus MC Cancer Institute, University Medical Center Rotterdam, PO Box 2040, 3000 CA Rotterdam, The Netherlands*

gpuppels@riverd.com, www.riverd.com

KEY WORDS: bio-equivalence, formulation, PBPK-modeling

In vivo Raman spectroscopy is a broadly accepted technique providing detailed information about the molecular composition of the skin.

We have recently introduced a method for quantitative analysis of *in vivo* skin penetration of topically applied products based on Raman spectroscopy[1]. The non-invasive nature of the method allows the monitoring of product concentration profiles (in mg/cm^3), total product uptake (in µg/cm^2) and determination of product flux (in µg/cm^2/h). This can e.g. be used to provide essential *in vivo* information for assessment of the bio-equivalence of generic topical products to the original product.

The *in vivo* data may also provide valuable input for the development and experimental validation of *in silico* PBPK-models.

Actives and other formulation constituents can be monitored simultaneously, providing input for optimization of product formulation[2,3].

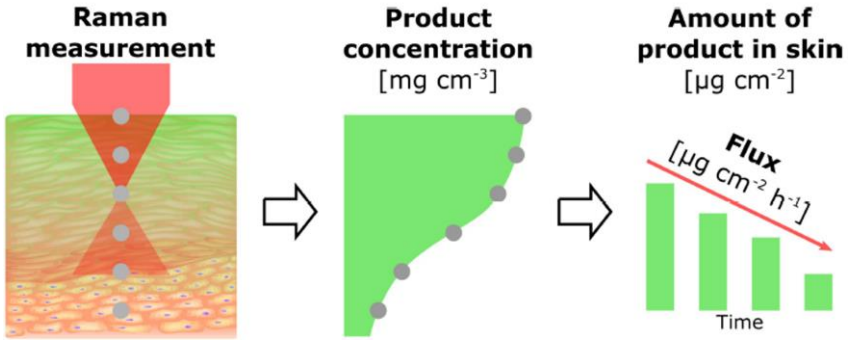

Confocal Raman spectra are measured at a range of depths in the skin and provide quantitative information about local product concentration. The area under the curve of the concentration profiles yields the tota amount of product in the skin. Monitoring its decrease over time after terminating the product application, enables calculation of the product flux through the skin.

[1]P.Caspers, Translational Biophotonics.2019;1:e201900004.
[2]A.Patel, Pharmaceutics 13:542, 2021
[3] Y. Zhang, Pharmaceutics13050726

Effects of Mechanotrasduction on Skin and Fascia with a Wave Stimulation

N. Qiao[1], L. Ouillon[1], A. Bergheau[1] , R. Vargiolu[1], V.Dumas[1], H. Zahouani[1]

University of Lyon, Laboratory of Tribology and Dynamic of Systems, UMR-CNRS 5513
Author email:na.qiao@ec-lyon.fr

KEY WORDS: Skin, Fascia, Mechanobiology

As the outermost organ of the human body, the skin is continuously exposed to various mechanical environments. Aging skin is known to undergo alterations in its structure, leading to changes in the response to external stimuli. Therefore, this research investigated the response of skin at different ages with distinct mechanical stimulations.

Utilizing human skin as the research object, two groups of males (20-35 and 50-65 years old) were mechanically stimulated for two weeks through two devices with alternative principles. LPG massager (no rhythm): Each subject was massaged for 2 minutes twice a day. Wave stimulation (independently developed by our research group): The volunteers were subjected to stimulation for 10 minutes once a day. Furthermore, the elasticity of the skin tissue was assessed by dint of Underskin® technology. In addition, ultrasounds were employed so as to analyze the changes in the subcutaneous fascia and even the muscles. Besides, the microenvironmental blood flow in the assay area was monitored by Laser-Doppler.

After a week of mechanical cues, the shear modulus of the skin increased in both stimulations. Since the wave stimulation generates shear waves and compression waves inside the skin, compared with the traditional massage, the effect of this system on the superficial fascia is emphasized: the shear modulus at the superficial fascia registered a 160% growth in the juvenile after the stimulus and 58% in the elderly. The ultrasound images illustrate, from the dermis to the deep fascia, an extension on both the X-axis and Y-axis concerning the two types of stimulated skin of elder volunteers, whereas the juvenile skin was compressed in the Y-direction and extended in the X-direction. Indirect contact with the skin, the LPG resulted in a leap in blood flow in all individuals, with an even more significant increase in younger participants. However, the wave propagation stimulation generated by the air yields little effect on blood flow.

Wave stimulation is an innovative method that can achieve a massage effect, and assist wound healing, fascia therapy, and the development of anti-aging products.

Fast and non-invasive estimates of SPF and UVA-PF on human skin with simplified diffuse reflectance measurements based on a single UV-LED

C. Reble[1*], S. Schanzer[2], S. Jansen[2], J. Schleusener[2], G. Wiora[1], G. Khazaka[1], J. Lademann[2], M. C. Meinke[2],

[1]Courage + Khazaka electronic GmbH, Mattias-Brüggen-Straße 91, 50829 Cologne, Germany
*[2]Charité – Universitätsmedizin Berlin, Department of Dermatology, Venerology and Allergology, Charitéplatz 1, 10117 Berlin, Germany, *creble@courage-khazaka.de, https://courage-khazaka.de*

KEY WORDS: in vivo skin measurements, sun protection factor

Non-invasive methods for the determination of the SPF open new research possibilities, since volunteers no longer experience sunburn and results are available immediately after the measurement.

In this contribution, we report on diffuse reflectance measurements, which are carried out with a compact technology based on a single LED and integral detection with photodiodes[1]. By this approach, an estimation of SPF or UVA-PF values, depending on the wavelength and spectral distribution of the LED emission, can be achieved. Previously, it was shown that a demonstrator setup using a single UVB-LED (308 nm) produces a good correlation with SPF reference values[2]. The results suggested the usefulness of the method in application studies, where a fast and simple measurement of relative changes of SPF values is advantageous and the accuracy of absolute SPF values is less relevant. Recent applications of the device are the measurement of inhomogeneity of sunscreen distribution by hand versus an electrohydrodynamic spray applicator[3], sweat resistance of sunscreen products[4] and the effect of an additional film former on the sunscreen homogeneity and transmission[5]. In addition, further results show the usefulness of a handheld demonstrator with a single UVA-LED.

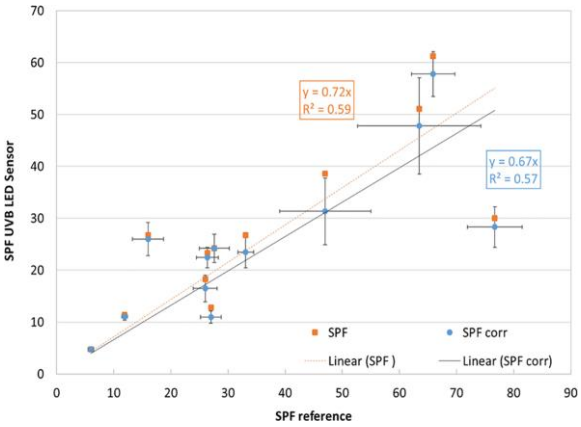

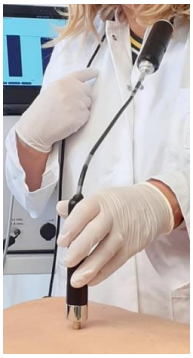

Fig. 1 : Left) Correlation of UVB-LED-based SPF estimate and SPF reference values[2]. Right) handheld demonstrator

Acknowledgements: The work is funded by the German Federal Ministry of Education and Research BMBF (FKZ 03ZZ0131D) within the program "Zwanzig20-Partnerschaft für Innovation", by Courage + Khazaka GmbH and carried out within the consortium "Advanced UV for Life".

[1] C. Reble, M. C. Meinke and J. Rass, "No more sun burn", Optic & Photonic, vol. 13, no. 1, pp. 32-35, (2018).
[2] S. Kobylinski et al, "Noninvasive measurement of the308 nm LED-based UVB protection factor of sunscreens. J. Biophotonics. 2021;14:e202000453.
[3] J. Schleusener et al., Electrohydrodynamic spray applicator for homogenous application and reduced overspray of sunscreen, Skin Res Technol 2021; 27:191-200.doi: 10.1111/srt.12924.
[4] A. Shahneh et al., "A new method for testing effective sunscreen products for skin cancer endangered professional groups", poster FOBI, (2020).
[5] V. H. P. Infante et al. "Influence of physical–mechanical properties on SPF in sunscreen formulations on ex vivo and in vivo skin", International Journal of Pharmaceutics 598 (2021) 120262.

Risk assessment of far-UVC-irradiation at 233 nm for eradication of microbes

J. Schleusener[1], P. Zwicker[2], L. Busch[1], S. B. Lohan[1], M. C. Meinke[1]

[1]*Center of Experimental and Applied Cutaneous Physiology, Department of Dermatology, Venerology and Allergology, Charité – Universitätsmedizin Berlin, Corporate Member of Freie Universität Berlin and Humboldt-Universität zu Berlin, Charitéplatz 1, 10117 Berlin, Germany.*
[2]*Institute of Hygiene and Environmental Medicine, University Medicine Greifswald, Ferdinand-Sauerbruch-Str., 17475 Greifswald, Germany.*
Corresponding Author: Johannes.schleusener@charite.de, https://ccp.charite.de/

KEY WORDS: Far-UVC LED irradiation, skin damage, CPD, 6-4PP

Using a newly developed 233 nm Far-UVC LED light source[1], the skin damage on excised human skin and reconstructed human epidermis models has been investigated at doses sufficient for the eradication of MRSA and MSSA[2]. At 40 mJ/cm², only minor superficial DNA damage occurred in skin models. While at 1/10 of a UVB MED for skin type III (3 mJ/cm²), which served as a positive control, >80% CPD damage occurred throughout the entire epidermis down to the basal cells (Fig. 1).

The superficial CPD damage disappeared after 24 h caused by enzymatic repair mechanisms. Further, after irradiating 4 times at this dose every 24 h, all CPD damage had disappeared.

After far-UVC irradiation with 40 mJ/cm², the radical formation was less than after exposition for 20 min with visible light at ≈100 mW/cm², which is <<1/4 of a UVA MED.

Our results suggest, that the exposition to far-UVC irradiation at 233 nm is harmless and causes negligible skin damage compared to positive controls, at doses that can be achieved by daily sunlight exposure. While several studies have shown similar results at 222 nm, with regard to the DNA damage, we show this behavior at 233 nm for the first time.

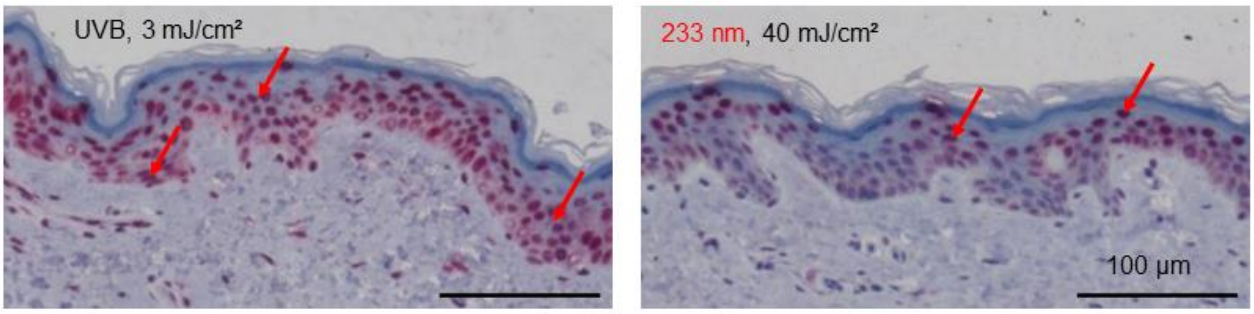

Fig. 2 : Images of histological analysis of DNA damage in excised human skin stained for CPD damage. Positive cells are stained in dark red. Human skin irradiated with 3 mJ/cm² UVB (left), which is 0.1 of a UVB MED for skin type III) showed >80% CPD damage throughout the whole epidermis. The CPD damage after 40 mJ/cm² irradiation at 233 nm (right) only occurred superficially in the epidermis. Scale bar: 100 µm.

This work was supported by the German Federal Ministry of Education and Research (BMBF) within the “Advanced UV for Life” project “VIMRE” under Grants 03ZZ0146A-D.

[1] Glaab, J., et al. (2021). "Skin tolerant inactivation of multiresistant pathogens using far-UVC LEDs." Scientific reports 11(1): 14647.
[2] Zwicker, P., et al. (2022). "Application of 233 nm far-UVC LEDs for eradication of MRSA and MSSA and risk assessment on skin models." Scientific reports 12(1): 2587.

From 20mhz ultrasound Scanning to focused ultrasound Treatment (HIFU) of dermatological Diseases: an innovative Danish Contribution to Dermatology developed in partnership with the Industry

Jørgen Serup
Bispebjerg University Hospital, Department of Dermatology, Copenhagen, Denmark
Joergen.vedelskov.serup@regionh.dk

KEY WORDS: 20 MHz HIFU, treatment, dermatology

Danish industry fostered together with the Technical University DTU a range of medical ultrasound devices sold worldwide. The 20MHz skin scanner produced by Cortex Technology, Hadsund pioneered by Jørgen Serup is today market leader for cross sectional imaging of the skin. TOOsonix, Hørsholm has developed a patented 20MHz high-intensity focused ultrasound (HIFU) device that is constructed to deliver high energy to a focal point inside the dermis at a predetermined level relevant for the condition to be treated. The thermal insult inside the skin is enough to kill cancer cells. Existing HIFU equipments used for skin rejuvenation works at lower frequency and target the subcutis exclusively because of low resolution at the dermis level. The treatment with the new 20MHz device is dosed guided by the inbuild dermoscope.
The device passed preclinical, animal and early clinical testing. It is CE-marked. The devise can be operated as an ablative method treating outer lesions and as a non-invasive device treating lesions that are hidden in the dermis without disturbing the outer skin thus with no wounding. This is superior in comparison with lasers. HIFU causes little pain only. The treatment was hitherto applied to actinic and seborrheic keratosis, basal cell carcinoma, Kaposi sarcoma, haemangioma, warts, xanthogranuloma, Fox-Fordyce disease, tattoo removal and other indications[1,2].
Ongoing two-centre studies on skin cancer (with Roskilde Hospital) and neurofibroma Recklinghausen (Sahlgrenska Sjukhuset, SE coordinated with the Wellman Institute and the Bloomberg Foundation, USA) are described.
Dermatology departments on all continents interested in this new method are invited for future projects on clinical application. The method can overcome some of the disadvantages of therapeutic lasers that work by penetrating thermal damage of very high temperature, associated with significant pain.

[1]Serup J. New Treatment of actinic keratosis, basal cell carcinoma, and Kaposi sarcoma Skin Research Technol 2020;26:824-831
[2]Serup J New ablative method for color-independent tattoo removal in 1-3 sessions. Skin Research Technol. 2020;26:839-850

Air pollution and the skin – two methods to measure the effect of air pollution in the skin

Tran PT[1], Tawornchat P[1], Beidoun B[1], Lohan SB[1], Sandig G[2], Meinke MC[1]

[1]Department of Dermatology, Venerology and Allergology, Charité – Universitätsmedizin Berlin, Corporate member of Freie Universität Berlin, Humboldt-Universität zu Berlin, and Berlin Institute of Health, Berlin, Germany, presenting author: phuong-thao.tran@charite.de; https://ccp.charite.de/
[2]Gematria Test Lab GmbH, Berlin

KEY WORDS: air pollution, electron paramagnetic resonance (EPR) spectroscopy, confocal Raman microscopy

The amount of air pollutants is increasing globally and causing serious health problems. It affects skin health and has been linked to the development of skin diseases. As one of the largest organs in our body, the skin is exposed to environmental stress everyday. This promotes the development of oxidative stress, which can lead to premature skin aging, skin barrier impairment and cellular damage caused by free radicals. To date, there is no established method for assessing the extent of pollution on skin or the protective effect of the substances used.

By the use of electron paramagnetic resonance (EPR) spectroscopy, a new method has been established which can assess the potential risk of air pollution in the skin and verify the effectiveness of products designed to protect the skin. Spin-labeled PCA (3-(carboxy)-2,2,5,5-tetramethyl-1-pyrrolidinyloxy) was used to study free radical formation in excised skin, with cigarette smoke as a model pollutant. In addition, the effect of combined smoke exposure and UVA radiation was investigated. A second method using confocal Raman microscopy has been established which allows a stress assessment without the use of an additional marker or external stressor. An increase of fluorescence intensity of the Raman bands can be an indicator for oxidative stress development. In this study, *ex vivo* and *in vivo* results will be presented.

A smoke chamber for *ex vivo* and *in vivo* studies was developed to expose skin to cigarette smoke under reproducible conditions. Initial studies have shown that cigarette smoke promotes the production of free radicals in the skin; a positive correlation between nicotine concentration and free radical production is given. These results will help to establish a new method for measuring the impact of pollutants and preventive measures.

Acknowledgments: The work is funded by European Regional Development Fund within the program “Pro FIT – Programm zur Förderung von Forschung, Innovationen und Technologien”

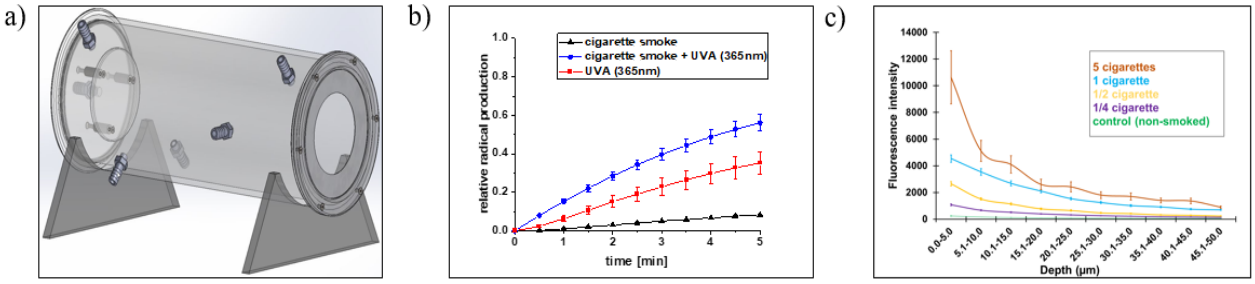

Figure: Assessment of the effect of cigarette smoke on excised porcine skin. a) To expose skin to cigarette smoke, a newly designed chamber was used for reproducible conditions. b) With Electron Paramagnetic Resonance Spectroscopy, radical production in skin was investigated after exposure to the smoke of five cigarettes. c) With confocal Raman microscopy, oxidative stress via fluorescence intensity in skin was analyzed.

Quantifying facial skin aging signs by deep learning-based algorithm

Fudi Wang[1], Yuhchi Lee[2], Zhiyang Li[2], Yonghao Luo[2], Jiani Wu[2], Sijia Wang[1]
1 CAS Key Laboratory of Computational Biology, Shanghai Institute of Nutrition and Health, Chinese Academy of Sciences
2 Eve Research & Innovation Center(ERIC), MeituEve, Inc, Xiamen, China
wangsijia@picb.ac.cn

KEY WORDS: facial skin aging, wrinkles, pigmented spots, deep learning

Facial skin aging signs, such as wrinkles and pigmented spots, have substantial individual variations, and require reliable quantification methods[1]. To solve the conventional object detection problems (e.g. unstable feature extraction and weak generalization ability), we decomposed the full-face into six sub-regions, and developed a two-step deep-learning network. We first performed multi-task learning of segmentation based on more than 25,000 labeled images. We then linearly fit the score of each sub-region with perceived age, an artificial skin aging label manually scored by dermatologists. Particularly, a novel melanoma detection solution[2] that won the ISIC Challenge was used for pigmented spots detection, while a MorphMLP architecture[3] was also proposed to capture local details and long-range information for wrinkle detection. To evaluate the performance of the algorithms, we collected facial images of 26 Chinese subjects aged between 22 and 49. Based on our deep learning-based algorithms, the wrinkle scores of various subregions were strongly correlated with age (PCC: 0.68-0.89). The overall wrinkle score also showed much stronger correlation with age than the score derived from other conventional algorithms (PCC_{Eve} =0.91 vs. PCC_{Visia}=0.54). The score of pigmented spots also showed the same pattern (PCC_{Eve}=0.31 vs. PCC_{Visia}=0.23). In conclusion, our deep learning-based algorithms could accurately quantify facial skin aging signs, and outperformed the conventional algorithms. It could be a useful instrument for skin aging related studies.

---

[1] Liu, Y., Gao, W., Koellmann, C., Le Clerc, S., Huls, A., Li, B., Peng, Q., Wu, S., Ding, A., Yang, Y., et al. (2019). Genome-wide scan identified genetic variants associated with skin aging in a Chinese female population. J Dermatol Sci 96, 42-49.

[2] C. Qian, T.L., H. Jiang, Z. Wang, P. Wang, M. Guan. (2018). A Detection and Segmentation Architecture for Skin Lesion Segmentation on Dermoscopy Images. In International Conference on Medical Image Computing and Computer. (Granada, Spain)

[3] KC.Li, YP.chen(2021) MorphMLP: A Self-Attention Free, MLP-Like Backbone for Image and Video. (arXiv:2111.12527)

Novel finger engineering technology to investigate the spatiotemporal sensitivity of human touch: TouchyFinger©

H. Zahouani, R. Vargiolu
Laboratory of Tribology and Dynamics of Systems. UMR CNRS 5513
University of Lyon. Ecole Centrale de Lyon France

KEY WORDS: Touch, Finger, Sensitivity, mechanoreceptors

In this work we present a multi-perspective view that encompasses both the perceptual and the motor aspects, as well as the response of skin mechano-receptors, to analyze and better understand the complex mechanisms underpinning the tactile representation of texture and motion. Such a better understanding of the spatiotemporal features of the tactile stimulus can reveal novel transdisciplinary applications in neuroscience and haptics.

The works that will be presented are based on the innovative "TouchyFinger" technology, figure (1). It is a connected and augmented technology, developed in our laboratory and patented. The device makes it possible to equip the human finger and measure the support force and the vibrations generated by friction during the movement of the finger. TouchyFinger is equipped with a vibration frequency analyzer and allows to identify the vibration level, the temporal frequencies and the wavelengths of the textures in each frequency band of the mechanoreceptors. The goal is to finely analyze the tactile feeling of textures by the mechanoreceptors of the human finger as well as the effect of the rigidity of the substrate on the spectral content. This technology responds to industrial and medical issues and makes it possible to generate useful databases for each application for the development of artificial intelligence. Illustrations of the tactile response of the human finger will be presented with an important contribution in understanding the mechano-biology and the effect of tribological stimulation on the mechano-transduction of touch.

Insert the text of your abstract here. The abstract including title, figure, references, etc. must not exceed one page. Use A4 paper format. Set all margins (left, right, top, and bottom) to 25 mm. The text should be written in a 12 pt Times New Roman font. Typeset the text in full justification.

References should be cited in "footnote fashion" using a superscript[1,2]. The references should be typed in a 10-point Times New Roman font in the format used below.

The inclusion of a figure that in graphical abstract style summarizes your contribution is encouraged.

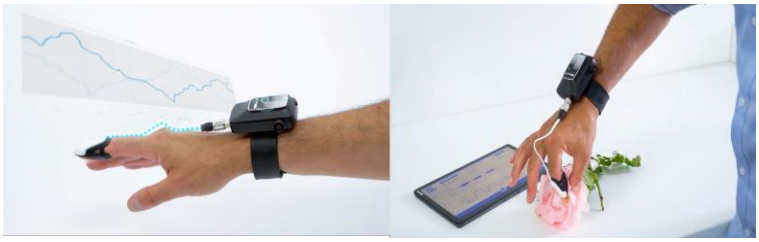

Figure.1 Touchy Finger Technology

Abstracts

Poster Presentations

In alphabetical order of the corresponding author

Kefir intake reduces the clinical severity in atopic dermatitis by improving epidermal "barrier"

E. Alves[1], J. Gregório[1], P. Rijo[1,2], C. Rosado[1], L. M. Rodrigues[1,*]

[1]CBIOS—Universidade Lusófona's Research Center for Biosciences & Health Technologies, Campo Grande 376, 1749-024 Lisboa, Portugal
[2]Instituto de Investigação do Medicamento (iMed.ULisboa), Faculdade de Farmácia, Universidade de Lisboa, 1649-003 Lisboa, Portugal

Corresponding Author e-mail address and URL: monteiro.rodrigues@ulusofona.pt

KEY WORDS: Skin health, atopic dermatitis, kefir

Skin barrier dysfunction correlates with clinical severity of atopic dermatitis (AD) and with immune dysregulation, are at the onset of AD[1]. Probiotics have shown beneficial effects on skin health, namely in the reduction of severity in AD[2]. Kefir is a traditional fermented food with numerous putative health benefits, attributed both to its unique microbial composition and the action of its metabolites, specially concerning lactic acid[3]. This study aimed to explore the effects of kefir ingestion on the skin of atopic individuals. The study was approved by the local ethics committee (CEECTS1/2018). All participants gave their informed consent. Participants (n=19), all clinically confirmed as atopic patients, were divided into two groups, the kefir group, which received and ingested 100 mL of kefir daily for 8 weeks, and the control group. Skin barrier function was assessed by measuring transepidermal water loss (TEWL) and stratum corneum hydration, while the degree of AD severity, was evaluated by the SCORing of Atopic Dermatitis index (SCORAD). Skin measurements were obtained in the volar forearm, before and after the intervention. Results have shown significant improvements of TEWL, hydration and SCORAD index in the kefir group ($p<0.001$, $p=0.001$, $p<0.001$ respectively) compared to control. The additional comparison of skin parameters, in the beginning and in the end of the intervention, has shown in the kefir group, showed a significant TEWL decrease ($p=0.008$) and hydration increase ($p=0.007$). No differences were observed in the control group for the same variables. This study suggests that the regular ingestion of kefir improves epidermal barrier and water balance in atopic skin patients, and mitigates AD clinical severity. To our knowledge, this was the first *in vivo* study design to provide evidence on the positive impact of kefir ingestion in atopic patients. Overall this work contributes to reinforce the interest on the beneficial effects of kefir on human skin.

[1] N. Stefanovic, A.D. Irvine, C. Flohr. Curr. Treat. Options Allergy, 8(2021)222-241.
[2] A. Makrgeorgou, J. Leonardi-Bee, F.J. Bath-Hextall, *et al*.. Cochrane Database Syst. Rev., 2018(2018)1-146.
[3] N.F. Azizi, M.R. Kumar, S.K. Yeap, *et al*.. Foods, 10(2021)1-26.

KEFIR INTAKE REDUCES THE CLINICAL SEVERITY IN ATOPIC DERMATITIS BY IMPROVING EPIDERMAL "BARRIER"

E. Alves[1], J. Gregório[1], P. Rijo[1,2], C. Rosado[1], L. M. Rodrigues[1,*]

[1]CBIOS—Universidade Lusófona's Research Center for Biosciences & Health Technologies, Campo Grande 376, 1749-024 Lisboa, Portugal
[2]Instituto de Investigação do Medicamento (iMed.ULisboa), Faculdade de Farmácia, Universidade de Lisboa, 1649- 003 Lisboa, Portugal
Corresponding Author e-mail address and URL: monteiro.rodrigues@ulusofona.pt

2022 ISBS Congress

INTRODUCTION

Skin barrier dysfunction correlates with clinical severity of atopic dermatitis (AD) and with immune dysregulation, are at the onset of AD[1].

Probiotics have shown beneficial effects on skin health, namely in the reduction of severity in AD[2].

Kefir is a traditional fermented food with numerous putative health benefits, attributed both to its unique microbial composition and the action of its metabolites, specially concerning lactic acid[3].

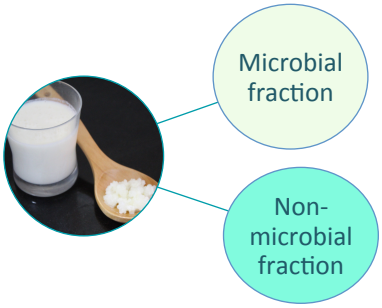

OBJECTIVE

This study aimed to explore the effects of kefir ingestion on the skin of atopic individuals.

MATERIALS & METHODS

The study was approved by the local ethics committee (CEECTS1/2018). All participants gave their informed consent.

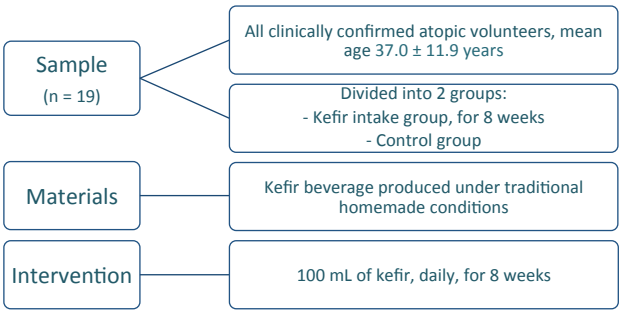

Skin measurements were obtained in the volar forearm, before and after the intervention.

RESULTS

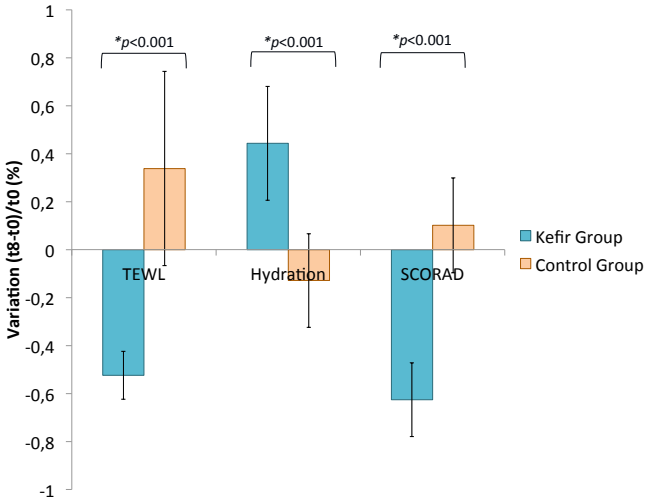

Figure 1 – Variation (%), between t0 and t8 of Transepidermal Water Loss (TEWL, g/m²/h) and hydration (AU) in the forearm and SCORAD Index (n=19, mean ± SD). Mann-Whitney test, significance level p<0.05.

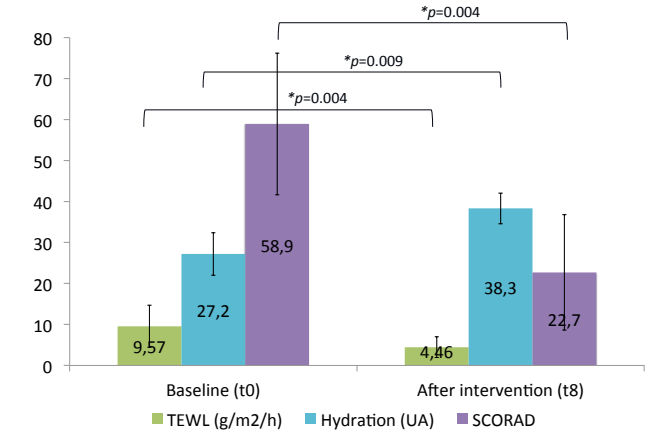

Figure 2 – Impact of kefir intake on Transepidermal Water Loss (TEWL, g/m²/h), hydration (AU) and SCORAD Index (n=9, mean ± SD). Wilcoxon test, significance level p<0.05.

CONCLUSION

This study suggests that the regular ingestion of kefir improves epidermal barrier and water balance in atopic skin patients, and mitigates AD clinical severity.

To our knowledge, this was the first *in vivo* study design to provide evidence on the positive impact of kefir ingestion in atopic patients. Overall this work contributes to reinforce the interest on the beneficial effects of kefir on human skin.

REFERENCES

[1] Stefanovic N., Irvine A.D. , Flohr C.. Curr. Treat. Options Allergy, 8(2021)222-241.
[2] Makrgeorgou A., Leonardi-Bee J., Bath-Hextall F.J., *et al*.. Cochrane Database Syst. Rev., 2018(2018)1-146.
[3] Azizi N.F., Kumar M.R., Yeap S.K., *et al*.. Foods, 10(2021)1-26.

Characterization of subcutaneous viscoelastic properties: application to dermatology

Ianis AMMAM[1], Amaury GUILLERMIN[1],Lucas Ouillon[1], Jean-Luc PERROT[2], Hassan ZAHOUANI[1].

[1] Univ Lyon, ENISE, LTDS, UMR 5513 CNRS, 58 rue Jean Parot, 42023 Saint-Etienne cedex 2, France.
[2] Dermatology Department, University Hospital of Saint-Etienne, Saint Etienne, France
Author email : ianis.ammam@ec-lyon.fr

KEY WORDS: Skin properties, viscoelastic properties, skin deformation

The skin is an envelope that covers the entire body. Today, understanding and studying its mechanical, biological or sensory properties is essential, particularly in dermatology or cosmetology. For example, in dermatology, the practitioner evaluates lesions by touch. Thus, the use of a device to assess the mechanical properties of the skin will help and complement the clinicians' diagnosis in an objective way. An extension device was developed to perform relaxation tests to mechanically characterize the cutaneous tissue. It was then coupled with imaging tools such as LC-OCT and ultrasound to understand the behavior in depth, layer by layer, during a relaxation test. The results of this study can be divided into two parts: the general behavior by studying the viscoelastic parameters and the superficial behavior by mapping the mechanical behavior in depth.

This work presents a method for studying the mechanical characteristic of the sublayer skin. First of all, the research on the general behavior, through the study of viscoelastic parameters, shows the influence of certain factors on the response. The relaxation test (n=12) show the strong skin anisotropy as well as its age and gender dependency. For example, we observed that the viscoelastic parameters were higher in the direction of the forearm Langer lines 45° than perpendicular to these lines 135° .This method could then be applied to other parameters such as the influence of a cosmetic product, the difference between healthy and pathological skin, etc. Furthermore, the combination of the extension system with LC-OCT and ultrasound allows us to understand the superficial behavior of the skin in depth during an extension. The analysis of the depth images confirm the non-homogeneity of the skin structure and the role of the fascia in the skin movement, by calculating the deformation layer by layer. In fact for a surface deformation, the depth deformation varies according to the skin layer.

Finally, this work provides the basis for a deeper understanding of the mechanical behavior of the skin in extension from surface to depth and the influence of certain factors.

Characterization of subcutaneous viscoelastic properties: application to dermatology

Laboratoire de Tribologie et Dynamique des Systèmes UMR 5513

I.Ammam, A.Guillermin, L.Ouillon, R.Vargiolu, J-L.Perrot, H.Zahouani

This study aims at developing an extension device to perform *in vivo* skin relaxation and/or extension tests. These results are divided into two parts: **the general behavior of the skin** through the investigation of the mechanical parameters and the **multi-layer mechanical behavior** through the coupling between the extension system and imaging tools.

Contexts and Objectives

- Understanding, studying, and characterizing the *in vivo* mechanical properties of the skin in order to objectify disciplines (Dermatology, Cosmetology, etc.) ;
- Characterizing and studying the viscoelastic parameters of the skin *in vivo* ;
- Investigating the multilayer behavior of the skin in extension by assessing the behavior of the skin in-depth ;
- Observing the skin's characteristics and, in particular, its anisotropy.

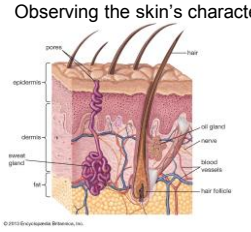

Skin Layer

Langer Lines [1]

Materials and Method

- Development of an *in vivo* skin extension system;
- ***Relaxation test*** : calculation of viscoelastic parameters from fits of relaxation curves → ***general behavior of the skin*** ;
- Extension test coupled with imaging test→ ***multi-layer mechanical behavior*** :
  - *LC-OCT : Superficial layers (Epidermis, superficial dermis);*
  - *Ultrasound: Deep layers (Deep dermis, Hypodermis, Fascia).*
- Calculation of the deformations layer by layer from a statistical approach, in which it allows the quantification of the deformations between 2 states: at rest and deformed rom images obtained through imaging devices. [*]

[*] Aüllo-Rasser, G., Dousset, E., Roffino, S. *et al.* Early-stage knee OA induced by MIA and MMT compared in the murine model via histological and topographical approaches. *Sci Rep* **10,** 15430 (2020). https://doi.org/10.1038/s41598-020-72350-7

Extension Device

Test Parameters

- $\epsilon_0 = 20\%$,
- speed = $1mm/s$,
- $l_0 = 20mm$
- 2 loading direction : Langer Lines, Orthogonal to the Langer Lines.

Results – General behavior

Viscoelastic parameters as a function of load direction and age (n=12)

Viscoelastic parameters						
Direction	45°			135°		
Parameters	$E_0\ (kPa)$	$E_1\ (kPa)$	η_1(Pa.s)	$E_0\ (kPa)$	$E_1\ (kPa)$	η_1(Pa.s)
Subject (n=12)	***654***	***1151***	***948***	***223***	***540***	***181***

Elastic moduli as a function of load direction (n=12)

Average elastic modulus [MPa]				
Direction	45°		135°	
Parameters	E1	E2	E1	E2
Subject (n=12)	***1,4***	***19.9***	***0.8***	***2,5***

- The parameters vary between 45° and 135°.
  - Influence of the direction of loading on the elastic and viscous character of the skin.

Results – Multilayer behavior

Multilayer ultrasound images of an extension test

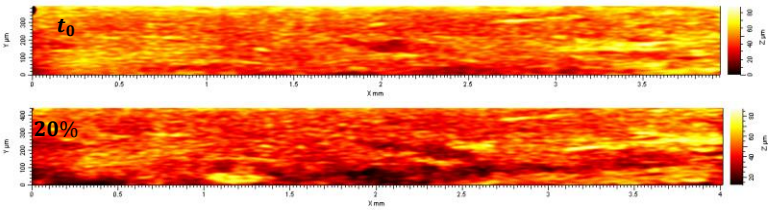

Layer by layer deformation table - 90° body axis

	Layers	ϵ_x	ϵ_y	ν
LC-OCT Extension	*Epidermis*	***0,22***	***-0,095***	***0,43***
	Superficial Dermis	***0,37***	***-0,15***	***0,41***
Ultrasound Extension	*Deep Dermis*	***0,193***	***-0,059***	***0,46***
	Hypodermis	***0,0948***	***-0,044***	***0,46***
	Fascia	***0,0618***	***-0,025***	***0,4***

Table of dermis déformations - anisotropy

Layers	*Langer Lines*		*Orthogonal to Langer Lines*	
Deformations	ϵ_x	ϵ_y	ϵ_x	ϵ_y
Dermis	***0,014***	***0,094***	***0,3***	***0,24***

Discussion

Study of the overall behavior of the skin

- A method was developed to understand and study the global behavior of the skin through its viscoelastic parameters *in vivo*;
- This pre-study illustrates the strong skin anisotropy, i.e., the great influence of the direction of loading on the viscous and elastic characteristics of the skin *in vivo*.

Study of the multilayer behavior of the skin

- A method was developed to understand and study the multilayered behavior of the skin by coupling: extension system and imaging tools (LC-OCT and ultrasound);
- In this pre-study, it was observed that the skin deforms from the surface to the depth during surface extension;
- These deformations are, nevertheless, heterogeneous according to the layers on the grounds of the structural differences between the different skin layers;
- The anisotropy of the skin is confirmed by calculating the deformations of the dermis in the two characteristic directions.

Conclusion

Conclusion

- The viscoelastic parameters of the skin *in vivo* are influenced by the direction of loading;
- The depth deformations display the multilayered and heterogeneous character of the skin in-depth;
- The anisotropy is confirmed by the deformation of the dermis in both characteristic directions.

[1] James C. Waldorf, Galen Perdikis, and Sarvam P. Terkonda. Planning incisions. Operative Techniques in General Surgery, 4(3) :199–206, September 2002

Cymbopogon citratus essential oil: Unraveling potential benefits on human skin

Sérgio Faloni de Andrade[1], Eucinário José Pinheiro[2], Catarina Pereira Leite[1], Maria do Céu Costa[1,2], Luis Monteiro Rodrigues[1]

[1]CBIOS - Research Center for Biosciences and Health Technologies, Universidade Lusófona de Humanidades e Tecnologias, Lisboa, Portugal.
[2] Mestrado em Produtos de Saúde e Suplementos Alimentares, Escola de Ciências e Tecnologias Saúde, Universidade Lusófona de Humanidades e Tecnologias, Lisboa, Portugal.
Corresponding Author e-mail address: sergio.andrade@ulusofona.pt

KEY WORDS: Essential oil; *Cymbopogon citratus*; lemongrass

Cymbopogon citratus (DC.) Stapf, commonly known as lemongrass, is an important aromatic medicinal plant cultivated in different regions of the world. Its essential oil is widely used for the production of fragrances, cosmetics, detergents, and pharmaceuticals. However, there is no clear evidence of the alleged effects of *C. citratus* (EOCC) on human skin. Thus, the aim of this study was to evaluate the effects of one formulation containing EOCC on skin's physiology in healthy volunteers. A Carboxymethyl cellulose (CMC) gel containing 5% EOCC (Cantinho das Aromaticas, Portugal) was prepared. Twelve healthy volunteers (4 men and 8 women) mean age 36.2 ± 16.3 years old were selected after informed written consent. All procedures were conducted respecting all principles of good clinical practice and approved by the institutional Ethics Committee (approval reference ECTS 04/13). Two areas (3cmx3cm) were drawn in forearm. In one area one formulation containing EOCC was applied with a spatula while in the other only gel (control) was applied. This procedure was repeated for 14 days twice/day (morning and night). In the beginning and by the end of the experiment, transepidermal water loss (Tewameter® CK electronics), hydration (Moisturemeter® DTec), and biomechanics skin (Cutiscan® CK electronics) parameters were measured. Images from High Resolution Sonography (HRS) were also taken at those sites with the Dermascan C (Cortex Tec). A methylnicotinate-provocation test was applied and followed with Laser Doppler Flowmetry (LDF, Perimed AB). A significant decrease in Transepidermal Water Loss (TEWL), as well as a significant increase in epidermal hydration, were observed at these areas treated with the formulation containing EOCC. An increase in firmness and elasticity was also noted. The HRS showed that epidermis is more echogenic after the application of formulation indicating that essential oil penetrates only the most superficial layers of the skin. Noteworthy, the site previously "protected" with the EOCC formulation revealed a reduced microinflammatory reaction following the methylnicotinate challenge. In conclusion, our results suggest that this formulation with EOCC is safe for topical application showing an interesting potential to be applied in skin care.

Acknowledgments: This work is funded by national funds through FCT - Foundation for Science and Technology, I.P., under the UIDB/04567/2020 and UIDP/ 04567/2020 projects.

---

1 Andrade, S. F., Rijo, P., Rocha, C., Zhu, L., & Rodrigues, L. M. (2021). https://doi.org/10.3390/cosmetics8020036
2 Ekpenyong, C. E., Akpan, E., & Nyoh, A. (2015). https://doi.org/10.1016/s1875-5364(15)30023-6
3 Majewska, E., Kozłowska, M., Gruczyńska-Sękowska, E., Kowalska, D., & Tarnowska, K. (2019). https://doi.org/10.31883/pjfns/113152

Cymbopogon citratus essential oil: Unraveling potential benefits on human skin

Sérgio Faloni de Andrade, Eucinário José Pinheiro, Catarina Pereira Leite, Maria do Céu Costa, Luis Monteiro Rodrigues

CBIOS - Research Center for Biosciences and Health Technologies, Universidade Lusófona Lisbon, Portugal

Corresponding Author e-mail address: sergio.andrade@ulusofona.pt

Introduction

Cymbopogon citratus (DC.) Stapf (Fig. 1), commonly known as lemongrass, is an important aromatic medicinal plant cultivated in different regions of the world. Its essential oil is widely used for the production of fragrances, cosmetics, detergents, and pharmaceuticals. However, there is no clear evidence of the alleged effects of C. citratus (EOCC) on human skin.

Fig. 1 - *Cymbopogon citratus* (DC) Stapf

Aim

The aim of this study was to evaluate the effects of a formulation containing EOCC on skin physiology in healthy volunteers.

Methods

- Gel containing 5% EOCC
- Negative Control

✓ 12 healthy volunteers (36.2±16.3 years old)

✓ All procedures were approved by the institutional Ethics' Committee.

Forearms

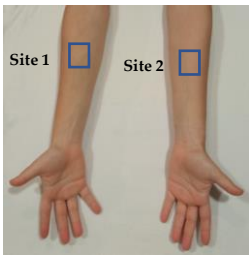

14 days/ 2 times per day

✓ Transepidermal Water Loss Meter (Tewameter TM300, CK electronics)

✓ Epidermal hydration (MoistureMeters (Delphin Technologies)

✓ Biomechanics properties (Cutiscan CS100 (CK electronics).

✓ Methyl Nicotinate Challenge (Laser Doppler Flowmetry , PeriFlux System 5000, Perimed, Sweden)

✓ Formulation Penetration (High Resolution Sonography-HRS, Dermascan C, Cortex Technology, Denmark)

✓ Variables measured before and after 14 days of treatment

Results

A significant decrease of Transepidermal Water Loss (TEWL), as well as a significant increase of epidermal hydration, were observed in the areas treated with the formulation containing EOCC compared with control (Table 1). A significant increase in firmness (V1) and elasticity (V3) was also noted (Table 2). The HRS showed that epidermis is more echogenic after the application of formulation indicating that essential oil penetrates only the most superficial layers of the skin (Fig. 2). Noteworthy, the site previously "protected" with the EOCC formulation revealed a reduced microinflammatory reaction following the methylnicotinate challenge (Fig. 3).

Table 1 - Effects of gel containing 3% *Cymbopogon citratus* (erva-príncipe) essential oil on TEWL and Hydration of the skin (treatment for 14 days)

	Site 1 (control)		Site 2 (Treated)	
	Before	After	Before	After
TEWL (g/m²/h)	5.22 ± 0.46	5.82 ± 0.48	5.69 ± 0.44	4.38 ± 0.38*
Hydration SC (A.U.)	29.48 ± 1.61	29.22 ± 2.73	28.99 ± 1.23	35.34 ± 2.25*
Hydration D (A.U.)	27.04 ± 2.63	29.16 ± 1.22	26.71 ± 1.82	35.18 ± 1.54**

*p < 0.05; **p < 0.01

Table 2 - Effects of gel containing 3% *Cymbopogon citratus* (erva-príncipe) essential oil on the Biomechanical parameters of the skin (treatment for 14 days)

	Site 1 (control)		Site 2 (Treated)	
Biomechanical parameters	Before	After	Before	After
V1 (firmness)	59.16 ± 6.18	61.18 ± 9.43	67.46 ± 6.92	44.81 ± 3.97*
V2 (viscoelasticity)	12.34 ± 2.96	7.85 ± 2.36	13.24 ± 3.76	15.29 ± 2.90
V3 (elasticity)	21.77 ± 6.31	18.44 ± 5.34	17.95 ± 4.10	39.25 ± 7.04*

*p < 0.05

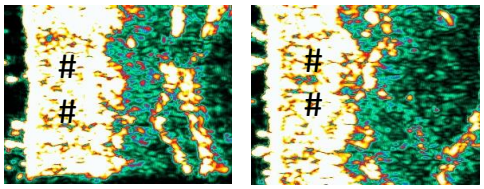

Treated group Control group

Fig. 4 – Illustrative Ultrasound image showing increase in epidermis echogenicity area (Shining area) after the application of essential oil formulation. ## Epidermis.

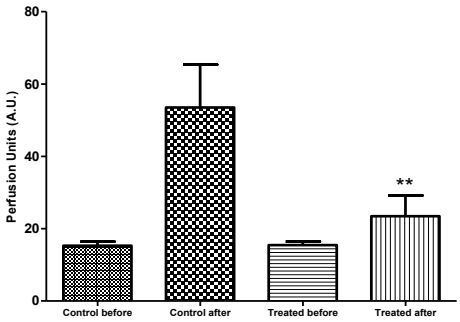

Fig. 2 - Perfusion on site control and treated after Methyl Nicotinate 0.5% stimulus (14 days of the treatment). **p < 0.05 compared with site 1 after

Conclusions

In conclusion, our results suggest that this formulation with EOCC is safe for topical application, and it could improve and protect the skin, showing an interesting potential to be applied in skincare.

Acknowledgments: This work is funded by national funds through FCT - Foundation for Science and Technology, Portugal, under the UIDB/04567/2020 and UIDP/04567/2020 projects.

Influence of the organization of the dermal fiber network on the mechanical properties of the human skin and its anisotropy *in vivo*

M. Ayadh[1,2], A. Guillermin[1], M-A. Abellan[1], M. Pedrazzani[3], E. Cohen[3], A. Bigouret[2], H. Zahouani[1]

1. Université de Lyon, ECL-ENISE, LTDS, 36, avenue Guy de Collongue, 69134 Ecully, France.
2. Laboratoires Clarins, 5 Rue Ampère, 95300 Pontoise, France
3. DAMAE MEDICAL, 14 Rue Sthrau, 75013 Paris, France
Corresponding Author e-mail address and URL: ayadhmeriem@gmail.com

KEY WORDS: *in vivo* test, anisotropy, LC-OCT imaging

Knowing the evolution of the mechanical properties of the skin and understanding the origin of these properties is very important in medicine, surgery, and cosmetics. Studies performed *in vitro* and *ex vivo* show that links exist between the mechanical properties of the skin and the collagen and elastin fibers network in the dermis[1,2].

In this study we propose a combination of two innovative experimental tests performed *in vivo* on the skin of the forearm and the thigh to show the influence of the organization of the dermal fiber network on the mechanical properties of the human skin and its anisotropy. The first method consists in non-contact impact tests using a device able to apply an air pressure onto the outer surface of the skin. It generates Rayleigh waves that spread in the skin. The speed of this wave is measured in 7 directions and values of the Young's moduli are deduced. The second method uses Line-field Confocal Optical Coherence Tomography (LC-OCT)[3] which allows to take images of human skin *in vivo* with very high spatial resolution. This technology allows two types of images: vertical section images and horizontal images. Thanks to these two modalities, it is possible to obtain the full 3D image of the volume of the skin. From these images we extract the densities of fibers and their orientation in the plan parallel to the surface of the skin. The study is carried out on 42 volunteers aged from 20 to 55 years old. The results show a correlation between the mechanical properties of the skin at the surface and the structure in depth of its layers in the volume ($0.31 < r_{(Spearman)} < 0.41$). We could observe that the Young's modulus of the skin in one direction depends on the density of the fibers in this same direction. The greater the fiber density, the higher the Young's modulus.

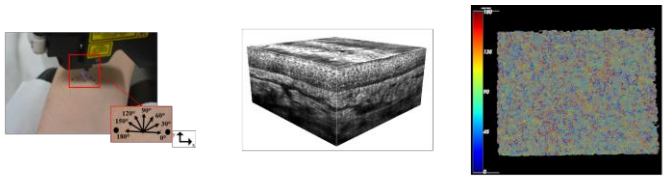

Figure 1: Non-contact impact test and LC-OCT images of skin

[1] M. Gasior-Głogowska et al., "FT-Raman spectroscopic study of human skin subjected to uniaxial stress," J. Mech. Behav. Biomed. Mater., vol. 18, pp. 240–252, 2013.

[2] A. Delalleau, G. Josse, J. M. Lagarde, and P. F. Dermo-cosmétiques, "Un modèle hyperélastique à réorientation de fibres pour l ' analyse des caractéristiques mécaniques de la peau," https://www.researchgate.net/publication/266492847, no. December 2014, 2014.

[3] J. Ogien, O. Levecq, H. Azimani, and A. Dubois, "Dual-mode line-field confocal optical coherence tomography for ultrahigh-resolution vertical and horizontal section imaging of human skin in vivo," *Biomed. Opt. Express*, vol. 11, no. 3, pp. 1327–1335, 2020.

Influence of the organization of the dermal fiber network on the mechanical properties of the human skin and its anisotropy *in vivo*

LTDS Laboratoire de Tribologie et Dynamique des Systèmes

Laboratoire de Tribologie et Dynamique des Systèmes
UMR 5513

GROUPE CLARINS

M. Ayadh. A. Guillermin. M-A. Abellan. M. Pedrazzani. E. Cohen. A. Bigouret. H. Zahouani

INTRODUCTION

Knowing the evolution of the mechanical properties of the skin and understanding the origin of these properties are very important in medicine, surgery and cosmetics. In this study we propose a combination of two innovative experimental tests: non-contact impact test and LC-OCT imaging performed *in vivo* on the skin of the forearm and the thigh to show the influence of the organization of the dermal fiber network on the mechanical properties of the human skin and its anisotropy. We thus compare the distribution of the Young's modulus of the skin to the orientation of the dermal fibers.

MATERIAL & METHODS

Panel and Test zone

Gender	Group	Age	Number	Body areas
Women	Young	[20 – 30] years old	21	Forearm - Thigh 12 cm above the wrist for the forearm, 12 cm above the knee for the thigh
	Elderly	[45 – 55] years old	21	

Non-contact impact test

Non-contact impact indentor applies an air pressure (P = 2 bar, t = 10 ms) onto the outer skin surface. The test is performed in 7 directions from 0 ° to 180 ° with a step of 30 ° . It generates Rayleigh waves that spread in the skin. The displacement of the skin is measured using a laser profilometer (800 sensors, l = 7 mm, 405 nm).

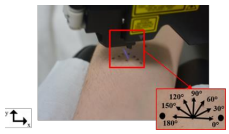

Forearm

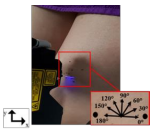

Thigh

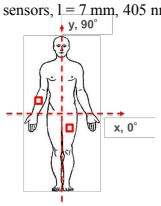

Data extraction

The Young's modulus (E) is calculated for the 7 measured speeds V using the relation below:

$$V = \frac{0.87 + 1.12\nu}{1+\nu}\sqrt{\frac{E}{2\rho(1+\nu)}}$$

ρ = 1000 kg/m³ the density
ν = 0.45 the Poisson's ratio

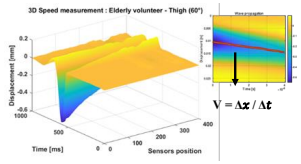

Example of 3D speed measurement at the outer surface of the skin *in vivo*

Line-field Confocal Optical Coherence Tomography imaging (LC-OCT)

LC-OCT provides 3D imaging modality, allowing to switch from a histology-like vertical mode to a confocal-like horizontal mode, and to record a 3D stack of tissue volumes.

Maximal resolution	Axial / Lateral< 1.3 µm
Penetration depth	> 400 µm
Laser wavelength	600-900 nm
Resolution	5 µm
3D stack size	1.2 × 0.5 × 0.5 mm

LC-OCT by DAMAE Medical

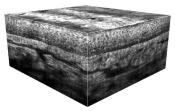

Stack of 3D LC-OCT images

Data extraction

The densities of the skin fibers are extracted from LC-OCT images by segmentation according to 9 intervals of directions ranging from 0 ° to 180 ° with a step of 20 °.

Original LC-OCT image of the papillary dermal layer of the skin *in vivo*

Segmented fibers

RESULTS

3D speed measurements and LC-OCT images

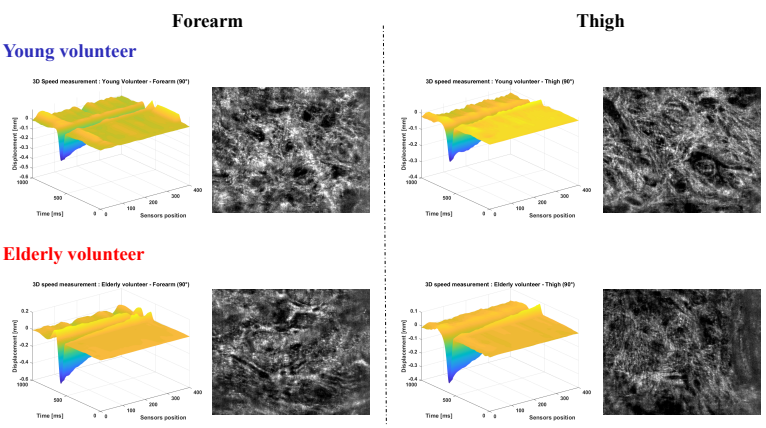

- Young skin is deformed more than aged skin when stressed by air pressure.
- Fiber density in young skin is greater than in aged skin.

Distribution of Young's modulus and skin fibers

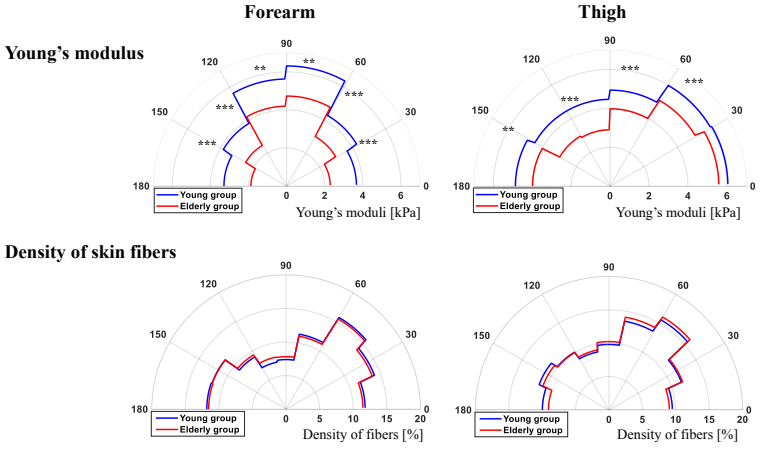

DISCUSSION & CONCLUSION

Age group	Zone	Directions of maximum Young's modulus	Directions of maximum density of skin fibers
Young	Forearm	[60 ° - 90 °] (E = 6.79 kPa ± 1.54 kPa)	[40 ° - 60 °] (d = 15.76 % ± 1.85 %)
	Thigh	[0 ° - 60 °] (E = 6.41 kPa ± 1.54 kPa)	[40 ° - 60 °] (d = 15.57 % ± 1.82 %)
Elderly	Forearm	[60 ° - 90 °] (E = 5.08 kPa ± 2.12 kPa)	[40 ° - 60 °] (d = 15.50 % ± 2.50 %)
	Thigh	[0 ° - 60 °] (E = 5.47 kPa ± 2.03 kPa)	[40 ° - 60 °] (d = 16.06 % ± 2.65 %)

Statistical analysis (ANOVA) show that the mechanical properties decrease significantly with age while no significant difference is observed for fiber densities.
For a group, the distributions of Young's modulus and skin fibers are significantly different between the forearm and the thigh.
For a group, we could observe a correlation between the distributions of Young's modulus and skin fibers for the same body area ($0.31 < r_{(Spearman)} < 0.41$). This correlation shows the link existing between the mechanical properties of the skin at the surface and the structure in depth of its layers in the volume.

The Young's modulus of the skin *in vivo* in one direction depends on the density of the dermal fiber network in this same direction.
The greater the fiber density, the higher the value of the Young's modulus.

ÉCOLE DOCTORALE SIS SCIENCES INGÉNIERIE SANTÉ UNIVERSITÉ DE LYON
cnrs
ÉCOLE CENTRALE LYON
CENTRALELYON ENISE
ENTPE
UNIVERSITÉ DE LYON

Contact-free Viscoelastography of skin and applications

A. Bergheau[1], R. Vargiolu[1], Jean-Luc Perrot[1], H. Zahouani[1]

University of Lyon - Ecole Centrale de Lyon - Laboratory of Tribology and System Dynamics (LTDS) - UMR 5513 CNRS, ECL-ENISE, 36 avenue Guy de Collongue, 69134, ECULLY
Corresponding Author e-mail address and URL: alexandre.bergheau@ec-lyon.fr

KEY WORDS: Skin Sublayers, Viscoelastography, Surface Waves

In the medical examination field, palpation is one of the exploration techniques of the human body and is part of the in-vivo diagnostic method. However, physical asperities are challenging to palpate, in which additional, quantifiable measurements are beyond necessary to gain an utter understanding of these. Indeed, many pathologies involve tissue structural changes resulting in modifying their mechanical properties. Numerous technologies came to light to assess these structural changes – e.g., elastography – yet they are primarily designed for profound tissue. So, they are unlikely to measure mechanical responses of the skin's outermost layers. A gap must be filled, and a specific device designed to analyze the mechanical properties of the thinnest layers of skin must heave into sight.

Following up on last year's UNDERSKIN®[1] introduction, novel investigations shed light on an inversion model utilizing the uttermost skin layer – Stratum Corneum – and viscoelastic parameters. Indeed, serendipitous characteristics lie in that layer, in which the removal of it, by dint of the tape stripping technique, yields astonishing outcomes. Moreover, not only was UNDERSKIN® capable of analyzing skin's elasticity, previously considered as a purely elastic material, but it now assesses it by taking heed of its viscosity. Besides, the viscoelastic model validation on phantoms came beforehand, for which the determination of their viscoelastic properties was analyzed via DMA testing. Therefore, including these improvements into experimental assessments representations, such as a map, and anisotropic plot, prove UNDERSKIN® to be earmarked as an excellent assistance device to gain objective knowledge of skin mechanical behavior such as cosmetic effects, tumoral skin, and skin aging.

[1] Patent filed in November 2020 with PULSALYS

UNDERSKIN®
Contact-free viscoelastography of skin and applications

Laboratoire de Tribologie et Dynamique des Systèmes
UMR 5513

A. Bergheau, R. Vargiolu, J-L Perrot, H. Zahouani

AWAKENED INTEREST

Assessing skin mechanical properties is of utmost importance on the grounds of the multiple applications in dermatology and cosmetology. Numerous technologies came to light to assess the mechanical structural changes – e.g., elastography – yet they are primarily designed for profound tissue. Therefore, a specific device designed to analyze the mechanical responses of the thinnest layers of skin must be developed. It will not only examine tumoral skin, but also determine the immediate and over-time viscoelastic effect of a cosmetic.

NOVEL TECHNOLOGY

DEVICE

- **Contact-free methodology**: Blast of air indenter
- **Surface wave propagation tracking**: Laser optical displacement sensor
- **Multi-jointed robotic arm**: To attain any human body zone

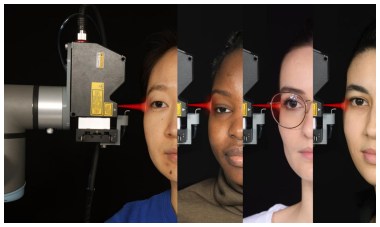

SIGNAL PROCESSING

- **Modal identification**
- **Dispersion curve computations:** $V_{shear}(f)$
- **Attenuation value computations**: $\beta_{shear}(f)$
- **Inversion model**: $\omega \rightarrow \lambda \rightarrow$ depth
- **Mechanical properties vs penetration depth:**
  - $V_{shear}(depth)$
  - $G'(depth)$
  - $G''(depth) \rightarrow \eta(depth)$

Figure 1: UNDERSKIN® device

Recorded Wave-field

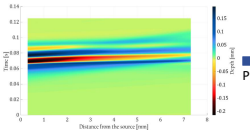

Figure 2: Recorded wave-field

Signal Processing

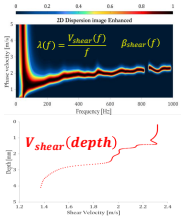

Figure 3: Dispersion image & Velocity profile

Viscoelastic model

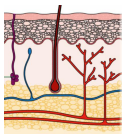

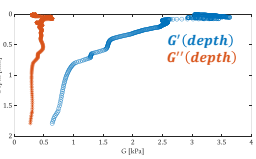

Figure 4: Storage and Loss Modulus vs Depth

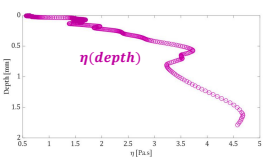

Figure 5: Viscosity vs Depth

ANISOTROPIC ASSESSMENT

- Owing to the **rotary table** of the multi-jointed robotic arm, the anisotropy of the mechanical properties can be assessed

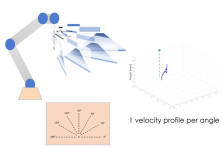

Figure 6: Anisotropic assessment method

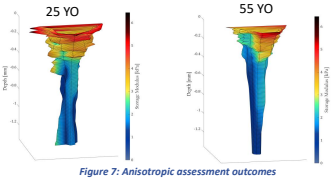

Figure 7: Anisotropic assessment outcomes

APPLICATIONS

DERMATOLOGY

- **Self-developed mapping algorithm**
- Storage modulus and Viscosity **gradient images**

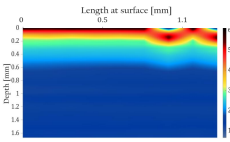

Figure 8: Healthy skin Storage Modulus

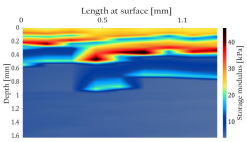

Figure 9: BCC Storage Modulus

- **Locate the firmness/softness** of skin tumors
- **Quantifiable data**

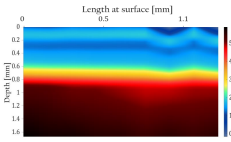

Figure 10: Healthy skin Viscosity

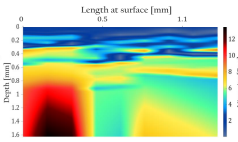

Figure 11: BCC Viscosity

COSMETOLOGY

SUBCUTANEOUS KINETIC TRACKING OF A COSMETIC

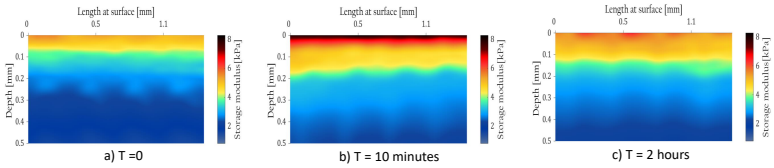

Figure 12: a) Storage Modulus before application, b) Storage Modulus 10 minutes after application , c) Storage Modulus 2 hours after application

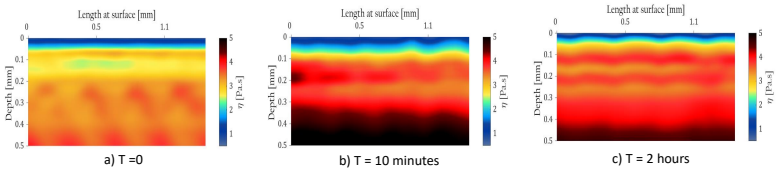

Figure 13: a) Viscosity before application, b) Viscosity 10 minutes after application , c) Viscosity 2 hours after application

- Being capable of measuring the **immediate effects** of a cosmetic product
- To evaluate the **over-time effects** of it
- To **locate/track** its effect

CONCLUSION

- **Comprehending the aging effect** in the skin's layers. **Cosmetic effect follow-up** in the subcutaneous layers.
- **Novel insights** conveyed to the dermatologist. Not only did the outcomes confirm diagnosis while employing human palpation, but the dermatologist is now able to **quantify** them and inform where the **firmness** or **softness** stems from.
- **To nourish AI algorithms** to create a database so that it will stand the practitioner in good stead for forthcoming diagnosis, prognosis, treatment, surgery, and teledermatology. A new way to enhance the digital palpation world.

Line-Field Confocal Optical Coherence Tomography compared with Confocal Laser Scanning Microscopy: a pilot study on three different age groups

Gaëtan Boyer[1], Clarence de Belilovsky[1], Pedro Pinto[2], Anaïs Barut[3], Mélanie Pedrazzani[3], Clara Tavernier[3], Gaëlle Bellemère[1], Caroline Baudouin[1]

1 Laboratoires Expanscience, Innovation R&D Direction, rue des Quatre Filles, 28233 EPERNON, FRANCE
2 PhDTrials, Av. Maria Helena Vieira da Silva, LISBOA, PORTUGAL
3 DAMAE, DAMAE Medical, 14 rue Sthrau, 75013 PARIS, France
gboyer@expanscience.com

KEY WORDS: LC-OCT, CLSM, epidermis

The aim of this work was to evaluate the performances of the recently developed in vivo imaging device Line-Field Confocal Optical Coherence Tomography (LC-OCT, DAMAE Medical, which has a better resolution that classical OCT) compared to the Confocal Laser Scanning Microscopy (CLSM, Vivascope 1500, Mavig) from a qualitative point of view and assessment of the epidermal thickness according to age.

We conducted a mono-centric open-label study. A total of 17 subjects divided into three groups (3–6 months, 5–7 years and 20–25 years) were recruited. Acquisitions have been performed on volar forearm. CLSM allows horizontal plane visualization. LC-OCT allows horizontal, vertical, and three-dimensional visualization with a better resolution in the vertical axis, a wider field of view and a faster image acquisition compared to CLSM. Full epidermis thickness was calculated as the mean value between the surface and the dermo-epidermal junction on a vertical reconstruction for CLSM and on a vertical acquisition for LC-OCT.

Acquisitions with both devices allow a visualization of the epidermis at cellular level. Results obtained with both devices give a slight decrease of full epidermis thickness according to age. This result is in accordance with a previous study using classical OCT but differs from those obtained using CLSM without reconstruction of the vertical plane of the epidermis.

This pilot study demonstrated the ability of both devices for the in vivo skin imaging on different age groups and their coherence. LC-OCT offers a new way for skin analysis and specially for pediatric applications. Larger studies are required to further interpret the discrepancies on epidermis thickness variation described by previous works.

Line-Field Confocal Optical Coherence Tomography compared with Confocal Laser Scanning Microscopy: a pilot study on three different age groups

Gaëtan Boyer[1], Clarence de Belilovsky[1], Pedro Pinto[2], Anaïs Barut[3], Mélanie Pedrazzani[3], Clara Tavernier[3], Gaëlle Bellemère[1], Caroline Baudouin[1]

1 - Laboratoires Expanscience, Innovation R&D Direction, rue des Quatre Filles, 28233 EPERNON, FRANCE
2 - PhDTrials, Av. Maria Helena Vieira da Silva, LISBOA, PORTUGAL
3 - DAMAE, DAMAE Medical, 14 rue Sthrau, 75013 PARIS, FRANCE

· Introduction ·

In vivo imaging of the skin in real time and non-invasively is of great interest for medical and cosmetic applications. Recently, improvement of Optical Coherence Tomography (OCT) has resulted to Line-Field Confocal Optical Coherence Tomography (LC-OCT) technique which has features comparable to well-known Confocal Laser Scanning Microscopy (CLSM) in terms of depth penetration in skin and resolution. The aim of this work was to compare side by side the performances of the recently developed *in vivo* imaging device LC-OCT (DAMAE Medical) compared to CLSM (Vivascope 1500, Mavig) from a qualitative point of view and for the assessment of the epidermal thickness according to age.

· Materials and Methods ·

We conducted a mono-centric open-label study. No product was applied. A total of 17 subjects divided into three groups (3–6 months, 5–7 years and 20–25 years) were recruited. Group characteristics are in table 1. Atopic skin subjects were excluded. Informed written consents were obtained from subject or legal representatives and the study was conducted in accordance with the principles of the Declaration of Helsinki following Good Clinical Practice. Measurements were performed on volar forearm in a fully controlled room and after an initial acclimatization process of at least 15 minutes.

CLSM (Vivascope 1500, Mavig) and LC-OCT (DAMAE Medical) acquisitions have been performed. CLSM allows "en-face" (horizontal plane) visualization with a field of view of 0.5 mm (x) x 0.5 mm (y) x 0.2 mm (z), a step in z direction of 1.52 µm and resolution of 1.25 µm (x) x 1.25 µm (y) x 5.0 µm (z). LC-OCT allows "en-face" (horizontal plane) but also "en-coupe" (vertical plane) visualization and three-dimensional imaging with a better resolution in the vertical axis and a wider field of view: 1.2 mm (x) x 0.5 mm (y) x 0.4 mm (z), step in z direction of 1 µm and resolution of 1.3 µm (x) x 1.3 µm (y) x 1.1 µm (z).

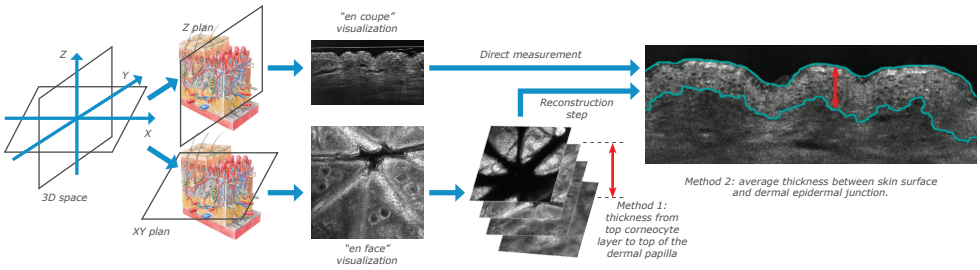

Figure 1: Illustration of "en-coupe" and "en-face" visualization with epidermis thickness measurement method associated. LC-OCT allows both "en-coupe" and "en-face" acquisitions. CLSM allows "en-face" visualization, requiring reconstruction step for method 2 application.

Group	N subjects	Mean age ± s.d. [min max]
3-6 months	5	4.0±0.8 [3-5] months
5-7 years	5	6.4±0.9 [5-7] years
20-25 years	7	22.1±2.0 [20-25] years

Table 1: Group characteristics.

Comparison of devices was performed from a qualitative point of view on acquisitions, and epidermis thickness was determined as the mean value between the surface and dermal epidermal junction on a vertical reconstruction for CLSM and vertical acquisition for LC-OCT. Figure 1 illustrates the "en-coupe" and "en-face" visualizations, and the 2 methods for thickness measurement depending on the approach.

· Results ·

Quality of acquisitions with both devices allows the visualization of the epidermis with a resolution at cellular level as illustrated figure 2 a) and 2 b) and also the visualization of the fibrillar dermis structure below the Dermal Epidermal Junction as illustrated figure 2 c) and 2 d) for each age group. LC-OCT advantages are the possibility to combine "en-face" (horizontal plane) but also "en-coupe" (vertical plane) acquisitions which allows to measure thickness as illustrated figure 1. Application of the same method with CLSM necessitates to reconstruct a vertical image from horizontal acquisitions stack.

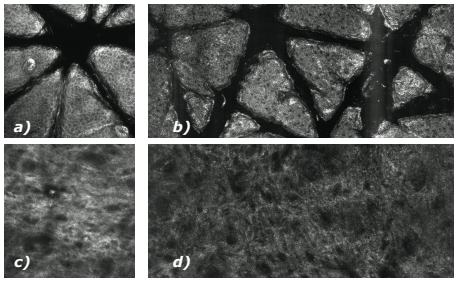

Figure 2: a) CLSM and b) LC-OCT acquisitions at the epidermis level allowing visualization of corneocytes. c) CLSM and d) LC-OCT acquisitions below the Dermal Epidermal Junction allowing visualization of the fibrillar dermis network.

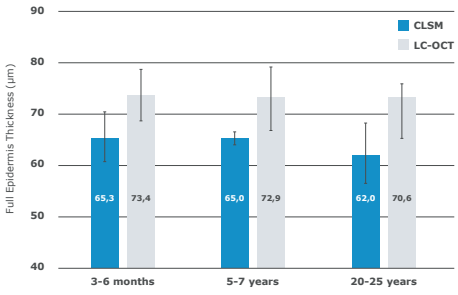

Figure 3: full epidermis thickness for each group measured on CLSM and LC-OCT acquisitions.

Epidermis thickness results obtained with both devices processed with the same method (measurement of mean value between the surface and dermal-epidermal junction on vertical reconstruction for CLSM and on vertical acquisition for LC-OCT) give a slight decrease of full epidermis thickness according to age as illustrated figure 3. This result is in accordance with a previous study using classical OCT[1] but differs from those obtained using CLSM without reconstruction of the vertical plane of the epidermis[2,3] (depth measured from the top corneocyte layer to the top of the dermal papilla). Slight offset between CLSM and LC-OCT results is observed.

· Conclusion ·

This pilot study demonstrated the ability of both devices for the in vivo skin imaging on different age groups and their coherence. LC-OCT offers a new approach for skin analysis and specially for pediatric applications. Larger studies are required to further interpret the discrepancies on epidermis thickness variation described by previous works. Recent work[4] shown that LC-OCT can assess several parameters on 3D acquisitions for example Dermal Epidermal Junction undulation. Considering a volume instead of a vertical section can certainly improve knowledge of skin morphology variation with age.

References: 1. Mogensen M. et al. Morphology and Epidermal Thickness of Normal Skin Imaged by Optical Coherence Tomography. Dermatology 2008;217(1):14-20.
2. Stamatas G N et al. Infant skin microstructure assessed in vivo differs from adult skin in organization and at the cellular level. Pediatr Dermatol. Mar-Apr 2010;27(2):125-31.
3. Fluhr J.W. Et am. Age-dependent transformation of skin biomechanical properties and micromorphology during infancy and childhood. J Invest Dermatol. 2019 Feb;139(2):464-466.
4. Chauvel-Picard J. et al. Line-field confocal optical coherence tomography as a tool for three-dimensional in vivo quantification of healthy epidermis: A pilot study. J Biophotonics. 2022 Feb;15(2):e202100236.

Assessment of a new transformative texture massage product in a pediatric population: effect on child, parent and child-parent interaction

Gaëtan Boyer[1], Clarence de Belilovsky[1], Pedro Pinto[2], Gaëlle Bellemère[1], Caroline Baudouin[1]

1 Laboratoires Expanscience, Innovation R&D Direction, rue des Quatre Filles, 28233 EPERNON, FRANCE
2 PhDTrials, Av. Maria Helena Vieira da Silva, LISBOA, PORTUGAL
gboyer@expanscience.com

KEY WORDS: massage, emotion, well-being

Massage is used for several centuries with well-known therapeutic benefits. Positive effects of massage on pediatric population are well documented for example on sleep disturbances, parent-child interaction and parental stress[1]. The aim of this work was to evaluate the effects of massage in a pediatric population using a new transformative texture product: study on the child, the parent and the parent-child interactions.

We conducted a mono-centric open-label study under dermatological and pediatric controls. 75 subjects were recruited aged from 7 days to 24 months. Massage has been performed daily by parents during 21 days at home after toilet and before sleep with a new transformative texture "gel to oil" massage balm. No instructions for the massage method were given. Tolerance evaluation was performed. Assessments of the effects of the massage just after the first application (performed on the study site), after 7 days (telephone questionnaire) and after 21 days have been performed using clinical scoring (redness, dryness, roughness and suppleness) and questionnaires related to the efficacy and cosmetic qualities of the product, the child well-being and sleep, the parent-child interaction and the mood and stress of the parent. Video recording of the parent face has been performed during the first massage and percentages of time of Joy and Disgust emotions detected using an artificial intelligence algorithm based on deep learning have been calculated.

Tolerance of the massage product was very good. Improvement of redness, dryness roughness and suppleness were observed immediately after the first application and after 21 days. After 21 days, parents perceived effects on moisturizing and nourishing of the child skin. The transformative texture was well appreciated for the massage and considered as a sensorial texture. Effect of the massage with the product on the child well-being has been positively perceived immediately and after 21 days. Improvement of the time for getting asleep has been observed. Parents perceived an improvement of the interaction, the complicity and the emotional bonds with their child. Effects on parent's mood and stress were also observed. During the first massage, Joy emotion was identified during 35.3±21.6% of the massage time and Disgust emotion during only 4.8±5.4%.

This study demonstrated that a "real-life" massage without any specific instructions has positive effects on the child well-being, the parent mind and the parent-child interaction. The transformative texture of the product was well perceived for the massage and the product improved child skin. Emotions assessment method used gave convincing results for a massage application.

[1] T. Field. Pediatric Massage Therapy Research: A Narrative Review. Children 2019, 6, 78

Assessment of a new transformative texture massage product in a pediatric population: effect on child, parent and child-parent interaction

Gaëtan Boyer[1*], Clarence de Belilovsky[1], Pedro Pinto[2], Gaëlle Bellemère[1], Caroline Baudouin[1]

1- Laboratoires Expanscience, Innovation R&D Direction, rue des Quatre Filles, 28233 Epernon, France
2- PhDTrials, Av. Maria Helena Vieira da Silva, Lisboa, Portugal
*gboyer@expanscience.com

· Introduction ·

Massage is used for several centuries with well-known therapeutic benefits and other positive impacts as relaxing effect, social interaction and well-being improvement[1]. Positive effects of massage on pediatric population are well documented for example on sleep disturbances, parent-child interaction and parental stress[2]. The aim of this work was to evaluate the effects of massage in a pediatric population using a new transformative texture product: study on the child, the parent and the parent-child interactions.

· Materials and Methods ·

We conducted a mono-centric open-label study under dermatological and pediatric controls. 75 subjects were recruited aged from 7 days to 24 months. Massage has been performed daily by parents during 21 days at home after toilet and before sleep with a new transformative texture "gel to oil" massage balm. No instructions for the massage method were given. Tolerance evaluation was performed. Assessments of the effects of the massage just after the first application (performed on the study site), after 7 days (telephone questionnaire) and after 21 days have been performed.

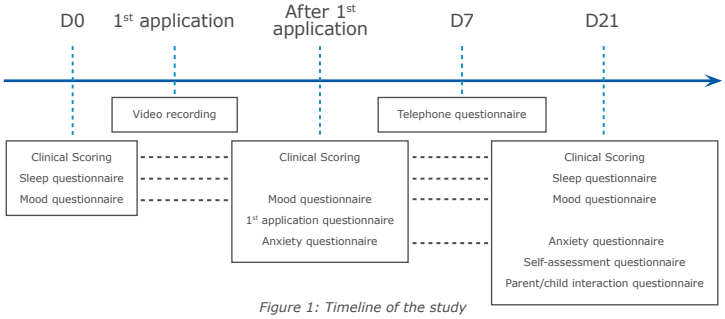

Figure 1: Timeline of the study

Assessments included clinical scorings (redness, dryness, roughness and suppleness) and questionnaires related to the efficacy and cosmetic qualities of the product, the child well-being and sleep, the parent-child interaction and the mood and stress of the parent. Different scales have been used:

- 5 points Likert scale (Totally agree – Agree - Neither agree or disagree – Disagree - Totally disagree) interpreted by comparison of the percentage of positive answers (sum of Totally agree and Agree related to the total number or answers) to the minimum percentage calculated to have a significant difference with a "random" percentage of 50%.
- 9 points scale from 0 (None/Disagree) to 9 (Important/Agree). Results obtained with this scale are expressed as mean ± standard deviation and processed by comparison of answer groups at each time using a statistical test. Normality of data is tested using Shapiro–Wilk test. Paired t-test (normal data) or Wilcoxon signed rank test (non-normal data) is then used with a significance level $\alpha<0.05$.
- Quantitative scale. Some questions involve a quantitative answer (for example: sleep duration). Results obtained with this scale are expressed as mean ± standard deviation and processed by comparison of answer groups at each time using a statistical test. Normality of data is tested using Shapiro–Wilk test. Paired t-test (normal data) or Wilcoxon signed rank test (non-normal data) is then used with a significance level $\alpha<0.05$.

Statistical analysis was performed using the R software version 4.0.3[3].

Video recording of the parent face has been performed during the first massage. Set up is illustrated figure 2. Face tracking and facial landmarks estimation was performed to evaluate the emotions of the parent by an artificial intelligence algorithm based on deep learning[4]. We considered the percentages of time of Joy and Disgust emotions detected during the massage as valence indicators.

Figure 2: Set up for recording the parent face during the first application

· Results ·

Tolerance of the massage product was very good. Clinical scorings demonstrated an improvement of redness, dryness, roughness and suppleness immediately after the first application and after 21 days (table 1).

	% of variation after 1st application compared to D0	% of variation after 21 days compared to D0
Redness	-32.1%*	-67.9%*
Dryness	-69.7%*	-93.9%*
Roughness	-64.1%*	-92.4%*
Suppleness	1.60%*	10.5%*

Table 1: Clinical scores variations after 1st and 21 days of application ***: p<0.05**

After 21 days, parents perceived effects on moisturizing (94.7%) and nourishing (98.7%) of the child skin. The transformative texture was well appreciated for the massage (94.7%) and considered as a sensorial texture (86.7%).

Effect of the massage with the product on the child well-being has been positively perceived immediately (93.3%) and after 21 days (82.3%). Improvement of the time for getting asleep has been observed (-22.9%).

Parents perceived an improvement of the interaction (98.7%), the complicity (86.7%) and the emotional bonds (80.0%) with their child. The massage with the product was considered as a tenderness moment with their child (97.3%) and a source of shared well-being (93.3%).

Effects on parent's mood and stress were also observed. Immediately and after 21 days of application, parents feel less tired and also more calm (table 2).

After this 1st / 21 days of application, would you say that you feel:	% of variation after 1st application compared to D0	% of variation after 21 days
Tired	-23.0%*	-30.0%*
Calm	8.2%*	8.0%°

Table 2: Mood variations of parents after 1st and 21 days of application ***: p<0.05 / °:p<0.1**

During the first massage, mean massage time was 5.52±2.35 min. During this time, the exploitable time for emotion assessment (face of the parent correctly detected) was 2.78±1.5 min (50.5±16.5% of the total massage time).

After image processing by the artificial intelligence algorithm, Joy emotion was identified during 35.3±21.6% of the exploitable time and Disgust emotion during only 4.8±5.4%.

Individual percentages of Joy and Disgust emotions are illustrated figure 3. For all subjects, time of Joy emotion was always higher that time of Disgust emotion.

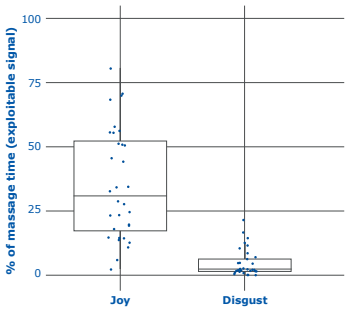

Figure 3: Emotions detected during the first massage

· Conclusion ·

This study demonstrated that a "real-life" massage without any specific instructions has positive effects on the child well-being, the parent mind and the parent-child interaction. The transformative texture of the product was well perceived for the massage and the product improved child skin. Emotions assessment method used gave convincing results for a massage application.

· References ·

[1] S. Iorio et al. Healing bodies: the ancient origins of massages and Roman practices. Medicina Historica 2018; Vol. 2, N. 2: 58-62.

[2] T. Field. Pediatric Massage Therapy Research: A Narrative Review. Children 2019, 6, 78.

[3] R Core Team (2020). R: A language and environment for statistical computing. R Foundation for Statistical Computing, Vienna, Austria. URL https://www.R-project.org/

[4] https://blog.affectiva.com/emotion-ai-101-all-about-emotion-detection-and-affectivas-emotion-metrics

Mapping of the biophysical properties of pregnant women abdomen skin: a pilot study

G. Boyer[1], G. Bellemère[1], C. de Belilovsky[1], C. Baudouin[1]

1 Laboratoires Expanscience, rue des Quatre Filles, 28233 EPERNON, FRANCE
gboyer@expanscience.com

KEY WORDS: pregnancy, mapping, skin properties

During pregnancy mechanical stretching of abdomen skin due to baby growth is very important and could lead to skin breakage (also known as striae distensae or stretch mark). Recent work demonstrated that biomechanical properties of healthy abdomen skin change drastically during pregnancy and that these properties remain altered 4 months after delivery[1]. It remains unclear if these observed modifications are homogeneous on the abdomen area or if a specific area is more affected. The aim of this pilot study is to perform a mapping of abdomen skin properties of a woman at 8 months of pregnancy using various non-invasive techniques in order to evaluate if gradient or specific pattern of these properties exist.

25 measurement points have been defined on one half of the abdomen. Assessments performed included hydration (Corneometer CM825), Transepidermal Water Loss (TEWL, Vapometer SWL-5), mechanical properties (Cutometer SEM 575) and thickness and echogeneicity of the skin (Dermascan 20 MHz). Mapping of each property has been performed by interpolation algorithm using Octave software.

Results obtained show that skin biophysical parameters were not homogeneous on abdomen as illustrated by figure 1 with skin thickness. Moreover, specific locations exhibited particular properties. High variations of the measurements between the 25 points were observed: 104% for hydration, 40% for TEWL, 134% for echogeneicity, 47% for thickness and 30% to 160% for biomechanical properties. Study of the relationships between all measured parameters demonstrated that some skin properties are significantly correlated while others are independent.

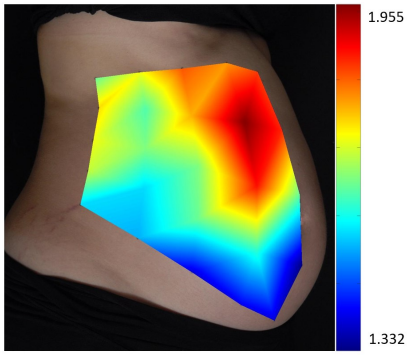

Figure 1: skin thickness mapping.

This pilot study demonstrated that the skin properties of women at 8 months of pregnancy are not homogeneous on the abdomen, tending to show that specific area could be more affected and therefore more subjected to stretch mark formation. A future study will compare women at different stages of pregnancy to quantify the variations of skin properties on the abdomen along pregnancy time.

[1] G. Boyer, N. Lachmann, G. Bellemère, C. De Belilovsky and C. Baudouin. Effects of pregnancy on skin properties: A biomechanical approach. Skin Res Technol. 2018 Nov;24(4):551-556.

Mapping of the biophysical properties of pregnant women abdomen skin: a pilot study

G. Boyer[1*], G. Bellemère[1], C. de Belilovsky[1], C. Baudouin[1]

1- Laboratoires Expanscience, Centre IRD, Epernon, France * gboyer@expanscience.com

· Introduction ·

During pregnancy mechanical stretching of abdomen skin due to baby growth is very important and could lead to stretch mark (also known as striae distensae). Recent work demonstrated that biomechanical properties of healthy abdomen skin change drastically during pregnancy and that these properties remain altered 4 months after delivery[1]. It remains unclear if these observed modifications are homogeneous on the abdomen area or if a specific area is more affected.

· Hypothesis ·

The aim of this pilot study is to evaluate if gradient or specific pattern of abdomen skin properties exist during pregnancy.

· Methods ·

A pilot study has been conducted. A healthy 28 years old woman at 8 months of pregnancy has been recruited. 25 measurement points have been defined on one half of the abdomen as illustrated figure 1. Non-invasive assessments performed were:

- Hydration using Corneometer CM825 (Courage + Khazaka, Germany),
- Barrier function via Transepidermal Water Loss (TEWL) using Vapometer SWL-5 (Delfin Technologies, Finland),
- Mechanical properties using Cutometer® SEM 575 (Courage + Khazaka, Germany),
- Thickness and echogenicity using Dermascan 20 MHz (Cortex Technology, Denmark).

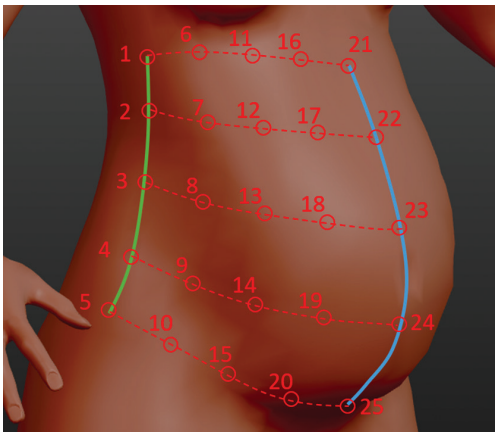

Figure 1: Positioning of the 25 measurement points.

Mapping of each property has been performed by interpolation algorithm using Octave software[2]. Evaluation of correlation between measured parameters has been performed using R[3].

· Results ·

Results obtained show that skin biophysical parameters were not homogeneous on abdomen.

Figure 2 to figure 6 illustrate respectively hydration, TEWL, echogenicity, thickness and biomechanical properties interpolated from the 25 measurement points. Specific locations exhibited particular properties. High variations of the measurements between the 25 points were observed: 104% for hydration, 40% for TEWL, 134% for echogenicity, 47% for thickness and 30% to 160% for biomechanical properties.

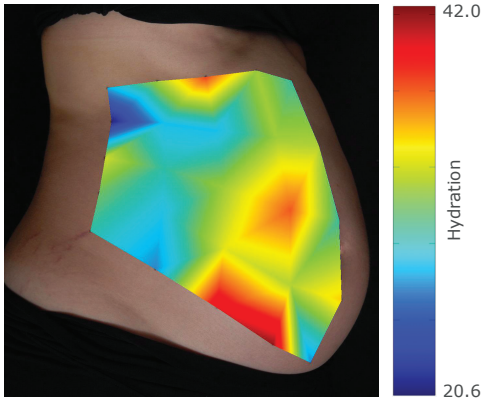

Figure 2: Interpolated hydration measured using Corneometer CM825 on 8 months pregnant woman abdomen.

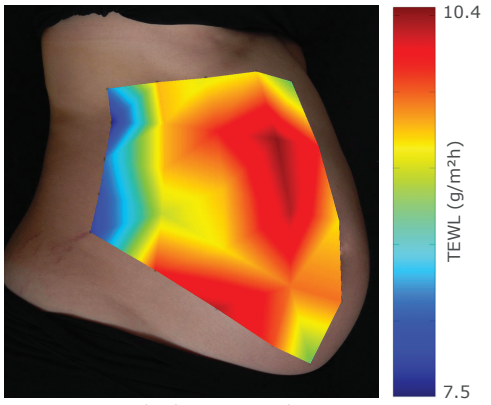

Figure 3: Interpolated TEWL measured using Vapometer SWL-5 on 8 months pregnant woman abdomen.

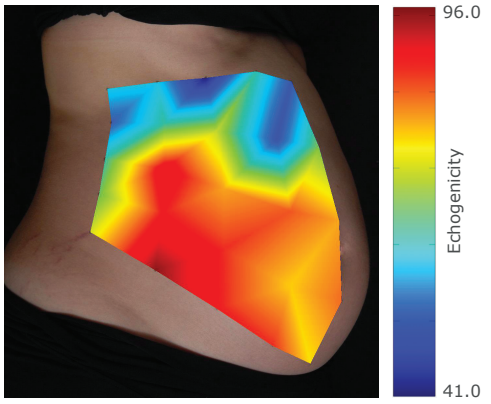

Figure 4: Interpolated echogenicity measured using echography on 8 months pregnant woman abdomen.

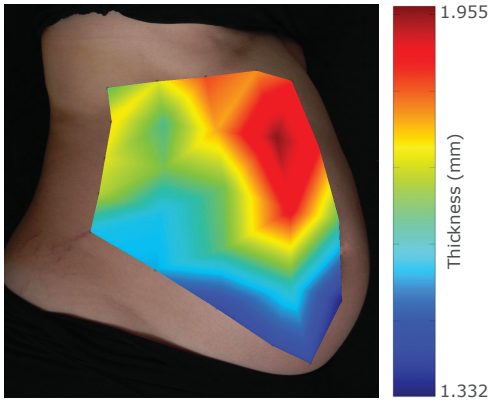

Figure 5: Interpolated thickness measured using echography on 8 months pregnant woman abdomen.

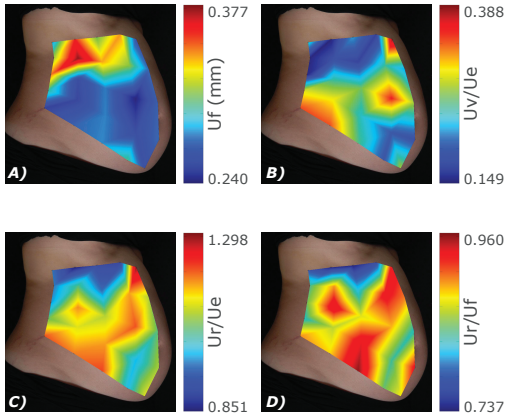

Figure 6: Figure 6. Interpolated biomechanical properties measured on 8 months pregnant woman abdomen
***A)** Firmness: Uf (mm) **B)** Ratio of viscoelastic to elastic distension: Uv/Ue*
***C)** Net elasticity: Ur/Ue and **D)** Elastic recovery: Ur/Uf*

Relationships between all measured parameters are illustrated in the correlation matrix figure 7. Positive correlations are in blue and negative correlations in red. Pearson correlation coefficient is indicated in each circle. Non significant coefficients are strikethroughs. Results show that some skin properties are significantly correlated while others are independent.

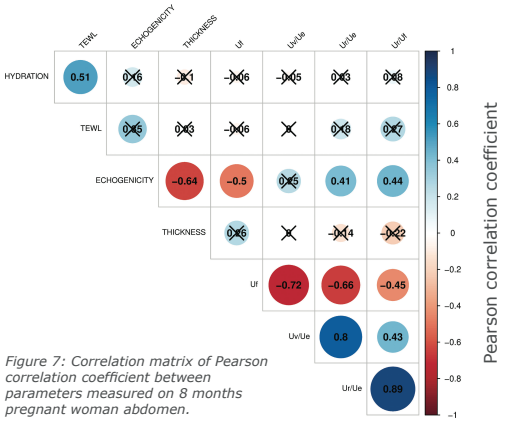

Figure 7: Correlation matrix of Pearson correlation coefficient between parameters measured on 8 months pregnant woman abdomen.

· Conclusion ·

This pilot study demonstrated that the skin properties of women at 8 months of pregnancy are not homogeneous on the abdomen, tending to show that specific area could be more affected and therefore more subjected to stretch mark formation. A future study will compare women at different stages of pregnancy to quantify the variations of skin properties on the abdomen along pregnancy time.

· References ·

[1] G. Boyer, N. Lachmann, G. Bellemère, C. De Belilovsky and C. Baudouin. Effects of pregnancy on skin properties: A biomechanical approach. Skin Res Technol. 2018 Nov; 24(4):551-556.

[2] J.W. Eaton, D. Bateman, S. Hauberg, R. Wehbring (2019). GNU Octave version 5.1.0 manual: a high-level interactive language for numerical computations. URL https://www.gnu.org/software/octave/doc/v5.1.0/

[3] R Core Team (2020). R: A language and environment for statistical computing. R Foundation for Statistical Computing, Vienna, Austria. https://www.R-project.org/

Acidic skin care promotes cutaneous microbiome recovery and skin physiology in an acute stratum corneum stress model

Razvigor Darlenski[2,3], Peter Menzel[7], Rolf Schwarzer[7], Benjamin Kaestle[6], Michaela Arens-Corell[6], Lina Praefke[6], Nikolai Tsankov[3], Dessyslava G. Nikolaeva[3,4], Laurent Miséry[5], Joachim W. Fluhr[1,5]

1- Department of Dermatology and Allergology, Charité Universitätsmedizin, Berlin, Germany; 2- Department of Dermatology and Venereology, Medical Faculty, Trakia University- Stara Zagora, Bulgaria; 3- Department of Dermatology and Venereology, Acibadem City Clinic Tokuda Hospital – Sofia, Bulgaria; 4- EuroDerma Clinic, Sofia, Bulgaria; 5- Department of Dermatology, Univ. of Brest, France; 6- Sebapharma GmbH & Co. KG, Boppard, Germany; 7- Labor Berlin – Charité Vivantes GmbH, Berlin, Germany

Background:
Context: skin microbiome and skin physiology are important indicators of the epidermal homeostasis status. Stress models are able to reveal pathological conditions and modulating effects. ***Purpose:*** we investigated the cutaneous microbiome (16S-rRNA-gene amplicon sequencing) in relation to skin physiology (barrier function, stratum corneum hydration, surface-pH) after mild tape stripping (TS) without treatment compared to two cosmetic leave-on lotions (pH5.5 vs. pH9.3) in 25 healthy volunteers.

Results
TS reduced the alpha-diversity with a recovery over 7 days without treatment. Both lotions significantly accelerated the recovery of the alpha-diversity after 2 days with a slightly higher rate for lotion pH5.5. After TS, the relative abundance of Proteobacteria was increased, whereas Actinobacteria were reduced. TS reduced the relative abundances of skin-associated genera. Taxa compositions normalized after 7 days in all treatment groups. Both lotions accelerated the normalization. Lotion pH9.3 induced a significant increase of skin-pH. Both lotions induced an increase in stratum corneum hydration.

Conclusion
The study proved the suitability of an experimental stress model to assess skin surface microbiome in relation to skin physiology. The positive effect of skin care on cutaneous microbiome in relation to skin physiology has a significant modulatory effect on exogenous stress-induced epidermal alterations.

Application of eNOSE in Odor Detection and Assessment in Cosmetic Testing

Lily Jiang[1], PhD., Aswathy VK[2], Av Abraham[2], PhD

1. SGS
2. SGS India
Corresponding Author e-mail address: Li.Jiang@sgs.com

KEY WORDS: eNOSE, odor detection

Sensory analysis of odor has traditionally been done by trained expert panels in the cosmetic testing field. With the advancement of sensor technology for artificial olfaction it is of great interest to explore the feasibility of applying this technology to achieve objective and quantitative assessment of odor in the cosmetic testing field. The Heracles Neo Electronic Nose (eNOSE) system is chosen to assess odor from a range of products. This eNOSE system is based on ultra-fast gas chromatography technology with an embedded temperature-controlled odor concentrator. Volatile compounds injected into the system are detected by two flame ionization detectors and identified using AroChemBase software. This system offers a wide dynamic range and high sensitivity. We have used this system in a proof-of-principle (POP) study in human odor detection and masking. Our preliminary result identified key signature molecules in human sweat such as acetic acid and dimethyl trisulfide. Use of deodorant appeared to mask the peak level of those sweat odor to certain extent. The effect of the deodorant can be quantified through multi-dimensional analysis. The masking effect tends to wear off over time as the multi-dimensional distance between the two conditions, with and without deodorant, is reduced at hour 8 when compared to hour 4. This POP study suggests that the eNOSE system may potentially be used for human odor detection and analysis therefore provide objective and quantitative result in odor sensory testing field.

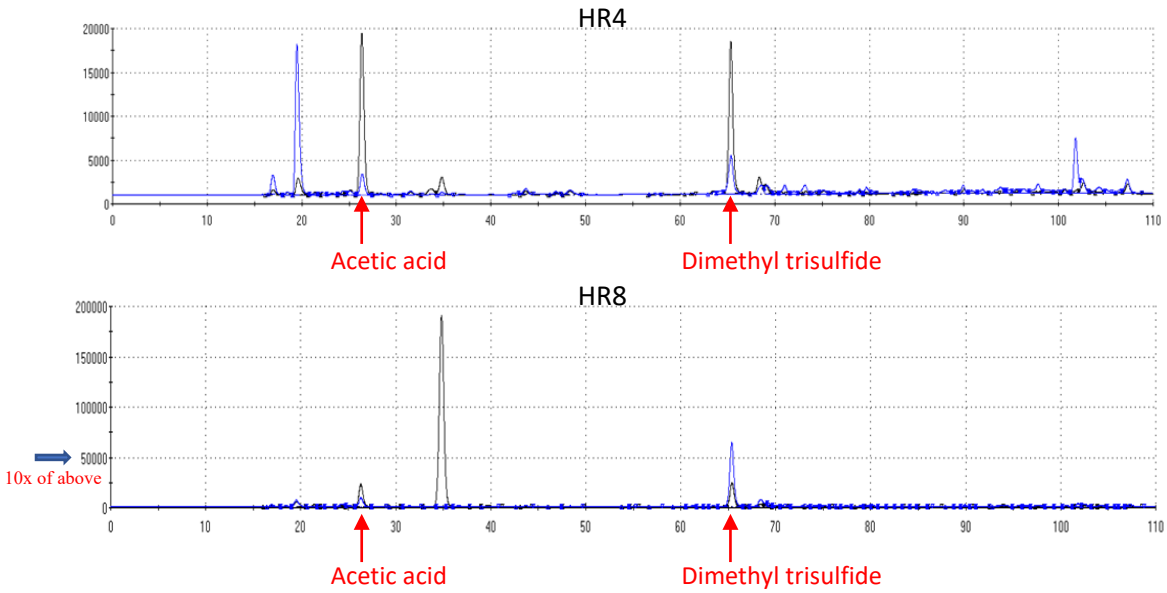

Application of eNOSE in Odor Detection and Assessment in Cosmetic Testing

Lily Jiang[1], PhD., Aswathy VK[2], Av Abraham[2], PhD
[1.] SGS; [2.] SGS India

Sensory analysis of odor has traditionally been done by trained expert panels in the cosmetic testing field. With the advancement of sensor technology for artificial olfaction it is of great interest to explore the feasibility of applying this technology to achieve objective and quantitative assessment of odor in the cosmetic testing field. The Heracles Neo Electronic Nose (eNOSE) system is chosen to assess odor from a range of products. This eNOSE system is based on ultra-fast gas chromatography technology with an embedded temperature-controlled odor concentrator. Volatile compounds injected into the system are detected by two flame ionization detectors and identified using AroChemBase software. This system offers a wide dynamic range and high sensitivity. We have used this system in a proof-of-principle (POP) study in human odor detection and masking. Our preliminary result identified key signature molecules in human sweat such as acetic acid and dimethyl trisulfide. Use of deodorant appeared to mask the peak level of those sweat odor to certain extent. The effect of the deodorant can be quantified through multi-dimensional analysis. The masking effect tends to wear off over time as the multi-dimensional distance between the two conditions, with and without deodorant, is reduced at hour 8 when compared to hour 4. This POP study suggests that the eNOSE system may potentially be used for human odor detection and analysis therefore provide objective and quantitative result in odor sensory testing field.

eNOSE Principle

The e-nose is an ultra- fast gas chromatograph with embedded odour concentrator, called trap. The trap is composed of Tenax TA polymer that allows volatile compound absorption at low temperature (usually 0 to 60ºC) and desorption at high temperature (typically 240ºC). The samples are subjected to agitation for different temperatures depending upon sample nature to generate the headspace. The headspace generated is then injected using an injector (the injector is heated at high temperature to allow the volatilization of liquid samples and prevent volatile molecule condensation) and concentrated in the cold trap during the loading phase. After flushing, the trap is heated, and the concentrated odor is injected rapidly and divided between the 2 columns namely DB5 and DB17 during the injection phase. The volatile compounds separated by each columns are detected by 2 flame ionization detector and recoded by the software for the data treatment.

Molecules detected by eNOSE is analyzed through AroChemBase software module. Based on the Kovats index, AroChemBase module delivers a list of possible compounds sorted by relevance index. With information on the sensory attributes related to the chemical compounds and human detection thresholds, samples can be further evaluated on their organoleptic features. AroChemBase is also a database of chemical compounds with related sensory notes that offers advanced search capabilities for smell analysis.

Method

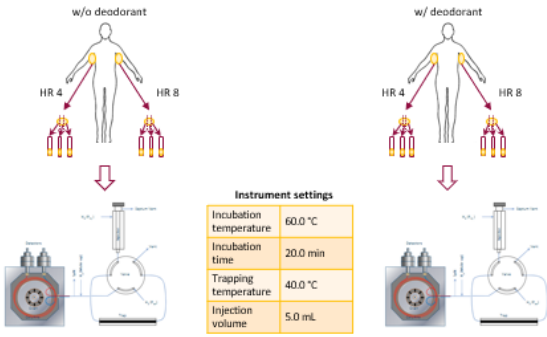

Instrument settings

Incubation temperature	60.0 °C
Incubation time	20.0 min
Trapping temperature	40.0 °C
Injection volume	5.0 mL

Result

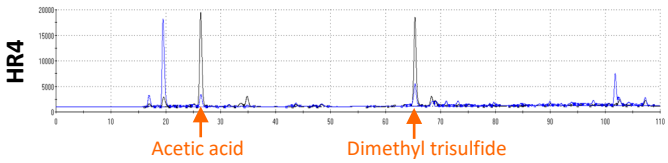

Retention time (seconds)	Name	Relevance index	Sensory descriptors
26.4	Acetic acid	57.04	acetic; acidic; pungent; sharp; sour;
65.36	Dimethyl trisulfide	14.08	alliaceous; sulfurous; pungent

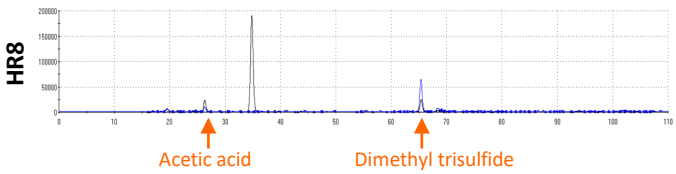

Chromatogram for Hr4 and Hr8 samples showing samples without deodorant in black superimposed with samples with deodorant in blue. The peaks at retention 26.40 second and 65.36 second indicate acetic acid and dimethyl trisulfide, respectively. The peaks intensity for acetic acid and dimethyl trisulfide has increased comparing to Hr4 samples.

Multi-dimensional analysis of the distance between samples with and without deodorant

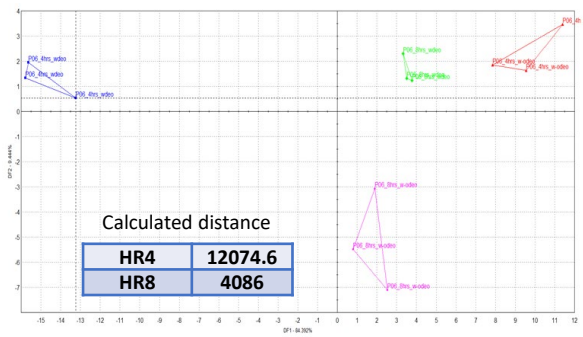

Conclusions

The eNOSE system can identify certain chemicals that are present in human sweat/human odor. Result from this pilot proof-of-principle study showed that the intensity of those molecules may be different with or without the presence of deodorant and the difference may relate to the wear time of the deodorant. A better controlled, split-body design study with more subjects is needed to further evaluate this method.

Contact Us

Ms. Aswathy V Krishnan
Aswathy.vk@sgs.com

Dr. A.V Abraham
Av.Abraham@sgs.com
www.sgsgroup.in

Lily Jiang, PhD
Li.Jiang@sgs.com

Feature-based Classification of Malignant Melanomas, Lesions, and Healthy Skin in Multiphoton Autofluorescence Skin Images

I. Lange[1], P. Prinke[1], S. Klee[1,2], Ł. Piątek[3], M. Warzecha[4], K. König[4,5], J. Haueisen[1]

[1]Institute for Biomedical Engineering and Informatics, Technische Universität Ilmenau, Gustav-Kirchhoff-Straße 2, 98639 Ilmenau, Germany
[2] Division Biostatistics and Data Science, Department of General Health Studies, Karl Landsteiner University of Health Sciences, Dr.-Karl Dorrek Straße 30, 3500 Krems, Austria
[3] Faculty of Applied Information Technology, University of Information Technology and Management, Sucharskiego 2, 35-225 Rzeszów, Poland
[4]JenLab GmbH, Johann-Hittorf- Straße 8, 12489 Berlin, Germany
[5]Department of Biophotonics and Laser Technology, Saarland University, Campus A5.1, 66123 Saarbrücken, Germany
Corresponding Author e-mail address: irene.lange@tu-ilmenau.de

KEY WORDS: skin cancer diagnosis, multiphoton fluorescence microscopy, biomedical image processing

Malignant melanoma is a highly aggressive tumour metastasising at an early stage and can lead to death. For this reason, early detection of malignant melanoma and differentiation from other skin lesions is of great importance[1]. Multiphoton tomography is a new non-invasive examination method in the clinical diagnosis of skin alterations that can be used for such early diagnosis[2].

We present a method for automated analysis of multiphoton images of the skin. To characterize the multiphoton images of the skin, the anatomical characteristics that are particularly important for distinguishing malignant melanoma, healthy skin, and lesions were selected and transferred into features extractable from multiphoton images of the skin[3]. The following features at the cellular and subcellular level were extracted: cell symmetry, cell distance, cell density, cell and nucleus contrast, nucleus cell ratio, and homogeneity of cytoplasm. The extracted features formed the basis for the subsequent classification. Two feature sets were used. The first feature set included all extracted features, while the second feature set included significantly different features. The classification was performed by a Support Vector Machine, the k-Nearest Neighbour algorithm, and Ensemble Learning.

The best classification results were generated with the Support Vector Machine using all features with an accuracy of 52 % and 79.6 % for malignant melanoma and healthy skin, respectively.

The main limitation of the present work is the small number of subjects. Nevertheless, our results indicate that the proposed method can distinguish malignant melanoma, lesions, and healthy skin.

---

[1] Leitlinienprogramm Onkologie der Arbeitsgemeinschaft der Wissenschaftlichen Medizinischen Fachgesellschaften e.V., Deutschen Krebsgesellschaft e.V., Deutschen Krebshilfe (Hrsg.), S3 - Leitlinie zur Diagnostik, Therapie und Nachsorge des Melanoms, AWMF-Register-Nummer: 032/024OL, Langversion 3.3, 2020.

[2] K. König, "Multiphoton tomography (MPT)" in K. König (ed.). Multiphoton Microscopy and Fluorescence Lifetime Imaging, (De Gruyter, Berlin, 2018: 247-263).

[3] I. Lange et al, Feature Extraction for Classification of Lesions and Malignant Melanomas in Multiphoton Tomography Skin Images, ISBS 2021 Digital Congress on Biophysics and Imaging of the Skin (Online, 2021).

Feature-based Classification of Malignant Melanomas, Lesions, and Healthy Skin in Multiphoton Autofluorescence Skin Images

I. Lange[1*], P. Prinke[1], S. Klee[1,2], Ł. Piątek[3], M. Warzecha[4], K. König[4,5], J. Haueisen[1]

[1] Institute for Biomedical Engineering and Informatics, Technische Universität Ilmenau, 98693 Ilmenau, Germany.
[2] Department of General Health Studies, Karl Landsteiner University of Health Sciences, 3500 Krems, Austria.
[3] Department of Artificial Intelligence, University of Information Technology and Management, 35-225 Rzeszów, Poland.
[4] JenLab GmbH, 12489 Berlin, Germany.
[5] Department of Biophotonics and Laser Technology, Saarland University, 66123 Saarbrücken, Germany.
*Irene.Lange@tu-ilmenau.de

Classification of skin cancer using image processing adapted anatomical characteristics

Introduction

Malignant melanoma is a highly aggressive tumour metastasising at an early stage and can lead to death. Therefore, early detection is of great importance. Multiphoton tomography is a new non-invasive examination method in the clinical diagnosis of skin alterations that can be used for such early diagnosis.

Aim: Automated analysis of multiphoton images of the skin for the purpose of skin cancer detection

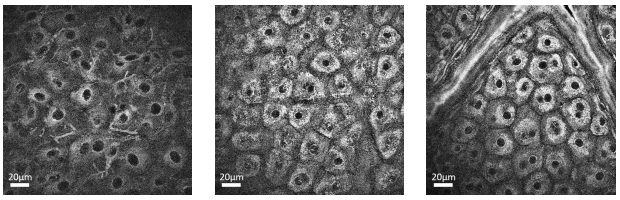

Figure 1: Multiphoton images of malignant melanoma, lesion, and healthy skin

Feature Extraction

Table 1: Anatomical characteristics and the extracted features used to distinguish malignant melanoma, lesions, and healthy skin

Anatomical Characteristics	Extracted Features
Architectural order	Cell symmetry, Cell distance, Cell density
Variance of cell shape	Cell symmetry
Size of intercellular distance	Cell distance, Cell density
Cell separability	Cell contrast
Nucleus separability	Nucleus contrast
Nucleus size	Nucleus cell ratio
Homogeneity of cytoplasm	Haralick texture feature homogeneity

Cell symmetry: Ratio of pixel sets along the symmetry axes determined with principal component analysis
Cell distance: Euclidean distances of neighboring cell centroids using Delaunay triangulation
Cell density: Ratio of the pixels within the cell and the total number of pixels [Discarded due to non-cell specificity]
Cell and nucleus contrast: Mean gradient estimation along a border area of the cell and the nucleus
Cell nucleus ratio: Ratio of the pixels of the nucleus and the pixels of the cell cytoplasm
Homogeneity of Cytoplasm: Haralick texture feature homogeneity on the cytoplasm of each cell

Feature-based Classification

Features sets:
A. All extracted cell-specific feature
B. Significant features [cell distance, homogeneity of cytoplasm, cell contrast] showing statistically significant differences among the three classes

Classifiers:
1. Support Vector Machine
2. k-Nearest Neighbour
3. Ensemble Learning

Classification Results

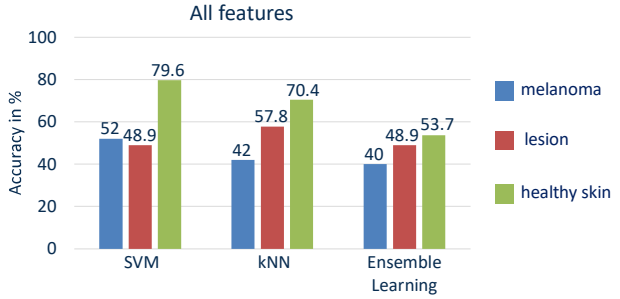

Figure 2: Accuracy of classification of test images of malignant melanoma, lesion, and healthy skin for the trained classification models of SVM, kNN , and Ensemble Learning based on all features

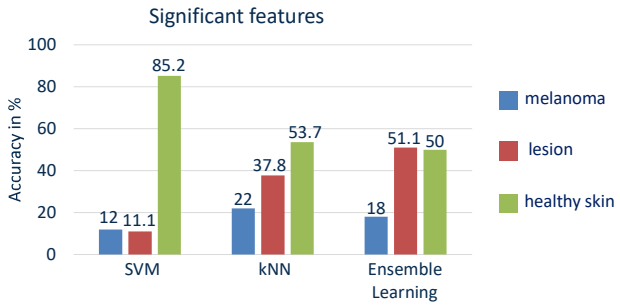

Figure 3: Accuracy of classification of test images of malignant melanoma, lesion, and healthy skin for the trained classification models of SVM, kNN, and Ensemble Learning based on significantly different features

Best classification results with the Support Vector Machine using all features

Conclusion

- Results indicate that the proposed method can distinguish malignant melanoma, lesions, and healthy skin
- Main limitation: small number of subjects

Acknowledgement

This work was supported by the Federal Ministry of Education and Research [grant number 01DS19012A] and by the Polish National Centre for Research and Development [grant number WPN-3/3/2019/DigiSkinDia].

Multimodal Multiphoton Tomography

D. Pankin1, HG. Breunig1, M. Warzecha1, A. König1, K.König[1,2]

JenLab GmbH, Berlin, www.jenlab.de
Saarland University, Department of Biophotonics and Laser Technology, Saarbrücken

Corresponding Author: pankin@jenlab.de, www.jenlab.de

KEY WORDS: two-photon, reflectance, multiphoton

Multiphoton tomography (MPT) is based on nonlinear excited autofluorescence and second harmonic generation (SHG) by 80 MHz near infrared femtosecond laser pulses. The major MPT signal is the fluorescence from the reduced coenzyme NADH. The second most important signal is the SHG signal from the extracellular matrix protein collagen. So far, most clinical MPT devices are based on a bulky tunable titanium:sapphire laser (670-950nm). The laser needs a water chiller. The laser beam is guided through an optical arm.

Here we report on the development of a compact MPT device that is based on an ultracompact chiller-free 80 MHz fiber laser at a "fixed" wavelength of 780 nm. The laser head is positioned within the measurement head that includes also a beam scanner, multiple photon detectors, and a high NA1.3 focusing optics. The use of an optical arm is no longer required.

The multimodal device has (besides autofluorescence/SHG detection) also modules for confocal reflectance, fluorescence lifetime imaging (FLIM), and dermoscopy. The novel tomograph was tested in a cosmetic research facility in Japan as well in two skin cancer clinics in Germany.

MULTIMODAL MULTIPHOTON TOMOGRAPHY

D. Pankin[1], HG. Breunig[1], M. Warzecha[1], A. König[1,2], K. König[1,2]
[1]JenLab GmbH, Berlin, www.jenlab.de
[2]Saarland University, Department of Biophotonics and Laser Technology, Saarbrücken

Modules, Components, and Technical Highlights of MPT*compact*

Multiphoton tomography (MPT) is based on nonlinear excited autofluorescence (AF) and second harmonic generation (SHG) by 50 MHz near infrared femtosecond laser pulses. The major MPT signal is fluorescence from the reduced coenzyme NADH. The second most important signal is SHG from the extracellular matrix protein collagen. So far, most clinical MPT devices are based on a bulky tunable titanium:sapphire laser (670-950nm). The laser needs a water chiller. The laser beam is guided through an optical arm.

Here, we report on the development of a compact MPT device that is based on an ultracompact chiller-free 50 MHz fiber laser at a "fixed" wavelength of 780 nm. The laser head is positioned within the measurement head that includes also a beam scanner, multiple photon detectors, and a high NA1.3 focusing optics. The use of an optical arm is no longer required. The multimodal device has (besides AF/SHG detection) also modules for confocal reflectance, fluorescence lifetime imaging (FLIM), and dermoscopy. The novel tomograph was tested in a cosmetic research facility in Japan as well in two skin cancer clinics in Germany.

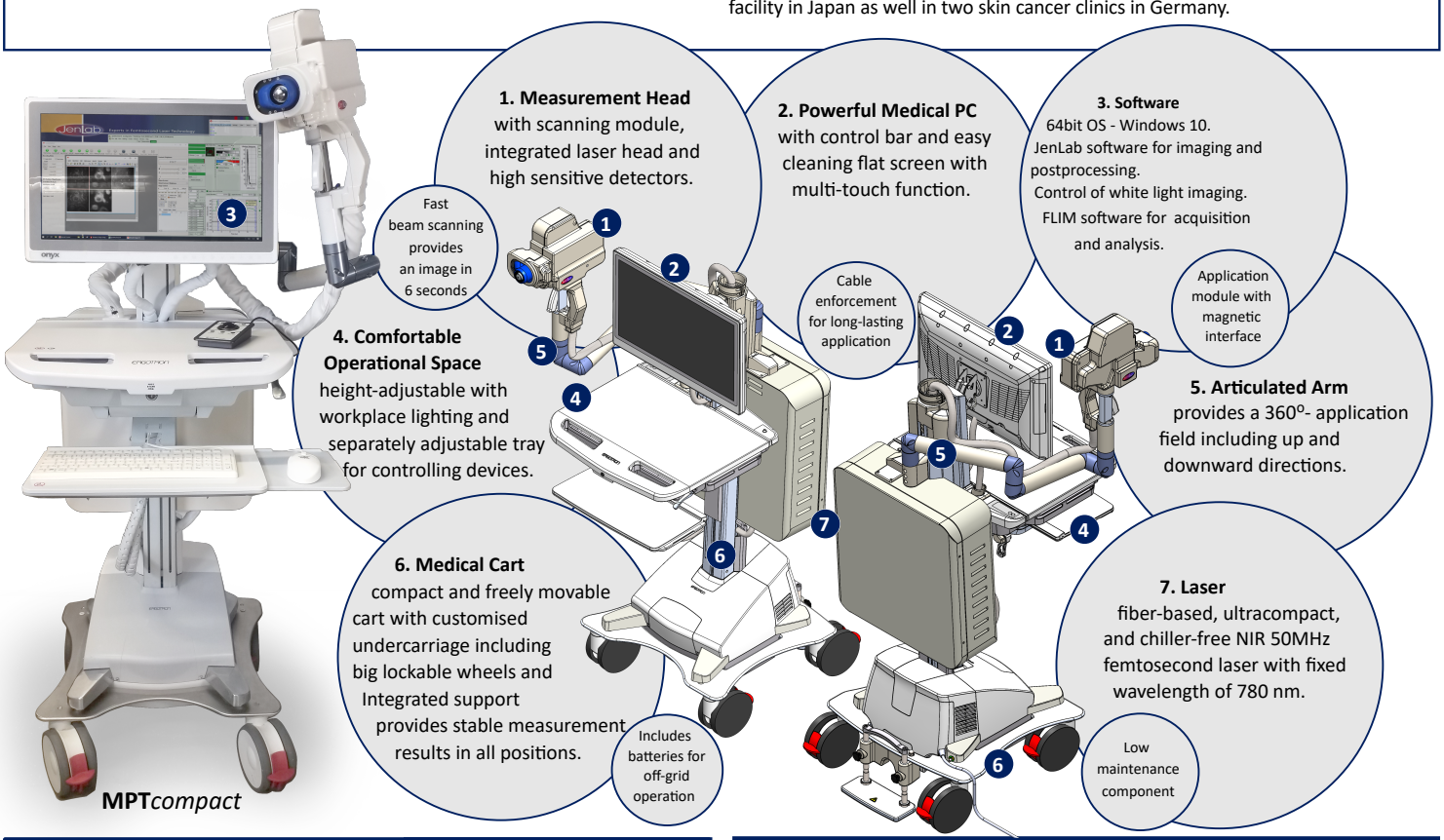

Technological Background

Advantages of Two-Photon Imaging

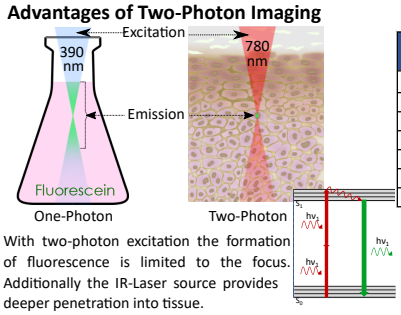

With two-photon excitation the formation of fluorescence is limited to the focus. Additionally the IR-Laser source provides deeper penetration into tissue.

Endogenous Skin Fluorophores

Fluorophore	Emission λ (nm)	Lifetime τ (ns)
NADH(P)H free	460	0.3
NADH(P)H-protein	440	2.0-2.3
Flavins	530	5 (bound: < 1)
Elastin	420-460	0.3/ 2
Collagen	420-460	0.3/ 2
Melanin	> 440	< 0.15
PPIX	635, 710	10-12

Types of Imaging

White Light Imaging

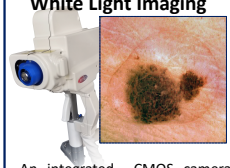

An integrated CMOS camera produces dermatoscopic images (area size 10mm x 10mm, image size 800 x 800 px).

Beam Scanning

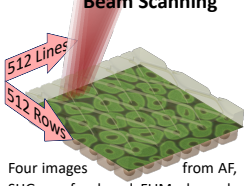

Four images from AF, SHG, confocal and FLIM channels are simultanously generated during beam scanning.

FLIM

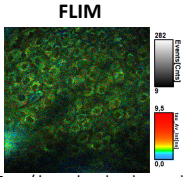

Free / bound molecules can be discriminated in FLIM images by pseudo-coloring their fluorescence decay times.

Composite from Single Channels

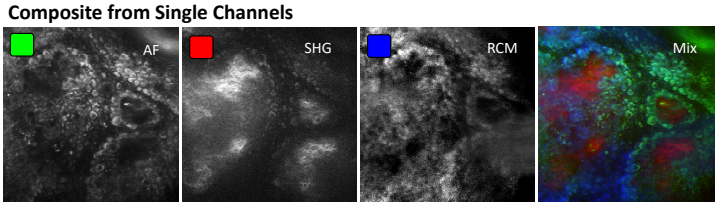

Application Examples

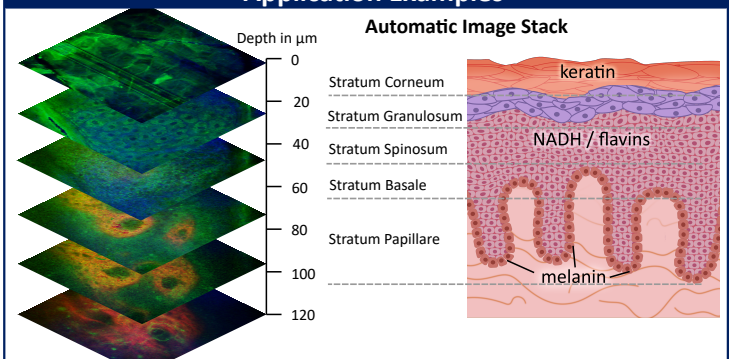

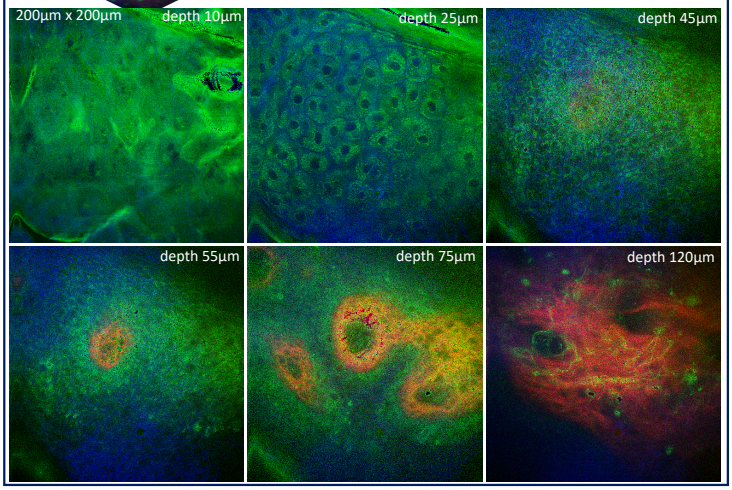

Skin Cell Segmentation using Superpixel-based Multi-Stage Merging on Multiphoton Autofluorescence Data

Philipp Prinke[1], Jens Haueisen[1], Sascha Klee[1,2], Muhammad Qurhanul Rizqie[1,3], Eko Supriyanto[1,4], Karsten König[5,6], Hans Georg Breunig[5,6], Łukasz Piątek[1,7]

[1]Institute for Biomedical Engineering and Informatics, Technische Universität Ilmenau, 98693 Ilmenau, Germany.
[2]Karl Landsteiner University of Health Sciences, Department of General Health Studies, Division Biostatistics and Data Science, Dr. Karl-Dorrek-Straße 30, 3500, Krems, Austria.
[3]Informatics Engineering Program, Universitas Sriwijaya, Palembang, South Sumatera, Indonesia.
[4]IJN-UTM Cardiovascular Engineering Centre, Universiti Teknologi Malaysia | UTM, Johor Bahru, Johor, Malaysia.
[5]Department of Biophotonics and Laser Technology, Saarland University, Campus A5.1, 66123 Saarbrücken, Germany.
[6]JenLab GmbH, Johann-Hittorf-Straße 8, 12489 Berlin, Germany.
[7]Department of Artificial Intelligence, University of Information Technology and Management, H. Sucharskiego 2 Str., 35-225 Rzeszów, Poland.
Corresponding author e-mail address: philipp.prinke@tu-ilmenau.de

KEY WORDS: two-photon-excited fluorescence (TPEF), malignant melanoma, nucleus classification

Malignant melanoma is a skin cancer that develops from melanocytes, which are pigment-containing cells found in the basal layer. The melanoma grows rapidly and metastasizes easily[1]. It is highly lethal in cases where it is not diagnosed early[2].

With a typical size of a skin cell in the basal layer of about 10 µm, a resolution of 1 µm or better is required to visualize subcellular details. Optical high-resolution, non-invasive, and non-destructive imaging techniques such as in vivo multiphoton tomography (MPT) are suitable for this purpose[3].

We propose a novel automatic segmentation algorithm for separating human skin cells from the rest of the tissue as the basis of an image processing pipeline for early diagnosis of human skin at the subcellular level in fluorescence data from three-dimensional multiphoton tomography scans. The high robustness of the segmentation to variable size and contrast ratios of different cell types and skin layers is achieved by the method of multi-stage merging on pre-processed superpixel images[4]. The assignment of segments to cell cytoplasm and nuclei is based on a feature-based cell model. In addition to local gradients and compactness, the relationship between outer cell and inner nucleus (OCIN) and the stability index are derived for the first time. The OCIN feature describes the topology of the model, while the stability index indicates the segment quality in the multi-stage merging process.

We illustrated our approach on a 200 x 200 x 100 μm^3 image stack containing the stratum spinosum and stratum basale skin layers of a healthy volunteer. Our image processing pipeline contributes to the fully automated classification of human skin cells in multiphoton data and provides a basis for the skin cancer detection by non-invasive optical biopsy.

---

[1] Tejera-Vaquerizo, A. et al. Chronology of metastasis in cutaneous melanoma: growth rate model. The Journal of investigative dermatology 132, 1215–1221 (2012).
[2] Noone, A. M. et al. Melanoma of the Skin. SEER Cancer Statistics Review 1975-2015 (2018).
[3] König, K. Multiphoton Microscopy and Fluorescence Lifetime Imaging, Applications in Biology and Medicine (De Gruyter, 2018).
[4] Prinke, P., Haueisen, J., Klee, S. *et al.* Automatic segmentation of skin cells in multiphoton data using multi-stage merging. *Sci Rep* **11,** 14534 (2021). https://doi.org/10.1038/s41598-021-93682-y

Skin Cell Segmentation using Superpixel-based Multi-Stage Merging on Multiphoton Autofluorescence Data

P. Prinke[1*], J. Haueisen[1], S. Klee[1,2], M.Q. Rizqie[1,3], E. Supriyanto[1,4], K. König[5,6], H.G. Breunig[5,6], Ł. Piątek[1,7]

[1] Institute for Biomedical Engineering and Informatics, Technische Universität Ilmenau, 98693 Ilmenau, Germany. *Philipp.Prinke@tu-ilmenau.de
[2] Department of General Health Studies, Karl Landsteiner University of Health Sciences, 3500 Krems, Austria.
[3] Informatics Engineering Program, Universitas Sriwijaya, Palembang, South Sumatera, Indonesia.
[4] IJN-UTM Cardiovascular Engineering Centre, Universiti Teknologi Malaysia | UTM, Johor Bahru, Johor, Malaysia.
[5] Department of Biophotonics and Laser Technology, Saarland University, 66123 Saarbrücken, Germany.
[6] JenLab GmbH, 12489 Berlin, Germany.
[7] Department of Artificial Intelligence, University of Information Technology and Management, 35-225 Rzeszów, Poland.

Novel segmentation pipeline for multiphoton autofluorescence cell images

Introduction

Malignant melanoma grows rapidly and metastasizes easily, leading to death if not diagnosed early. Visualization of subcellular alteration can be realized by high-resolution, non-invasive, and non-destructive in vivo multiphoton tomography [1]. A novel automatic multi-stage segmentation method is proposed to recognize human skin cells [2] for subsequent early diagnosis at the subcellular level in fluorescence data from three-dimensional multiphoton tomography scans.

Pipeline

Layer-wise skin cell recognition modules:

a. Pre-processing
[top hat transform, CLAHE*, anisotropic diffusion]

b. Segmentation
[watershed transformation, multi-stage merging]

c. Semantic assignment
[feature-based cell model using local gradient, compactness, OCIN-topology†, and stability index‡]

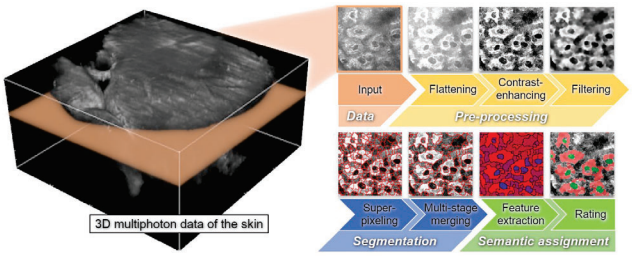

Fig.1: 3D representation of the image stack (left) and processing pipeline (right) showing from top left to bottom right: input image, plateauing by Top Hat transform, contrast enhancement by CLAHE, edge preserving filtering by anisotropic diffusion, segmentation by Watershed transform with subsequent segment fusion by multi-stage merging (boundaries are red), feature extraction with model matching by vector 2-norm (blue corresponds to higher similarity) and final thresholding (cytoplasm (red), nuclei (green))

Pipeline-Output is segment-wise data:

I. Label as nucleus, cytoplasm or intracellular matrix

II. Score as a measure of similarity to the cell model

** contrast-limited adaptive histogram equalization*
† the relationship between outer cell and inner nucleus (OCIN)
‡ indicates segment quality in the multi-stage merging process

Feature-based cell model

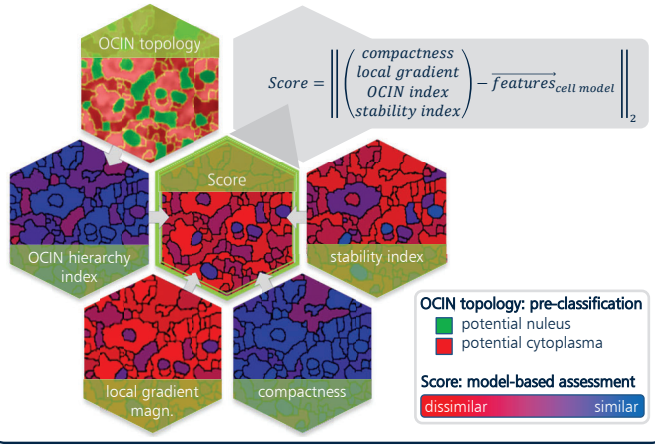

Results

$$Dice\ coefficient = \frac{2 \cdot true\ positives}{2 \cdot true\ positives + false\ positives + false\ negatives}$$

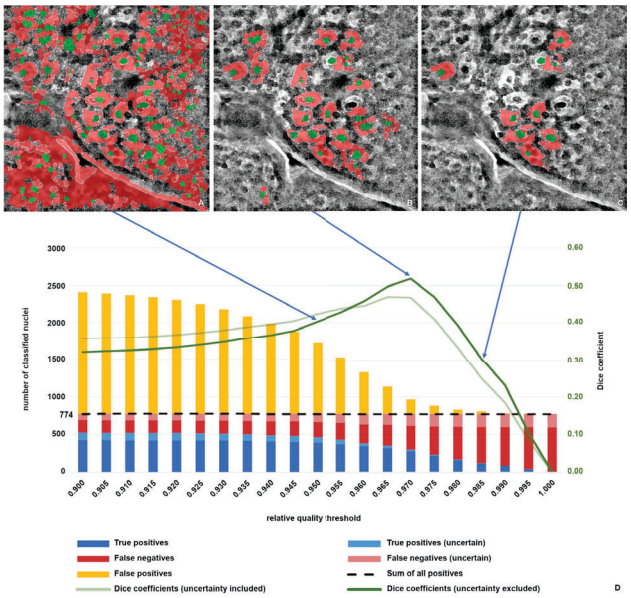

Fig.2: Classification results. A–C: Overlay of cell cytoplasm (red) and nuclei (green) using Score-related quality thresholds 0.95 (A), 0.97 (B), and 0.985 (C) (blue arrows), D: Accumulated true positives and misclassifications (left ordinate) and Dice coefficient (right ordinate) using different thresholds (abscissa) over the entire image stack with 774 nuclei.

Conclusion

- High robustness to variable size and contrast ratios of various cell types and skin layers by multi-stage merging
- Score for potential nuclei by feature-based cell model
- Adjusted score thresholds for the trade-off between true pos. and false neg. due to ambiguities caused by large intercellular intensity variations and less structured nuclei

References

[1] König, K. Multiphoton Microscopy and Fluorescence Lifetime Imaging, Applications in Biology and Medicine (De Gruyter, 2018).

[2] Prinke, P., Haueisen, J., Klee, S. et al. Automatic segmentation of skin cells in multiphoton data using multi-stage merging. Sci Rep 11, 14534 (2021). https://doi.org/10.1038/s41598-021-93682-y

Acknowledgement

This work was supported by the Federal Ministry for Economic Affairs and Energy on the basis of a decision by the German Bundestag [grant no. 16KN053021], the Federal Ministry of Education and Research [grant no. 01DS19012A] and by the Polish National Centre for Research and Development [grant no. WPN-3/3/2019/DigiSkinDia].

TECHNISCHE UNIVERSITÄT ILMENAU
Federal Ministry for Economic Affairs and Energy
Federal Ministry of Education and Research
The National Centre for Research and Development

Time for change - Non-invasive determination of SPF and UVA-PF with LED-HDRS

C. Reble[1*], C. M. Throm[2], G. Wiora[1], S. Schanzer[2], J. Schleusener[2], G. Khazaka[1], M. C. Meinke[2], J. Lademann[2]

[1] Courage + Khazaka electronic GmbH, Mattias-Brüggen-Straße 91, 50829 Cologne, Germany
*[2] Charité-Universtitätsmedizin Berlin, Department of Dermatology, Venerology and Allergology, Charitéplatz 1, 10117 Berlin, Germany, *creble@courage-khazaka.de, https://courage-khazaka.de*

KEY WORDS: UV-LEDs, sun protection, diffuse reflectance spectroscopy

Since the current gold standard for SPF testing is an invasive procedure that requires the generation of erythema on at least ten volunteers (ISO 24444), new alternative methods for SPF testing were developed in the last years.

The international ring study ALT-SPF[1] will compare different alternatives to the current gold standard. One of participating methods is LED-HDRS, where multiple UV-LEDs are utilized in a customized UV-light source combined with a customized system for diffuse reflectance spectroscopy on human skin. The resulting UV-transmission spectra allow calculation of SPF and UVA-PF according to the equations as in ISO 24443.

In this contribution, we describe the method and report on the results of our recent study[2], which showed that SPF and UVA-PF values obtained by this new approach correlated well with reference values by certified test institutes (R^2 =0.86 and 0.92, respectively). Further evaluations in test institutes were carried out.

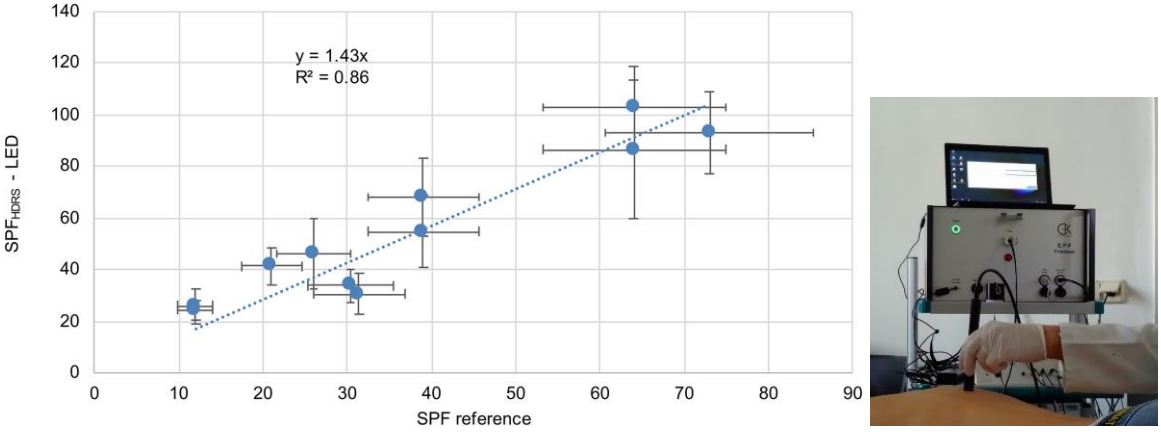

Fig. 1 : Correlation of SPF with LED-HDRS[2] and measurement device during the study

Acknowledgements: The work is funded by the German Federal Ministry of Education and Research BMBF (FKZ 03ZZ0131D) within the program "Zwanzig20-Partnerschaft für Innovation", by Courage + Khazaka GmbH and carried out within the consortium "Advanced UV for Life".

[1] www.ALT-SPF.com
[2] C. M. Throm et al., "In vivo SPF and UVA-PF determination using (hybrid) diffuse reflectance spectroscopy and a multi-lambda-LED light source", J. Biophotonics.2021;14:e202000348.

Impact of Pollution on the skin in real-life conditions

J. Robic [1]*, A. Nkengne[1], A. Bigouret, B. Lua[2] K. Vie[1]

1 Laboratoires Clarins, 5 rue Ampère 95300 Pontoise
2 Clarins Cosmetics Technology (Shanghai) Co., Ltd.
Corresponding Author: Julie ROBIC e-mail address: julie.robic@clarins.com

KEY WORDS: Skin aging, Pollution, real-life condition

Background
The impact of pollution on the skin has been investigated in over the recent years. Nevertheless, there is a need for characterizing its impact on the skin in real-life conditions.

Objective
The objective of this work is to study the impact of different pollutants in-vivo on the skin of women living in urban cities.

Methods
The study took place in 2019 over 6 months in France. 157 women between 20 and 60 years old were recruited, 131 women finished the study. The volunteer should be living near Paris and spending more than 200 days a year in this area. Pollutant's concentrations (particulate matter, gas, Air quality index) were retrieved daily with the Breezometer platform for 6 months, between June 2019 and January 2020. The Breezometer platform captures the concentration of each pollutant in a radius of 250m from the volunteer GPS position. In January 2020, a clinical study has been carried out with the following evaluated parameters: mechanical properties, hydration, sebum content, transepidermal water loss, spectrophotometer, pores, wrinkles, skin texture, color. Volunteers' cumulated exposure over 6month is calculated. Two groups of lower and higher cumulated exposure are then created for each pollutant. Each group is composed of around 50 volunteers, with no age difference between the two groups. Statistical comparison of skin parameters is performed.

Results
The group of women with a higher cumulated exposure of particulate matter (10µm) show a significantly lower hydration content on the cheek and a rougher skin texture under the eyes. Higher cumulated exposure of pollen induces a more yellow skin tone (b*) on the cheek and a darker skin tone (L*) under the eyes. We also highlighted the impact of air pollution on average wrinkles severity, skin elasticity and pores surface.

Conclusion
This clinical study, paired with an air-tracking solution, aims to be a first step in bringing awareness to the consumer and developing specific self-care routines.
Additional lifestyle questionnaires were included, to quantify the volunteer's stress score, sleep quality, screen use, and self-perception of their skin. Further work will focus on the relationship between other aspects of lifestyle and skin condition.

Impact of Pollution on the skin in real-life conditions

J. Robic [1]*, A. Nkengne[1], A. Bigouret[1], K. Vie[1]
[1] **Laboratoires Clarins**, 5 rue Ampère 95300 Pontoise

Introduction

The impact of pollution on the skin has been investigated in recent years. Nevertheless, there is a need for characterizing its impact on the skin in real-life conditions. The objective of this work is to study the impact of different pollutants in-vivo on the skin of women living in an urban city (Paris). The change in skin condition is looked at against exposure to the various pollutants that are gases (O3, NO2, SO2, CO), fine particles (PM25, PM10), and pollen over a 6-month period.

Materials and Methods

157 women between 20 and 60 years old were recruited, 131 women finished the study (**Table 1**).

Evaluation of skin condition (**Table 2**) aims to collect objective measurements characterizing facial skin appearance. This evaluation was carried out during measurement sessions conducted at the start of the study, and at T6 months. Wrinkles, skin color, skin roughness, pores measurements are obtained by image analysis.

The volunteer should be living near Paris and spending more than 200 days a year in this area. Pollutant's concentrations (**Table 3**) were retrieved daily with the Breezometer platform for 6 months, between June 2019 and January 2020. The Breezometer platform captures the concentration of each pollutant in a radius of 250m from the volunteer GPS position.

Table 1. Population

	Number of vol.
Start	151
End	131

Table 2. Skin parameters measurements.

Methods
Photos (Colorface)
Hydration (Corneometer)
Firmness (Cutometer)
Sebum (Sebumeter)
TEWL (Vapometer)
Colour (Spectrocolorimeter)

Table 3. Pollutants evaluated by Breezometer.

Parameters	Description	Unit of measurement
Air quality - BAQI	Proprietary index by Breezometer which combines all solid and gaseous pollutants depending on their hazardousness to health. Small values on this scale represent poor air quality.	A.U (1-100)
PM10	Concentration in the air of fine particles measuring less than 10 µm	µg/m3
PM 2.5	Concentration in the air of fine particles measuring less than 2.5 µm	µg/m3
NO2	Nitrogen dioxide air concentration	ppb
O3	Ozone air concentration	ppb
SO2	Sulphur dioxide air concentration	ppb
CO	Carbon monoxide air concentration	ppb
NOx	Nitrogen oxide air concentration	ppb
Tree/Flower/Leaf pollen	Relative quantity of pollen in the air on a scale of 0 (None) to 5 (High)	A.U (0-5)

Fig. 1 describes the pipeline to create two exposure groups for each pollutant. The two groups' skin measurements at T6month are then statistically compared. The volunteers are separated in such a way that the difference in the level of exposure to the pollutants between the two final is significant by using the median of the cumulative exposure to pollutants. Also, the final groups are chosen so there is no significant difference in terms of their age.

Figure 1. Exposure groups creation pipeline.

1 The cumulative exposure of each pollutant over the 6-month is calculated for each volunteer.

2 Exposure groups are created using the median of the pollutant exposure distribution as a threshold.

3 Exposure groups descriptions. N is the number of volunteers in each group. The mean exposure of each group is described and underlined if above the OMS warning threshold recommendation.

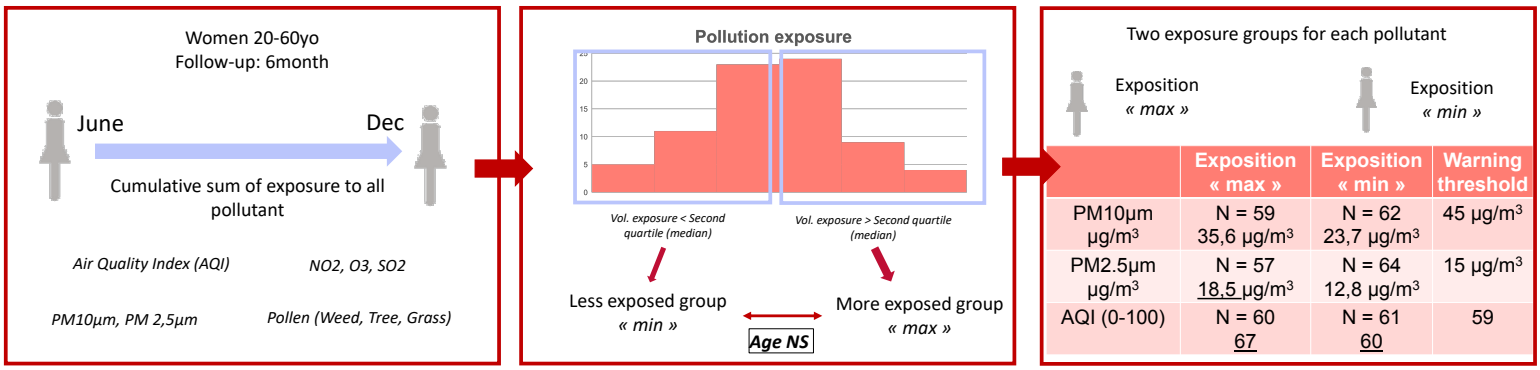

Results and Discussion

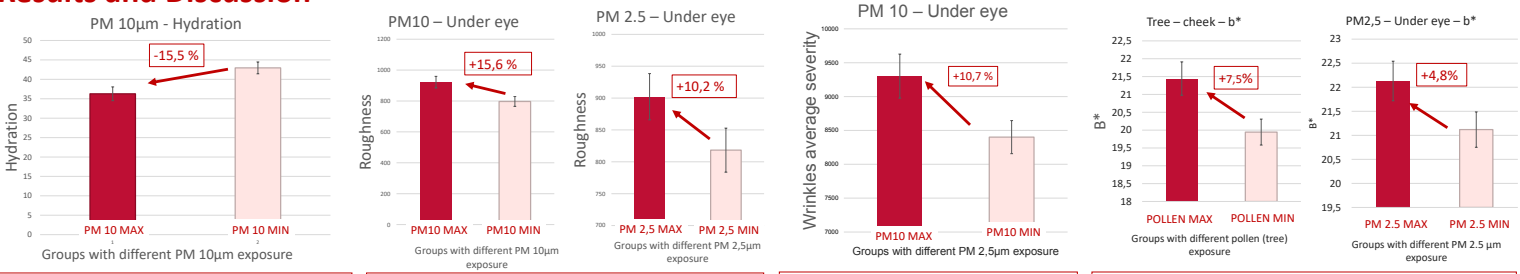

Exposure to particulate matter **PM 10µm** induces a **loss of hydration** (-15%)

Exposure to **fine particles PM 10µm, PM 2.5 µm** increases the **roughness under the eyes**

Exposure to **PM 10µm** increases the **wrinkles severity under the eye**

Exposure to a **Pollen (tree), PM2.5** induces a **more yellow skin tone on the cheek (Pollen) and under the eye (PM)**

The group of women with a higher cumulated exposure of particulate matter (10µm) show a significantly lower hydration content on the cheek and a rougher skin texture under the eyes. Higher cumulated exposure to pollen induces a more yellow skin tone (b*) on the cheek and a darker skin tone (L*) under the eyes. We also highlighted the impact of air pollution on average wrinkles severity, skin elasticity, and pores surface.

Conclusion

This clinical study, paired with an air-tracking solution, aims to be a first step in bringing awareness to the consumer and developing specific self-care routines. Additional lifestyle questionnaires were included, to quantify the volunteer's stress score, sleep quality, screen use, and self-perception of their skin. Further work will focus on the relationship between other aspects of lifestyle and skin condition.

Modeling of Global Skin Aging Indexes among Caucasian and Asian women

J. Robic [1]*, A. Nkengne[1], Bee Leng Lua[2], A. Bellanger1, R. Hu[2], K. Vie[1]

1 Laboratoires Clarins, 5 rue Ampère 95300 Pontoise
2 Clarins Cosmetics Technology (Shanghai) Co., Ltd.
Corresponding Author: Julie ROBIC e-mail address: julie.robic@clarins.com

KEY WORDS: Skin aging index, clinical evaluation, instrumental measurements

Background
The skin aging process is defined as the gradual degradation of several skin properties such as firmness, color, or the appearance of wrinkles. These properties can be assessed by trained experts, who perform an overall evaluation of the entire face.

Objective
The objective of this paper is the construction of two Global Skin Aging Indexes specifically designed to model the overall skin aging process of Caucasian and Asian women.

Methods
240 Asian women and 129 Caucasian women aged between 20 and 60 years old are recruited. Parameters related to wrinkles, sagging, elasticity and, skin tone are measured (Clinically or instrumentally). The global skin aging index is defined as the normalized projection on the first principal component of a Principal component analysis (PCA) of the skin measurements. Then, linear regressions are performed between the indexes and age of both panels. New data were selected to determine whether the model could generate accurate predictions. 32 Chinese women, aged between 30 and 45 years old, and 36 French women, aged between 41 and 60, were recruited.

Results
The first principal component carries around 50% of the initial variance for both indexes. Both Global Skin Aging Indexes statistically correlate with age ($R^2 \geq 0.7$, p-val < 0.05). We validated our model's generalization ability to process, adapt and react appropriately to previously unseen. New data projections fall within the prediction interval for both populations.

Conclusion
The proposed indexes are good indicators of the overall aging process for Caucasian and Asian women. The contribution of each initial parameter in the construction of the indexes are almost evenly balanced for both populations, giving our models the capacity to deal with inter-individual variability and assess the global skin aging status of the face. They offer new approaches to assess anti-aging product efficacy.

Modeling of Global Skin Aging Indexes among Caucasian and Asian women

J. Robic [1]*, A. Nkengne[1], Bee Leng Lua[2], A. Bellanger[1], R. Hu[2], K. Vie[1]
[1] **Laboratoires Clarins**, 5 rue Ampère 95300 Pontoise
[2] **Clarins Cosmetics Technology** (Shanghai) Co., Ltd.

Introduction

The efficacies of cosmetics products are usually evaluated through the clinical or instrumental measurement of various skin parameters, and the improvement is determined via statistical analysis. Several multidimensional approaches propose to combine several aspects of skin conditions to assess its overall status.
This study aims to describe the method used to build two Global Skin Aging Indexes specific to Caucasian and Asian women, by combining both clinical and instrumental skin parameters. The Global Skin Aging Indexes are meant to represent the overall skin aging of a population, i.e., to provide information about several skin parameters involved in the aging process, such as skin tone, sagging, and wrinkles. Therefore, the Global Skin Aging Indexes would be highly correlated with age.

Materials and Methods

Population

Table 1. Population

	Asian panel	Caucasian panel
20-30yo	60	21
30-40yo	60	29
40-50yo	60	42
50-60yo	60	37
Total	**240**	**129**

Materials and methods

Table 2. Skin parameters measurements. ┼ indicates Instrumental measurements

	Asian panel	Caucasian panel
Wrinkles	Forehead wrinkles[2], Glabellar wrinkles[2], Nasolabial fold[2]	Forehead wrinkles[1], Glabellar wrinkles[1], Nasolabial fold[1]
Sagging	Sagging of the lower cheek[3], Sagging of the upper cheek[3]	Ptosis[1], Plumpness
Elasticity	R2 ® ┼, R7 ® ┼	R2 ® ┼, R7 ® ┼
Skin tone	Radiance L* ┼, Color Homogeneity H76 ┼	Radiance, Skin tone homogeneity

Results and Discussion

The datasets are first standardized before entering a Principal Component Analysis (PCA) procedure. The variance explained, or information captured, by the principal components (PC) is presented in **Fig.1**.

The first principal component explains more than 50% of the initial variance for both populations, while the second and third principal components only explain around 15% of each of the remaining variance. The remaining principal components only explain slight variance. Note that the PCA is determined without any information about the age, only the skin parameters. Our goal is to build an index that captures meaningful information on the skin aging process.

Figure 1. Percentage of information/variance explained by each principal component (PC) of the PCA.

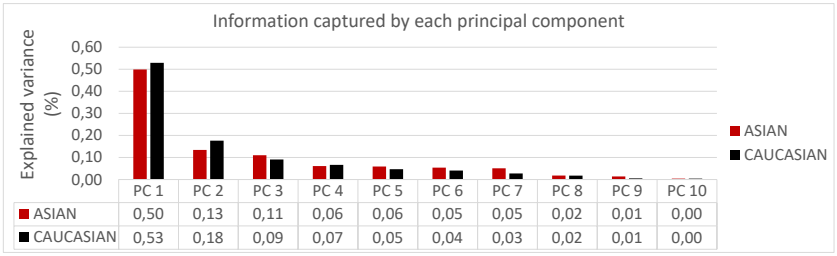

	PC 1	PC 2	PC 3	PC 4	PC 5	PC 6	PC 7	PC 8	PC 9	PC 10
ASIAN	0,50	0,13	0,11	0,06	0,06	0,05	0,05	0,02	0,01	0,00
CAUCASIAN	0,53	0,18	0,09	0,07	0,05	0,04	0,03	0,02	0,01	0,00

The Global Skin Aging Indexes are defined as the projections on the first principal components of the PCA analysis. The correlation coefficients (R^2) for PC1 are superior or equal to 0.70 for both populations and are statistically significant (p-value < 0.001 given by Spearman statistical test), see **Fig. 2**. The remaining principal components do not correlate with age (R^2<0.1), and correlations are insignificant (p-values > 0.05).

Figure 2. Normalization of projected data on the first principal component and its correlation with age. These are defined as the Caucasian and Asian Global Skin Aging Indexes.

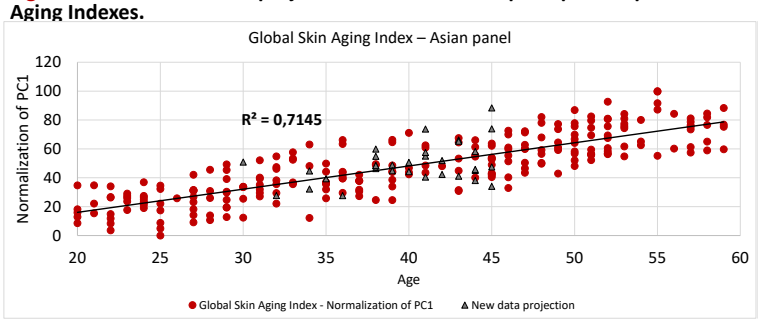

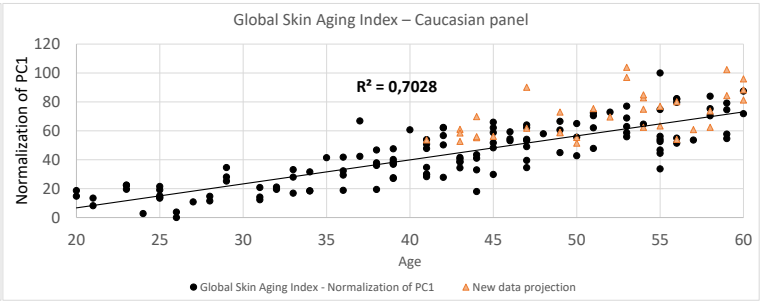

The projection on the first principal component of the PCA is a good indicator of the overall aging process. To model the skin aging process between 20 and 60 years old, the Global Skin Aging Index values are normalized between 0 and 100%,

We validated our model's generalization ability to process, adapt and react appropriately to previously unseen; new data were selected to determine whether the model could generate accurate predictions. 32 Chinese women, aged between 30 and 45 years old, and 36 French women, aged between 41 and 60, were recruited. The same skin parameters are measured, clinical studies are conducted the same way as for the Global Skin Aging Indexes constructions. **Fig.2** presents the projection of the estimated age of the new panels into the one of the Global Skin Aging Model. New data projections fall within the prediction interval for both populations. This proves the model's ability to process new data and generate accurate predictions after being trained on a training set. Thus, this Global Skin Aging Indexes can be used as skin aging referential.

Conclusion

The construction of Global Skin Aging Indexes is non-supervised, yet they are both highly correlated with age. When looking at the contribution of each initial parameter in the construction of the indexes (data not shown), we can observe that the ranking are different between the Asian and Caucasian populations, but the weights are almost evenly balanced for both populations. The sagging, elasticity and wrinkles-related parameters are of most importance in constructing the indexes, followed by parameters related to skin tone. The balance between weights does not bring much information on the differences between the two populations. However, it does provide to the models the capacity to deal with inter-individual variability. For instance, it is known that wrinkles appear with age, but not all women will have wrinkles appearing at the same rate on the exact location. Some women might have visible glabellar wrinkles, while others have visible nasolabial folds. Our models manage this variability. As the weights of the wrinkles are similar, women with a high grade of glabellar wrinkles will have a similar index value as a woman with a high grade of nasolabial fold (provided that other skin parameters are the same). It gives our model the capacity to assess the global skin aging status of the face.

1. Atlas du vieillissement cutané, Vol.1. Population européenne (R. Bazin & E. Doublet)
2. Atlas du vieillissement cutané, Vol.2 Population asiatique (R. Bazin & F. Flament)
3. Ezure, T., Hosoi, J., Amano, S., & Tsuchiya, T. (2009). Sagging of the cheek is related to skin elasticity, fat mass and mimetic muscle function. Skin Research and Technology, 15(3), 299-305

Advanced metabolic NADH/FAD/FMN FLIM to investigate cell metabolism with focus on human skin cells

A. Rueck[1], J. Wieland[1], K. Reess[1], J. M. Weise[2], T. Blatt[2], and N. Naskar[1]

[1] *University Ulm, Core Facility Optical Microscopy N24, Albert-Einstein-Allee 1189081 Ulm, Germany, Germany: e-mail: angelika.rueck@uni-ulm.de*
[2] *Research and Development, Beiersdorf AG, Unnastrasse 48, Hamburg, 20245, Germany*

KEY WORDS: metabolic FLIM, Q10, OXPHOS

Fluorescence lifetime imaging (FLIM) of metabolic coenzymes, as NAD(P)H and FAD, is now widely accepted to be one of the most important imaging methods for cell metabolism; different algorithms are investigated to get reproducible results. Whereas the intensity based optical redox ratio, defined by Britton Chance in 1979 (Britton Chance et al., J. Biol. Chem., 1979) determines the redox state of cells and distinguishes oxidized from reduced cells a correlation with the fluorescence lifetime is valid only for special conditions, if the NADH/NAD^+ pool is stable. New algorithms are needed to circumvent these problems and to image cell metabolism and redox state from fluorescence lifetimes in complex cellular systems. With respect to this, results will be presented for various cell systems with special attention to human skin cells. The significance of a metabolic index based on NAD(P)H FLIM will be explained and compared with the fluorescence lifetime induced redox ratio (FLIRR) where FLIM of NAD(P)H and FAD is considered (Alam and Periasamy, Sci Rep., 2017). In detail metabolic FLIM was used to demonstrate enhanced oxidative phosphorylation (OXPHOS) in Q10 treated cells. The coenzyme Q10 is known to play an important role in the functioning of the respiratory chain within complex I, II and complex III of the mitochondrial membrane.

Acknowledgment:
This work is supported by the Deutsche Forschungsgemeinschaft DFG, GZ: RU 473/12-1.

ISBS 2022 conference, 2nd – 3rd June 2022, Langenbeck-Virchow-Haus, 10117 Berlin

Advanced metabolic NADH/FAD/FMN FLIM to investigate cell metabolism with focus on human skin cells

A.Rueck[1], J.Wieland[1], K.Reess[1], J.M.Weise[2], T.Blatt[2], S. Kalinina[1]*, and N.Naskar[1]

[1] University Ulm, Core Facility Optical Microscopy, N24, Albert-Einstein-Allee 11, 89081 Ulm, Germany
[2] Research and Development, Beiersdorf AG, Unnastrasse 48, Hamburg, 20245, Germany

angelika.rueck@uni-ulm.de

Introduction

Fluorescence lifetime imaging (FLIM) of metabolic coenzymes, as NAD(P)H, FAD and FMN is now widely accepted to be one of the most important imaging methods for cell metabolism; different algorithms are investigated to get reproducible results. With respect to this, results will be presented for various cell systems with special attention to human skin cells. The significance of a metabolic index based on NAD(P)H FLIM will be explained and compared with the fluorescence lifetime induced redox ratio (FLIRR) where FLIM of NAD(P)H and FAD is considered (Alam and Periasamy, Sci Rep., 2017). In detail metabolic FLIM was used to demonstrate enhanced oxidative phosphorylation (OXPHOS) in Coenzyme Q_{10} treated cells. The CoQ_{10} is known to play an important role in the link within complex I and III, as well as complex II and III of the mitochondrial membrane.

Metabolic coenzymes and energy metabolism, the role of CoQ_{10} in the mitochondrial membrane

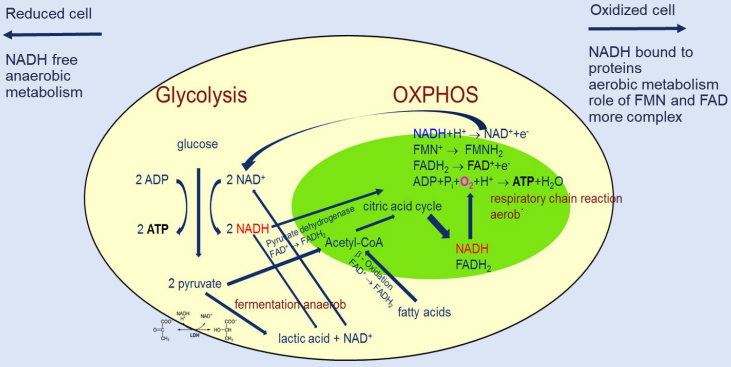

Metabolic coenzymes and metabolic FLIM

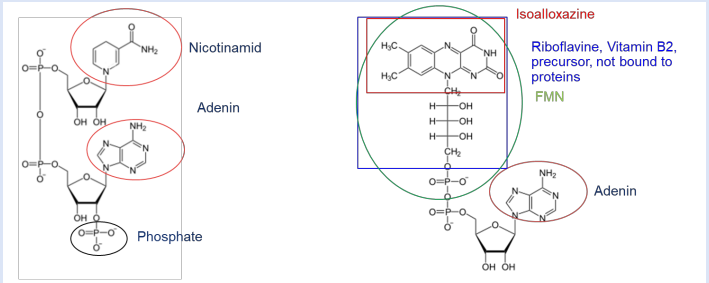

NAD(P)H: Nicotinamid-Adenin-Dinukleotide; exc.360 nm

NAD(P)H is fluorescent at 460 nm, if unbound Φfl: 0,02
at 440 nm, if bound, Φfl: 0,1

FAD/FMN: Flavin-Adenindinukleotide/-mononucleotide; exc.450 nm

FAD^+ is fluorescent at 530 nm, Φfl: 0,04
FMN^+ is fluorescent at 530 nm, Φfl: 0,22

$NADH_{free}$ λ_{em} = 460 nm, $\tau_1 \cong$ 0.4 ns (short)	FAD^+_{free} λ_{em} = 530 nm, $\tau_2 \cong$ 1.7- 1.9 ns (long)
$NADH_{bound}$ λ_{em} = 440 nm, $\tau_2 \cong$ 2.5 ns (long)	FAD^+_{bound} λ_{em} = 530 nm, $\tau_1 \cong$ 0.1- 0.3 ns (short)
	FMN^+_{bound} λ_{em} = 530 nm, $\tau_2 \cong$ 4.5- 6.0 ns (long)

Coenzyme CoQ10

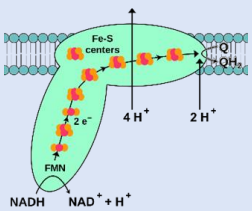

Complex I (NADH-Dehydrogenase)

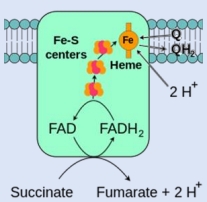

Complex II (Succinate-Dehydrogenase)

$NADH + FMN^+ \longrightarrow NAD^+ + FMNH_2$
$FMNH_2 + Q \longrightarrow FMN^+ + QH_2$

$FAD^+ \longrightarrow FADH_2$
$FADH_2 + Q \longrightarrow FAD^+ + QH_2$

Experimental background: metabolic TCSPC FLIM/PLIM

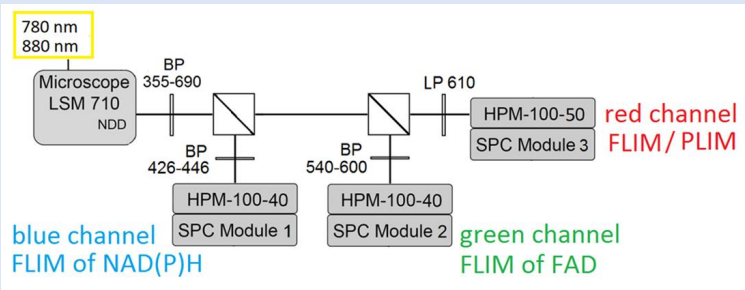

Algorithms: NADH metabolic Index versus FLIRR Indices

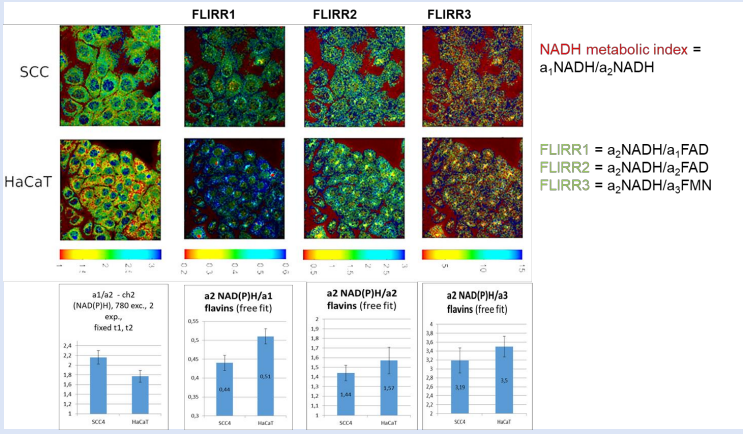

NADH lifetime fitted biexponential
FAD/FMN lifetime fitted triexponential

Cell metabolism and CoQ_{10}: Study on primary fibroblasts NADH fluorescence excitation with 2p 740 nm

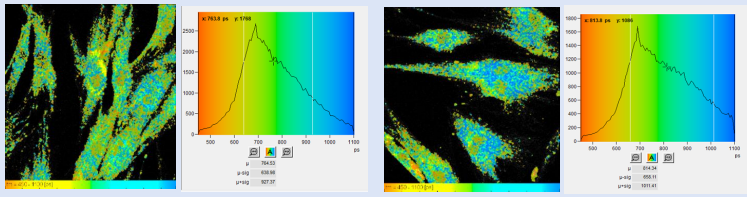

without Q_{10} 24h Q_{10}

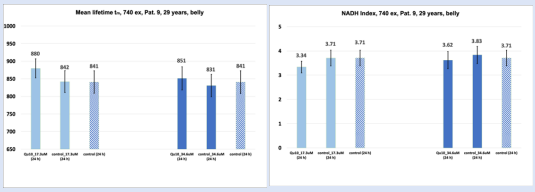

from 9 fibroblasts with different origin
7 showed a significant stimulation of Q10 towards OXPHOS
2 where not significant

Conclusion

Investigation of metabolic NADH FLIM in primary fibroblasts during CoQ_{10} treatment showed significant increase of the NADH lifetime and decrease of the metabolic index, which is correlated with a switch of cell metabolism towards OXPHOS. Further FAD/FMN FLIM and calculation of extended FLIRR will improve mechanistic understanding of CoQ_{10} functioning as well as supercomplex formation within the mitochondrial membrane.

Publications:
Kalinina S, et al., Rück A, J. Biophotonics. e201800085 (2018).
S. Kalinina, et al., A. Rueck, Int. J. Mol. Sci. 2021, 22, 5952.

This work was carried out with financial support by the Company Beiersdorf AG, Unnastrasse 48, Hamburg, Germany, the Ministry of Research and Development, FKZ order: 13N14508 ("OMOXI") and the Deutsche Forschungsgemeinschaft (DFG).

*The work is dedicated to Sviatlana Kalinina who died on September 24th 2021 after a long-term disease.

Image Analysis of Anti-Aging Parameters on Specific Facial Areas after Automated Area-Detection on High Definition Facial Photographs

M. Seise[1], S. Bielfeldt[1], I. Kruse[1], .K-P. Wilhelm[1]

[1]proderm GmbH, Kiebitzweg 2, 22869 Schenefeld
mseise@proderm.de, www.proderm.de

KEY WORDS: Image analysis, facial photography, anti-aging

The human face is a mirror of intrinsic and extrinsic skin aging. Cosmetic treatments are therefore focused to rejuvenate the view of the face by use of decorative cosmetics as well as skincare products. The impression of facial youth and attractiveness are the result of a complex process in the human brain[1]. Nevertheless, an inner judgmental impression as the result of this process arises almost immediately in the consciousness of the observer[1].

Research revealed that visible irregularities of skin surface and pigmentation are key parameters forming the subjective impression of youth and beauty[2].

Image analysis on high definition facial photographs can objectively quantify such irregularities. As they appear in specific regions of the face, e.g. the sun exposed part of the cheek under the eye or the temple, individual detection and recovery of the correct test areas are crucial for a reliable measurement.

The software we introduce here, enables an individual definition of test areas in the images at baseline of a study and their recovery at consecutive time points of cosmetic treatment, even months later.

As an example to demonstrate the advantages of the automated recovery of facial test areas, the facial images of 6 female subjects, 35 years and older with visible pigmentation irregularities were investigated before and after a decorative treatment by a cosmetician.

Our work demonstrates how strongly test area variations produce a bias, when investigating the effect of a decorative cosmetic treatment on pigmentation irregularities. We could show a clear reduction of this bias by using the automated software compared to interactive area definition. Also, the evaluation time and effort could be clearly reduced.

---

[1] Bielfeldt, S., Henss, R., Koop, U., Degwert, J., Heinrich, U., Jassoy, C., ... & Blume, G. (2013). Internet□based lay person rating of facial photographs to assess effects of a cleansing product and a decent cosmetic foundation on the attractiveness of female faces. *International Journal of Cosmetic Science*, *35*(1), 94-98.

[2] Bielfeldt, S., Springmann, G., Seise, M., Wilhelm, K. P., & Callaghan, T. (2018). An updated review of clinical methods in the assessment of ageing skin–new perspectives and evaluation for claims support. *International Journal of Cosmetic Science*, *40*(4), 348-355.

proderm

Image analysis of anti-aging parameters on specific facial areas after automated area-detection on high definition facial photographs

proderm GmbH, M. Seise, S. Bielfeldt, I. Kruse, K.-P. Wilhelm

Introduction

The human face is a mirror of intrinsic and extrinsic skin aging. Cosmetic treatments are therefore focused to rejuvenate the view of the face by use of decorative cosmetics as well as skincare products. The impression of facial youth and attractiveness are the result of a complex process in the human brain . Nevertheless, an inner judgmental impression as the result of this process arises almost immediately in the consciousness of the observer[1]. Research revealed that visible irregularities of skin surface and pigmentation are key parameters forming the subjective impression of youth and beauty[2]. Image analysis on high definition facial photographs can objectively quantify such irregularities. As they appear in specific regions of the face, e.g. the sun exposed part of the cheek under the eye or the temple, individual detection and recovery of the correct test areas are crucial for reliable measurements.

Methods

The proderm Image Analysis Software (PIAS) is an in-house developed software for interactive analysis of various image analysis parameters. It facilitates manual as well as automatic definitions of skin regions to be analyzed. Combined with facial imaging systems, like the proderm USRCliP (Unit for Standardised Clinical Photography, proderm) or VISIA-CR (Canfield, USA) it allows for fully automatic region definitions. It uses a trainable algorithm for detecting facial keypoints like nose, eyes, mouth[3]. These keypoints are used to register pre-defined regions on the investigated face.

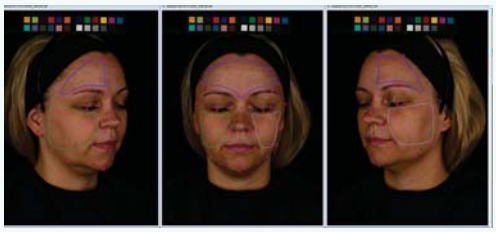

Image 1 Frontal & Side images before makeup application taken with USRCliP including automatically detected key points (pink) and automatically defined regions of cheek and forehead using PIAS (proderm Image Analysis Software)

Experiment

To demonstrate the advantages of the automated recovery of facial test areas, the facial images of 6 female subjects, 35 years and older with visible pigmentation irregularities were investigated before and after a decorative treatment by a cosmetician. Frontal and side pictures were taken by USRCliP. The subjects were acclimated at 22°C and 50% relative humidity for 20 minutes before taking baseline images between the makeup application and before final image acquisition. Pigmentation irregularities were evaluated using two different parameters for homogeneity:

(1) Global unevenness ,H_{76}, is calculated as the standard deviation in CIELAB color space

where l_i, a_i, b_i are the CIELAB values for each pixel and

$$H_{76} = \frac{1}{N} \sum_{i=1...N} \sqrt{(l_i - \mu_l)^2 + (a_i - \mu_a)^2 + (b_i - \mu_b)^2}$$

μ_l, μ_a, μ_b are the average CIELAB values of the region of interest. Lower values are showing less inhomogeneity.

(2) H_b^{lc} as the local homogeneity parameter of CIELAB b*. This parameter is calculated for every pixel as the inverse of the standard deviation of CIELAB b* in a small sub-image realized by a moving window approach. The average value for each region of interest is reported. In this parameter higher values are showing higher homogeneity.

Results

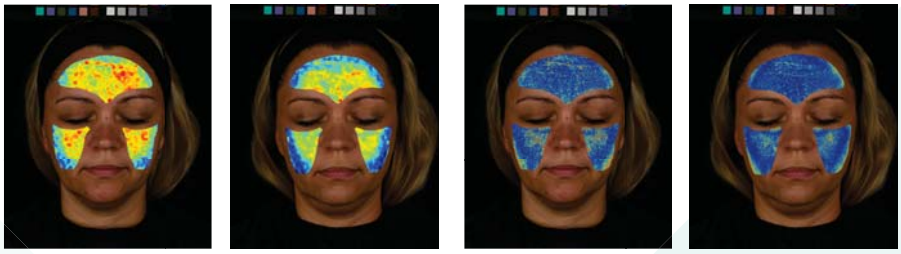

Images 2 - 3 Local homogeneity H_b^{lc} before (left) and after makeup application (right) for subject #2. Red indicates regions of low values of H_b^{lc}, thus low homogeneity.

Images 4 - 5 Global unevenness H_{76} before (left) and after makeup application (right) for subject #2. Red indicates regions of high values of H_{76}, thus low homogeneity.

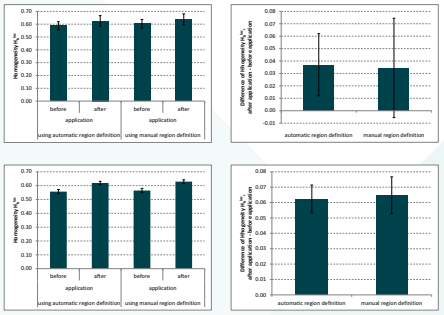

Graphs 1 - 4 The graphs are showing the local homogeneity H_b^{lc} before and after makeup application for all subjects using manual and automatic region detection (1) and separately for subject#7 (3). Further differences between H_b^{lc} after makeup application and before application for all subjects (4) and separately for subject#7 (2) are displayed. The errorbars are showing 95% CI. The difference of H_b^{lc} between before and after application images shows an improvement of the homogeneity after makeup application. The confidence intervals were smaller when using automatic region definition compared to manual definition.

For single subject evaluation, the difference in homogeneity can have a high variation, so that the results are not significant for manual definition of the region of interest, only for the automatic region definition.

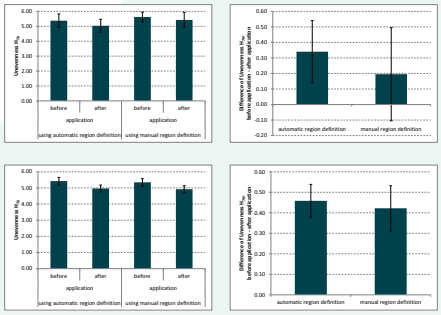

Graphs 5 - 8: The graphs are showing the unevenness H_{76} before and after makeup application for all subjects using manual and automatic region detection (5) and separately for subject#7 (7). Further differences between H_{76} after makeup application and before application for all subjects (8) and separately for subject#7 (6) are displayed. The errorbars are showing 95% CI. The difference of H_{76} between before and after application images shows an improvement of the homogeneity after makeup application. The confidence intervals were smaller when using automatic region definition compared to manual definition.

For single subject evaluation, the difference in homogeneity after manual region detection can have an even higher variation compared to H_b^{lc}. The results are clearly different and not significant for manual definition of the region of interest, compared to the automatic region definition.

Conclusion

Our work demonstrates how strongly test area variations can produce a bias, when investigating uneven skin pigmentation. We could show a reduction of this bias by using the automated definition of areas compared to manual area definition. The moving windows approach could reduce the bias even further.

A clear advantage of the automated software is the reduction of evaluation time as well as the avoidance of subjective influences on the results. Thanks to the automated landmark detection exact fusion of the images with overlay images of other sources (e.g. infrared imaging) is easy.

References

1. Bielfeldt, S., Henss, R., Koop, U., Degwert, J., Heinrich, U., Jassoy, C., ... & Blume, G. (2013). Internet based lay person rating of facial photographs to assess effects of a cleansing product and a decent cosmetic foundation on the attractiveness of female faces. International Journal of Cosmetic Science, 35(1), 94-98.

2. Bielfeldt, S., Springmann, G., Seise, M., Wilhelm, K. P., & Callaghan, T. (2018). An updated review of clinical methods in the assessment of ageing skin—new perspectives and evaluation for claims support. International Journal of Cosmetic Science, 40(4), 348-355.

3. Davis E. King. Dlib-ml: A Machine Learning Toolkit. Journal of Machine Learning Research 10, pp. 1755-1758, 2009

Clinical Knowledge Enabled Deep Learning Networks for Skin Cancer Detection

Yuheng Wang[1,2,3,4], Jiayue Cai[5,6], Daniel Louie[1,2,3,4], Z. Jane Wang[1,5], Harvey Lui[2,3,4], Tim K. Lee[1,2,3,4,*]

[1.] School of Biomedical Engineering, University of British Columbia, Vancouver, BC, Canada
[2.] Department of Dermatology and Skin Science, University of British Columbia, Vancouver, BC, Canada
[3.] Photomedicine Institute, Vancouver Coast Health Research Institute, Vancouver, BC, Canada
[4.] Departments of Cancer Control Research and Integrative Oncology, BC Cancer, Vancouver, BC, Canada
[5.] Department of Electrical and Computer Engineering, University of British Columbia, Vancouver, BC, Canada
[6.] School of Biomedical Engineering, Health Science Center, Shenzhen University, Shenzhen, China
[.] Corresponding Author e-mail address and URL: tlee@bccrc.ca*

KEY WORDS: 7-Point checklist, Multi-modality, Melanoma detection

The 7-point checklist is one of the most well-known and well-validated dermoscopic algorithms for melanoma screening. The method comprises three major (atypical network, blue-white veil, and atypical vascular pattern) and four minor criteria (irregular streaks, irregular dots, irregular blotches, and regression structures). Two and one point are allocated to each major and minor criterion, respectively. A minimum of 3 points would identify a melanoma. Several deep learning studies have recently attempted to detect melanoma using all seven content-based features simultaneously; however, these systems did not distinguish between the major and minor criteria of the checklist. In this project,[1] we developed a deep network that fully employed clinical domain knowledge of the checklist's major and minor criteria and the scoring mechanism. To improve the detecting accuracy, the proposed deep architecture allowed dermoscopic and clinical images, if available, to be processed together. Deep features were independently extracted by parallel networks and classified into 7 criterion classes, where the major and minor criteria were considered and handled by a constrained classifier chain method. The order within the major and minor categories was optimized based on the training data. Finally, the seven-point checklist scoring method was applied, i.e. 2 and 1 scoring points and a minimum of 3 points for identifying a melanoma. The proposed framework was trained and tested using 1,011 paired dermoscopic and clinical images and matched 7-point checklist annotations acquired from a publicly available dataset. The testing results demonstrated a substantial improvement over melanoma detection with an average accuracy of 81.3%, outperforming state-of-the-art methods in the literature. The resultant technique would potentially make the deep learning approach more interpretable and enhance diagnostic accuracy by incorporating expert clinical knowledge.

[1]Wang, Y., et al. "Incorporating Clinical Knowledge with Constrained Classifier Chain into a Multimodal Deep Network for Melanoma Detection." Computers in Biology and Medicine 137.2(2021):104812.

Clinical Knowledge Enabled Deep Learning Networks for Skin Cancer Detection

Yuheng Wang[1,2,3,4], Jiayue Cai[5,6], Daniel Louie[1,2,3,4], Z. Jane Wang[1,5], Harvey Lui[2,3,4], Tim K. Lee[1,2,3,4,*]

[1.] School of Biomedical Engineering, University of British Columbia, Vancouver, Canada
[2.] Department of Dermatology and Skin Science, University of British Columbia, Vancouver, Canada
[3.] Photomedicine Institute, Vancouver Coast Health Research Institute, Vancouver, Canada
[4.] Departments of Cancer Control Research and Integrative Oncology, BC Cancer, Vancouver, Canada
[5.] Department of Electrical and Computer Engineering, University of British Columbia, Vancouver, Canada
[6.] School of Biomedical Engineering, Health Science Center, Shenzhen University, Shenzhen, China
[*.] Corresponding Author e-mail address and URL: tlee@bccrc.ca

Background

- Incorporating clinical domain knowledge has become a new trend in applying AI to medical problems
- The 7-point checklist is one of the well-known and validated dermoscopic algorithms for melanoma detection
- Considering the dependencies between criteria of 7-point checklist will help the interpretation of AI prediction

Objective

- Propose a novel multimodal deep learning framework for automatic melanoma detection
- Fully utilized the clinical knowledge and made use of the major and minor criteria of the checklist

Table 1. An overview of 7-point checklist.

Criteria	*Abbreviation*
Pigment network	**PN**
Blue-whitish veil	**BWV**
Vascular structures	**VS**
Streaks	STR
Pigmentation	PIG
Dots and globules	DaG
Regression structures	RS

Bold ones refer to major criteria.

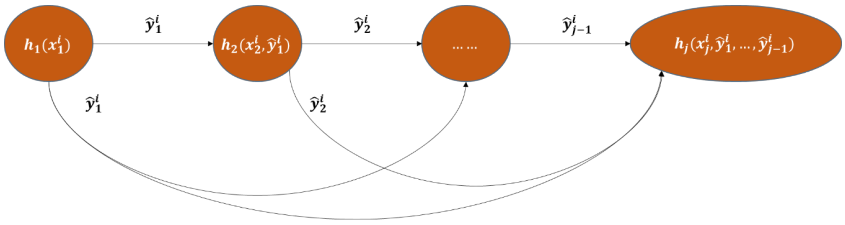

Fig.1. A graphical illustration of the classifier chain

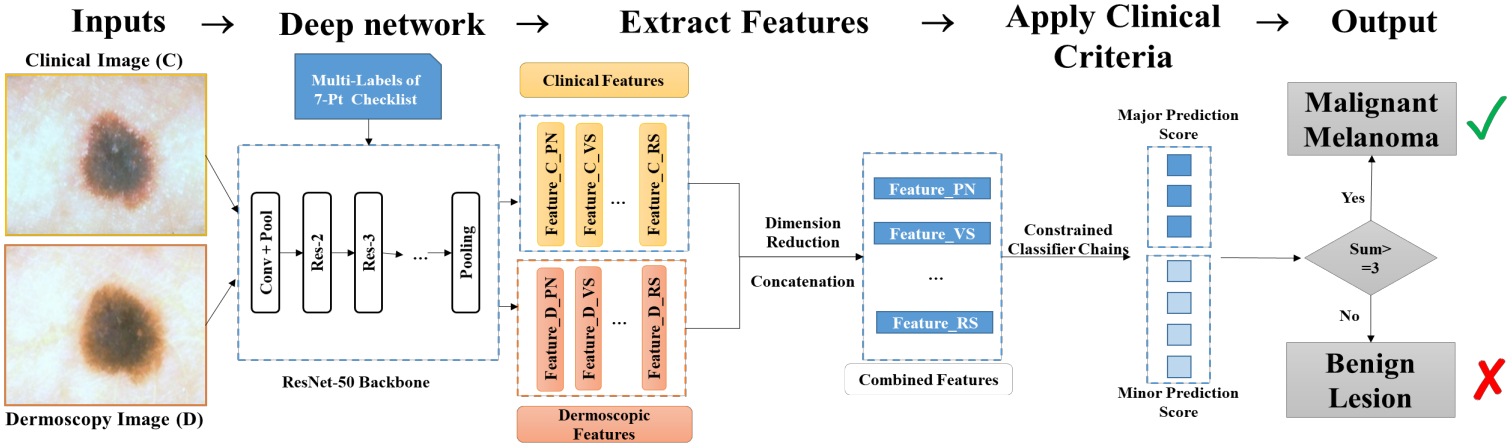

Fig.2. An overview of the proposed workflow for malignant melanoma detection

Method

- 1011 pairs of dermoscopic images and clinical images with 7-point annotations
- ResNet-based deep convolutional neural networks for classification
- Clinically constrained classifier chain is used to optimized the order of criteria for melanoma

Results and Conclusion

- An average accuracy of 81.3% for detecting melanoma and all 7 criteria
- Incorporating the clinical knowledge and providing human-interpretable results
- Utilization of clinical features help physicians to interpret the results

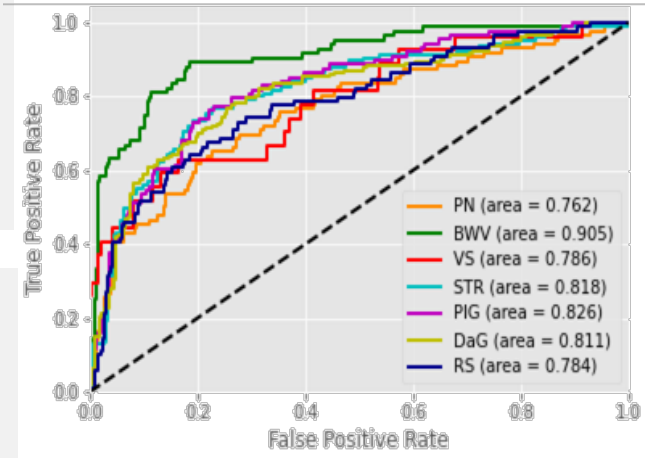

Fig.3. ROC curve for all 7-point checklist

Link to the peer-reviewed publication

SCAN ME

Dermoscopy Imaging with a Compact Multiphoton Tomograph for Prediction of Malignant Melanoma

M. Warzecha[1], Ł. Piątek[2], J. Dąbrowski[3], P.Prinke[4], J. Haueisen[4], K. König[1,5]

[1]*JenLab GmbH, Johann-Hittorf- Straße 8, 12489 Berlin; info@jenlab.de*
[2]*Facultiy of Applied Information Technology, University of Information Technology and Management, Sucharskiego 2, 35-225 Rzeszów, Poland*
[3]*Info-Projekt IT Sp. z. o.o., Ul. Załeska 63b, 35-332 35-225 Rzeszów, Poland*
[4]*Institute of Biomedical Engineering and Informatics, Technische Universität Ilmenau, 98693 Ilmenau, Germany*
[5]*Department of Biophotonics and Laser Technology, Saarland University, Campus A5.1, 66123 Saarbrücken, Germany*

KEY WORDS: Dermoscopy, multiphoton tomography, deep learning, artificial intelligence

Dermoscopy as a rapid and non-invasive method offers great potential for detecting changes of the skin surface, but cannot provide high-resolution images from deeper skin layers. Examination of the suspicious skin areas by means of multiphoton tomography using pulsed laser radiation also provides information from the cellular and subcellular areas[1]. The MPT*compact*™ of JenLab GmbH provides the acquisition of dermoscopy images by a CMOS camera with LED lighting, as well as the generation of multiphoton (MP) images, Second Harmonic Generation (SHG), Fluorescence Lifetime Imaging (FLIM) and confocal reflection realized by a femtosecond NIR-laser. The software-controlled menu navigation of the system allows the user to select any point on the recorded dermoscopic image and then to generate a multi-photon investigation at the desired position. Stolz et al. have developed a scoring method to assess whether a suspected lesion is benign or malignant by applying a relatively simple ABCD rule to a skin pattern[2,3]. Other groups developed similar evaluation criteria, namely the 7-point check list[4] or chaos and clues[5]. Due to a relatively large number of dermoscopy data, which were generated in a clinical multimodal multiphoton study on suspicious pigmented lesions, already presented by König et al.[6], we were able to examine the data using algorithms and deep learning methods. First evaluations of dermoscopic data revealed that the pictures can be used for cancer prediction in the early stage. Additionally, the association between dermoscopy and FLIM results, such as fluorescence lifetimes, is examined in this study. Therefore, using computer-aided diagnosis, the MPT*compact* is excellently suited to support the physician in diagnosing skin cancer and to minimizing surgical interventions.

We acknowledge financial support from the Federal Ministry of Education and Research under the DigiSkinDia-project (project number 01DS19012B).

---

[1] K. König, "Multiphoton Tomography (MPT)," in *Multiphoton Microscopy and Flourescence Lifetime Imaging*, De Gruyter, 2018.
[2] Stolz, W., Reimann, A. and Cognetta, A. B. : "ABCD rule of dermatoscopy: A new practical method for early recognition of malignant melanoma." *European Journal of Dermatology,* Vol. 4, No. 7, pp. 521 – 527, (1994).
[3] Stolz, W., et al.: *Farbatlas der Dermatoskopie.* Stuttgart: Thieme Verlagsgruppe, 2004.
[4] Argenziano, G. et al.: "Epiluminescence Microscopy for the Diagnosis of Doubtful Melanocytic Skin Lesions", *Archives of Dermatology,* Vol. 134, No.12, pp. 1563 – 1570, (1998).
[5] Rosendahl, C. (2014) "Dermatoscopy: Chaos and Clues". *Practical Dermatology*.
[6] König. K., Pankin, D., Paudel, A., Hänßle H., Winkler, J. K., Ziegler, M., Kaatz, M.:"Skin Cancer Detection with a Compact Multimodal Fiber Laser Multiphoton FLIM Tomograph" Proc. SPIE 11648, Multiphoton Microscopy in the Biomedical Sciences XXI, 116480A (2021).

Dermoscopy Imaging with a Compact Multiphoton Tomograph for Prediction of Malignant Melanoma

M. Warzecha[1], G. Breunig[1], D. Pankin[1], Ł. Piątek[3], G. Lisowicz[4], P. Prinke[2], J. Haueisen[2], K. König[1,5]

[1]JenLab GmbH, Johann-Hittorf- Straße 8, 12489 Berlin, info@jenlab.de

[2]Institute of Biomedical Engineering and Informatics, Technische Universität Ilmenau, 98693 Ilmenau, Germany

[3]Faculty of Applied Information Technology, University of Information Technology and Management, Sucharskiego 2, 35-225 Rzeszów, Poland

[4]Info-Projekt IT Sp. z. o.o., Ul. Załeska 63b, 35-332 35-225 Rzeszów, Poland

[5]Department of Biophotonics and Laser Technology, Saarland University, Campus A5.1, 66123 Saarbrücken, Germany

Abstract

Dermoscopy as a rapid and non-invasive method offers great potential for detecting changes in the skin surface, but cannot provide high-resolution images from deeper skin layers. Examination of the suspicious lesions by multiphoton tomography (MPT) provides additional information from inside the skin with subcellular resolution [1]. The tomograph MPT*compact*™ provides dermoscopy images by a CMOS camera with LED lighting as well as autofluorescence (AF) images, Second Harmonic Generation (SHG) images, Fluorescence Lifetime Imaging (FLIM), and confocal reflection images. The software-controlled menu navigation of the system allows the user to select any point on the recorded dermoscopic image and then to perform a multiphoton investigation at the desired position.

Stolz et al. have developed a scoring method to assess whether a suspected lesion is benign or malignant by applying a relatively simple ABCD rule to a skin pattern [2,3]. Other groups developed similar evaluation criteria, namely the 7-point checklist [4] or chaos and clues [5]. Due to a relatively large number of dermoscopy data, which were generated in a clinical multimodal multiphoton study on suspicious pigmented lesions, already presented by König et al. [6], we were able to examine the data using algorithms and deep learning methods. First evaluations of dermoscopic data revealed that the pictures can be used for cancer prediction at an early stage. Additionally, the association between dermoscopy and FLIM results, such as fluorescence lifetimes, is examined in this study. Therefore, using computer-aided diagnosis, the MPT*compact* is excellently suited to support the dermatologist in diagnosing skin cancer and to minimizing surgical interventions.

Concept

MPT*compact*

Femtosecond laser system combined with a LED camera for acquisition of multiphoton and white light images.

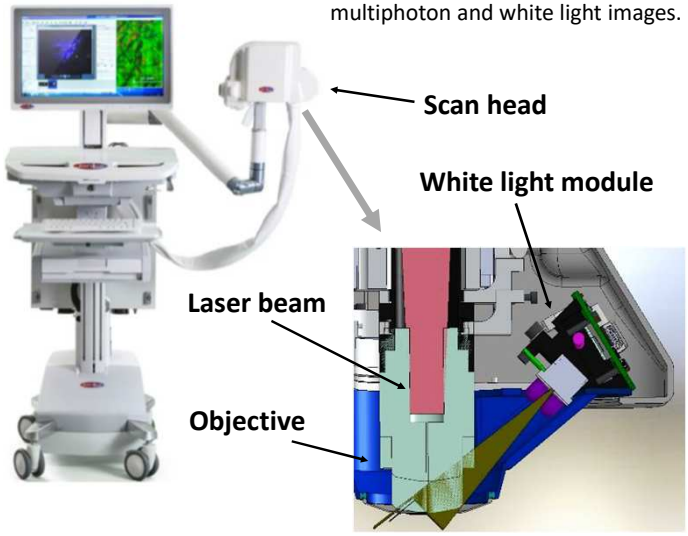

- White light image (10 mm x 10 mm) recording in bmp-format
- By clicking with a computer mouse on the white light image, the laser focus can be moved to the desired location for MP measurement.

→ Data acquisition from clinical studies (100 patients) to determine the symmetry from the criteria of the ABCD rule [2,3], the 7-point checklist [4], or the Chaos and Clues [5].
→ Determination of specificity and sensitivity.

Project partners

JenLab

TECHNISCHE UNIVERSITÄT ILMENAU

UNIVERSITY of INFORMATION TECHNOLOGY and MANAGEMENT in Rzeszow, POLAND

Info-Projekt IT Spółka z o.o.

Analysis

Application of Symmetry Algorithms:

Total Dermoscopy Score = 1.3 x [Score_A]
+ 0.1 x [Score_B] + 0.5 x [Score_C] + 0.5 x [Score_D]

Examples of white light images + analysis:

Whitelight image	Naive approach	Symmetry	Score_A	Medical diagnosis
	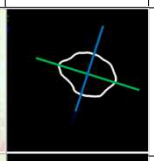	2 axes	0	Benign
		2 axes	0	
		1 axis	1	Malignant
	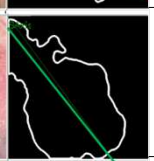	1 axis	1	
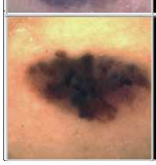	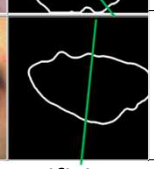	1 axis	1	

Specificity: 78.8%, Sensitivity: 37.2 %

Conclusion

- A camera module for white light recordings of skin lesions integrated into the tomograph MPT*compact* can be used for dermoscopy.
- Verification of the whole system was performed in clinical studies.
- Specificity of up to 78.8 % for the symmetry determination in the dermoscopic images calculated.
- Next step: Evaluation of multiphoton combined with dermoscopic images.

Acknowledgement

We acknowledge financial support from the Federal Ministry of Education and Research under the DigiSkinDia-project (project number 01DS19012B).

References

[1] K. König, "Multiphoton Tomography (MPT)", in *Multiphoton Microscopy and Fluorescence Lifetime Imaging*, De Gruyter, 2018.

[2] Stolz, W., Reimann, A. and Cognetta, A. B. : "ABCD rule of dermatoscopy: A new practical method for early recognition of malignant melanoma." *European Journal of Dermatology,* Vol. 4, No. 7, pp. 521 – 527, (1994).

[3] Stolz, W., et al.: *Farbatlas der Dermatoskopie.* Stuttgart: Thieme Verlagsgruppe, 2004.

[4] Argenziano, G. et al.: "Epiluminescence Microscopy for the Diagnosis of Doubtful Melanocytic Skin Lesions", *Archives of Dermatology,* Vol. 134, No.12, pp. 1563 – 1570, (1998).

[5] Rosendahl, C. (2014) "Dermatoscopy: Chaos and Clues". *Practical Dermatology*.

[6] König. K., Pankin, D., Paudel, A., Hänßle H., Winkler, J. K., Ziegler, M., Kaatz, M.:"Skin Cancer Detection with a Compact Multimodal Fiber Laser Multiphoton FLIM Tomograph" Proc. SPIE 11648, Multiphoton Microscopy in the Biomedical Sciences XXI, 116480A (2021).

Direct Diode Pumped Ti:sapphire Oscillator for Biomedical Imaging

Marco Andreana[1], Caterina Sturtzel[2], Ming Yang[3], Richard Latham[4], Rainer A. Leitgeb[1], Wolfgang Drexler[1], Manuel Zimmer[4], Tuan Le[3], Martin Distel[2], and Angelika Unterhuber[1]

[1] Center for Medical Physics and Biomedical Engineering, Medical University Vienna, 1090 Vienna, Austria; [2]Innovative Cancer Models, St. Anna Children's Cancer Research Institute, 1090 Vienna, Austria;[3] VIULASE GmbH, 1230 Vienna, Austria;[4]Research Institute of Molecular Pathology (IMP), Vienna Biocenter (VBC), 1030 Vienna, Austria.

ming.yang@viulase.com

KEY WORDS: biomedical microscopy, ultrafast laser, laser applications

Among various optical imaging modalities, nonlinear optical microscopy is extremely powerful for multimodal contrast imaging capable to deliver functional, molecular and morphological information in living systems. However, the widespread of this technology strongly depends on the integration of highly sophisticated laser systems ensuring optimized signal excitation by providing the best balance among peak power, average power, and optical noise. We have developed a 5nJ direct diode pumped femtosecond Kerr-lens-mode-locked Ti:sapphire oscillator in order to relax the complexity, the footprint and the cost of conventional Ti:saphhire oscillators. For optimal biomedical optical imaging, the pulsed laser emission has a nominal repetition rate of 80MHz and 440mW mode-locked output power. The wavelength is centered at 805nm with a spectral bandwidth of 15nm allowing for two-photon excited fluorescence (TPEF) and second harmonic generation (SHG) microscopy. Moreover, noise performance and beam quality are characterized and results are comparable and in good agreement with conventionally used Ti:sapphire oscillator pumped by diode pumped solid state lasers. Due to the low noise performance of the direct diode pumped scheme, we demonstrate a stable supercontinuum from a photonic crystal fiber to create an inherently synchronized Stokes beam centered at 1050nm used for coherent anti-Stokes Raman scattering (CARS) microscopy. An in vivo imaging of C. elegans and zebrafish larvae with SHG, CARS and multicolor TPEF of green fluorescent protein was performed.

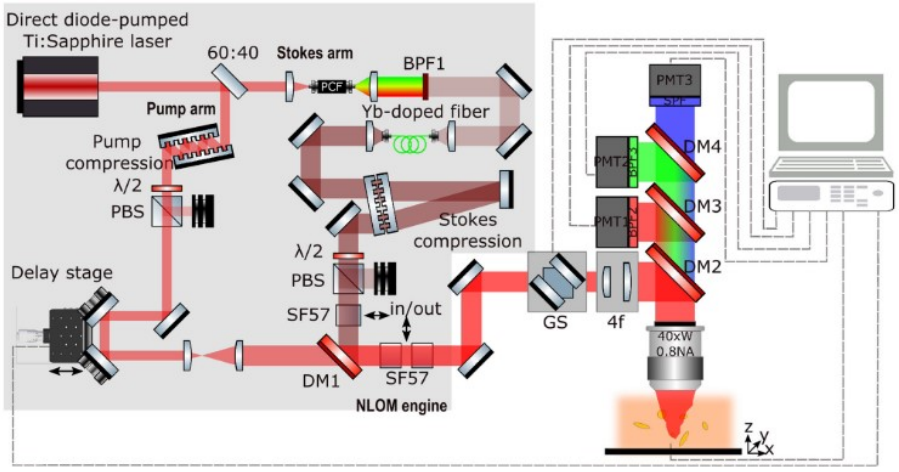

Figure 1: Multimodal nonlinear optical microscopy setup based on direct diode pumped Ti:Sapphire laser. BPF, band-pass filter; PMT, photomultiplier tube; DM, dichroic mirror; GM, galvanometric scanning mirrors.

Direct Diode Pumped Ti:sapphire Oscillator for Biomedical Imaging

Marco Andreana[1], Caterina Sturtzel[2], Ming Yang[3*], Richard Latham[4], Rainer A. Leitgeb[1], Wolfgang Drexler[1], Manuel Zimmer[4], Tuan Le[3], Martin Distel[2], and Angelika Unterhuber[1]

[1] Center for Medical Physics and Biomedical Engineering, Medical University Vienna, 1090 Vienna, Austria; [2]Innovative Cancer Models, St. Anna Children's Cancer Research Institute, 1090 Vienna, Austria;[3] VIULASE GmbH, 1230 Vienna, Austria;[4]Research Institute of Molecular Pathology (IMP), Vienna Biocenter (VBC), 1030 Vienna, Austria. *Email:ming.yang@viulase.com

Abstract:

Among various optical imaging modalities, nonlinear optical microscopy is extremely powerful for multimodal contrast imaging capable to deliver functional, molecular and morphological information in living systems. However, the widespread of this technology strongly depends on the integration of highly sophisticated laser systems ensuring optimized signal excitation by providing the best balance among peak power, average power, and optical noise. We have developed a 5nJ direct diode pumped femtosecond Kerr-lens-mode-locked Ti:sapphire oscillator in order to relax the complexity, the footprint and the cost of conventional Ti:saphhire oscillators. For optimal biomedical optical imaging, the pulsed laser emission has a nominal repetition rate of 80MHz and 440mW mode-locked output power. The wavelength is centered at 805nm with a spectral bandwidth of 15nm allowing for two-photon excited fluorescence (TPEF) and second harmonic generation (SHG) microscopy. Moreover, noise performance and beam quality are characterized and results are comparable and in good agreement with conventionally used Ti:sapphire oscillator pumped by diode pumped solid state lasers. Due to the low noise performance of the direct diode pumped scheme, we demonstrate a stable supercontinuum from a photonic crystal fiber to create an inherently synchronized Stokes beam centered at 1050nm used for coherent anti-Stokes Raman scattering (CARS) microscopy. An in vivo imaging of C. elegans and zebrafish larvae with SHG, CARS and multicolor TPEF of green fluorescent protein was performed.

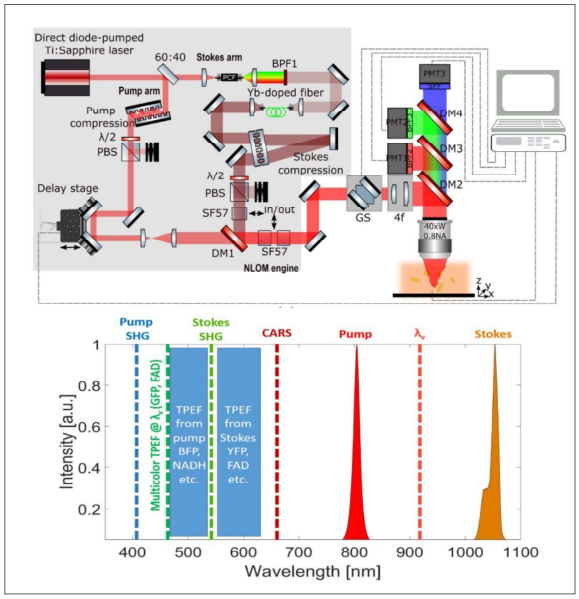

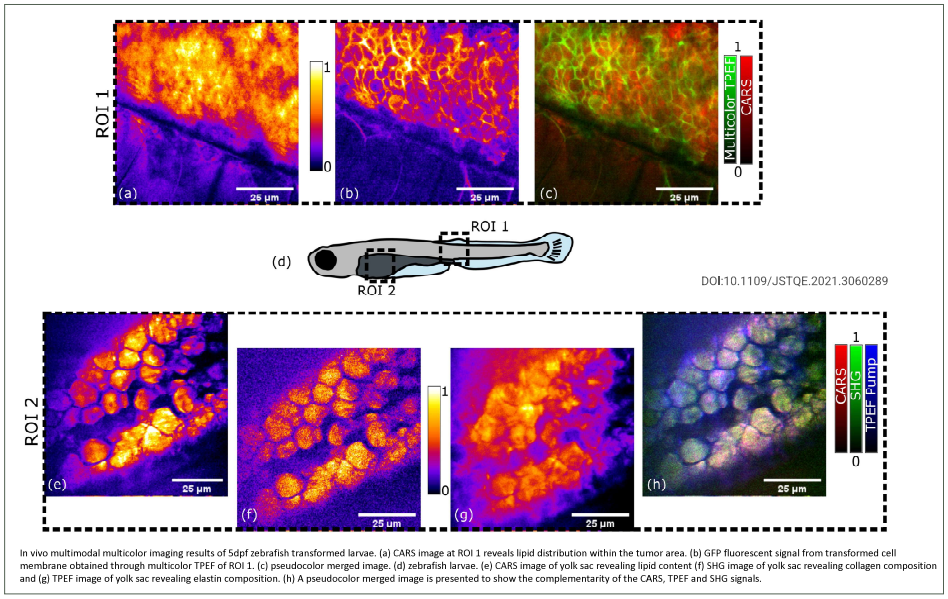

In vivo multimodal multicolor imaging results of 5dpf zebrafish transformed larvae. (a) CARS image at ROI 1 reveals lipid distribution within the tumor area. (b) GFP fluorescent signal from transformed cell membrane obtained through multicolor TPEF of ROI 1. (c) pseudocolor merged image. (d) zebrafish larvae. (e) CARS image of yolk sac revealing lipid content (f) SHG image of yolk sac revealing collagen composition and (g) TPEF image of yolk sac revealing elastin composition. (h) A pseudocolor merged image is presented to show the complementarity of the CARS, TPEF and SHG signals.

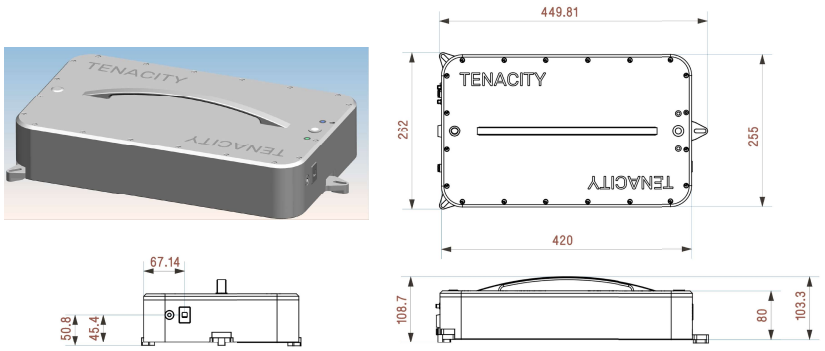

Compactness

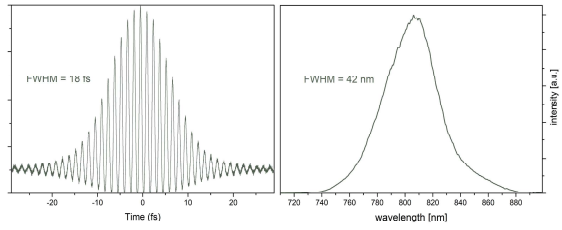

Beam Quality

Divergency H	0.5 mrad
Divergency V	0.9 mrad
M^2 Horizontal	1.07
M^2 Vertical	1.14

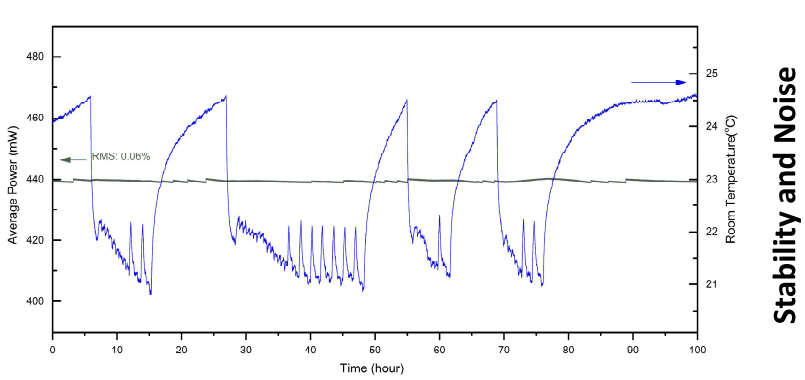

Stability and Noise

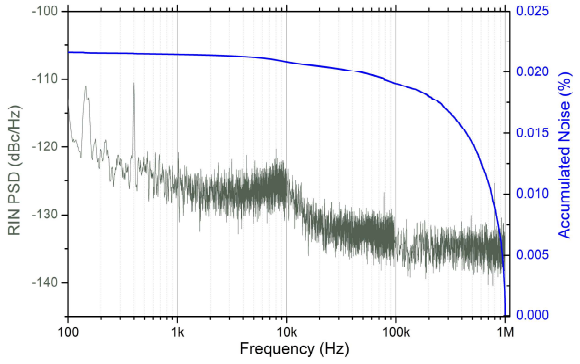

Conclusion:

The multimodal imaging experiment demonstrated that a direct diode pumped Ti:sapphire oscillator is capable of serving as the light source in a bioimaging experiment. The combination of its excellent performance, its outstanding compactness and potential cost reduction of the laser outperform the traditional Ti:sapphire lasers and ultrafast fiber lasers. Therefore, it is an ideal laser source for the bioimaging applications.

Project supported by austria wirtschafts service aws

Development of an in-vitro platform for dynamic maturation of lab grown skin tissues

Hamza Zaidi[1], Stéphane Avril[2] and Christophe Marquette[1]
1 : Institut de Chimie et Biochimie Moléculaires et Supramoléculaires (ICBMS) UMR 5246, Université Lyon 1, Lyon, France
2 : INSERM Sainbiose U1059, Ecole Nationale Supérieure des Mines de St Etienne, France
Corresponding author email: hamza-raza.zaidi@univ-lyon1.fr

KEY WORDS: Skin Bioreactor, Maturation, Tissue model

Skin is the largest organ of the human body. Natural human skin growth occurs simultaneously as the human body is exposed to multiple stresses and environmental conditions. So far, current skin models have not been able to achieve mimicking these stresses during the development of skin. There has yet not been a dedicated bioreactor available in the market for dynamic maturation of skin tissues.

A new bioreactor platform has been developed and validated based on the principles of fluid dynamics. This bioreactor is simple to use, has a defined air / liquid interface mechanism, avoids degradation & contraction of skin structure, provides mechanical forces in a controlled manner and delivers continuous maturation to cells embedded in the skin hydrogel. The bio-ink consisting of fibroblasts and keratinocytes cells used on this bioreactor was developed in the group previously for scaffold free skin bioprinting[1]. This whole bioreactor setup is designed to fit on standard 6 and 12 well plates and the whole setup can be placed on any laboratory shaking system. Also, the bottom of the bioreactor is open to expose the hydrogel for microscopy. At this orientation, the skin maturation can be visualized in real-time during its development.

Computational fluid dynamics simulation studies showed the fluid velocity and shear stress around the skin hydrogel can be controlled using various shaking parameters. Initial results using this bioreactor device validate the design principle and are matching the expected hypothesis. Preliminary results using this bioreactor demonstrates higher collagen production, higher cellular viability, reduced hydrogel degradation and faster skin maturation. This bioreactor could be used for in-vitro skin model production.

1. Pourchet, L. J. *et al.* Human Skin 3D Bioprinting Using Scaffold-Free Approach. *Adv. Healthc. Mater.* **6**, (2017).

Exhibiting Companies

In alphabetical order

Courage + Khazaka electronic GmbH
Skin Testing Instruments as a Solution for a Variety of Tasks

Beate Becker

info@courage-khazaka.de; www.courage-khazaka.de

KEY WORDS: parameters, testing, skin properties

Courage + Khazaka electronic GmbH is the world market leader for scientific measurement tools to objectively quantify a complete range of parameters (sebum, moisture, pH, TEWL, elasticity, melanin, colour, roughness, gloss, lines and wrinkles and others) on the skin. The instruments are standard in dermatology and cosmetology and are used for efficacy testing and claim support as well as basic research.

Cutometer® dual MPA 580

The Multiprobe Adapter System MPA is modular and can therefore be configurated according to the required measurement parameters. The versatile software MPA CTplus makes it easy to create a full study and handle all measurement data.

The imaging systems give information on the topography of the skin: The Visioscan® VC 20plus evaluates lines and wrinkles, the MoistureMap MM 200 shows the moisture distribution over the stratum corneum and the Visioface® RD allows high resolution full face photography. Other instruments evaluate pores, dandruff on the scalp or the skin behaviour during suction.

For the growing field of in-vitro measurements the Tewitro® TW 24 is a valuable tool to measure the water evaporation from cultured tissue sets (wells in a plate with medium) in up to 24 wells simultaneously with the worldwide most used open chamber measurement of the Tewameter®.

A completely new approach for investigation of skin properties in connection with applied substances leads to the development of the Drop Angle Meter DM 300. The analysis of the shape of a drop applied to the skin (or other materials) gives a value for the wettability. This information can be used for testing the effect of products on the skin or the water repellence of substances.

The SPF Skin Scan HDRS 290 is another future innovative development. It allows quick and painless in-vivo SPF testing being based on LED Hybrid Diffuse Reflectance Spectroscopy.

Boiler

Damae Medical is reinventing skin imaging, revolutionizing the screening, management, and follow-up of skin cancers (melanoma and carcinoma) with its deepLive™ solution, which provides an accurate, fast and reliable optical examination without performing a biopsy.

CE marked, the deepLive™ medical device is based on LC-OCT (Line-field Confocal Optical Coherence Tomography) proprietary optical imaging technology that provides 3D images of the different layers of the skin at the cellular level, complemented by several software and Artificial Intelligence (AI) modules.

This innovation is protected by 6 patent families and has already been published in more than 50 scientific and medical publications.

Present in 10 countries and used in more than 30 referral centers, deepLive™ transforms the daily practice of dermatologists making the management of skin pathologies efficient, reassuring, and non-invasive for the patient.

The product is also used by leading cosmetic and pharmaceutical players for research and evaluation purposes.

Based in Paris, Damae Medical currently employs 25 people. Winner of several innovation awards (MIT Technology Review, Bpifrance, European Commission), the company has been able to invest more than €20 million since its creation in 2014.

www.damae-medical.com

Innovative manufacturer of solid-state and fiber lasers, from customized systems to small and medium OEM series. In-house R&D team and more than 27 years of experience ensure professional laser design, customization and manufacturing of reliable and state of the art products. 76 out of the 100 top universities use EKSPLA lasers. Customers like CERN, NASA, ELI, Max Planck Institutes, Cambridge University, Massachusetts Institute of Technology and Japan University of Science showed trust in Ekspla lasers & systems.

A broad range of available laser parameters, such as pulse duration, wavelength, average power, pulse energy, repetition rate and others make it easy to select an appropriate laser source from EKSPLA and to tailor it, if needed, for various applications. A wide range of available options, accessories and modifications enable you to tailor lasers to better fit your requirements.

PhotoSonus X

High Output Power DPSS Tunable Laser for Photoacoustic Imaging

FEATURES

- *Ultra-wide signal tuning range from 660 to 1300 nm*
- *Fully motorized wavelength tuning*
- *High, up to 90 mJ pulse energy from OPO*
- *100 Hz or 50 Hz pulse repetition rate*
- *Fast Wavelength Switching*

PhotoSonus X is a perfect solution for photoacoustic imaging in pre-clinical and clinical use and when fast sample scanning is required. Having high output energy of up to 90 mJ at the peak, a broad wavelength tuning range from 660 to 2600 nm, high pulse repetition rate up to 100 Hz and fast wavelength switching makes it a perfect photoacoustic imaging source for high-resolution images and high data acquisition rate. Being built on a DPSS laser platform, PhotoSonus X assures significantly quieter operation (<60 dB) compared with flash-lamp pumped lasers, which is very beneficial for clinical use. Diode pumped laser technology and well-engineered system design ensures high reliability and low-cost system operation. PhotoSonus X output can be coupled with almost any type of fiber bundle.

PhotoSonus M

High Energy, Mobile, Tunable Wavelength Laser Source for Photoacoustic Imaging

FEATURES

- *Wide tuning range from 330 to 2300 nm*
- *Ultra-wide OPO signal tuning range from 660 to 1320 nm*
- *High up to 250 mJ output energy*
- *10 Hz or 20 Hz pulse repetition rate*
- *Integrated pump laser, OPO and PSU in single mobile unit*

Following the demand for high output energies in the photoacoustic market for imaging larger volumes of tissue, PhotoSonus M, an updated high energy tunable laser source for photo-acoustic imaging, was introduced. Time-tested Ekspla nanosecond pump laser, parametric oscillator, power supply and cooling unit are integrated in a single robust housing to provide mobility, ease of use and low maintenance cost. It is fully motorized and computer controlled, with user trigger outputs and inputs and special options such as motorized switching between OPO Signal and Idler, motorized attenuator, internal energy meter and electromechanical output shutter.
For convenience, the outputs of PhotoSonus M and PhotoSonus M+ lasers can be coupled with almost any type of fiber bundle.

EKSPLA
SAVANORIU AV. 237, LT-02300 VILNIUS, LITHUANIA TEL +370 5 2649629 E-MAIL SALES@EKSPLA.COM WWW.EKSPLA.COM

EOTECH presentation

Jean-Jacques SERVANT[1]
Eotech, 1 ZI du fond des Près, 91460 Marcoussis France
jj.servant@eotech.fr, www.eotech-sa.com

KEY WORDS: Skin measurement, Skin surface, 3D shape, volume, efficacy

The Eotech Company develops and manufacture non-contact 2D/3D imaging based measuring solutions as well as thermography camera for skin research and evaluation of cosmetic products and treatments efficacy.

We have developed complete solutions for multi-scaling analysis of the skin relief ranging from pores, fine lines and wrinkles to shape and volume of the face or parts of the body.

The combination of positioning benches, 3D scanners based on fringe projection technique and powerful software allow to record reproducible data and perform automated evaluations over a complete study.

Products:

- AEVA-HE: Universal solution for skin, face and body 3D measurements
- dermaTOP-HE : Dedicated to measure local areas of the face with the highest definition
- Evaskin : Standard solution for fine lines and wrinkles 3D measurements
- Evaface : Standard solution for face ageing analysis
- VisioTOP benches: Table top benches for panelist repositioning
- EvaTHERM: Infrared camera for temperature changes evaluation on skin, face and body
- CBright: Standardized and compact Photo Studio.

iThera Medical develops and markets optoacoustic imaging (OAI) systems for preclinical and clinical research. OAI utilizes the photoacoustic effect to visualize and quantify optical contrast at several millimeters to centimeters depth, at high spatiotemporal resolution. In the context of dermatology, OAI has shown the potential to visualize and quantify changes in vascular morphology as well as skin perfusion and oxygenation associated with inflammatory skin diseases and skin cancer.

Experts in Femtosecond Laser Technology

JenLab GmbH was founded as High-Tech spin-off company of the Friedrich Schiller University Jena in 1999 in Jena (Germany).

JenLab pioneered clinical multiphoton tomography (MPT) and femtosecond laser nanoprocessing microscopy in Life Sciences.

The company is technology provider of the multiphoton tomographs *DermaInspect*, MPTf*lex*, and MPT*compact*. The major application is high-resolution *in vivo* human skin imaging. Optical *in vivo* biopsies are provided label-free within seconds with 0.3 µm lateral and 2 µm axial resolution by latest turn-key femtosecond laser technology.

MPT is based on the detection of the (i) endogenous fluorophores NAD(P)H, flavins, keratin, elastin, melanin, and porphyrins by two-photon autofluorescence, (ii) the collagen network by second harmonic generation (SHG), optical metabolic imaging (OMI) by fluorescence lifetime imaging (FLIM), and lipids/water by Coherent AntiStokes Raman Spectroscopy (CARS).

JenLab's tomographs are employed in hospitals (e.g. Charite, Princess Alexandra Hospital in Brisbane), in the cosmetic industry (e.g. Beiersdorf, L'Oreal, Shiseido), in the pharmaceutical industry (e.g. GSK), as well as in large research institutions (e.g. University of California Irvine, Skin Research Lab Singapore) in Europe, the US, Russia, Japan, China, Singapore, and Australia.

MPT projects include early detection of malignant melanoma, testing of anti-ageing means, in vivo pharmacokinetics, *in situ* nanoparticle tracing, and skin evaluation on astronauts after long-term space flights.

CEO Dr. Karsten König

JenLab GmbH
Campus Berlin-Adlershof
Johann-Hittorf-Strasse 8
12489 Berlin
info@jenlab.de
www.jenlab.de

TOPAG Lasertechnik

Founded in 1993, TOPAG Lasertechnik supplies lasers, optics and metrology for innovative research projects and 24/7 industrial applications. The main focus is consultation, sales and service of nanosecond to femtosecond lasers with fixed or tunable wavelength. Our team is experienced in designing customer-specific laser systems and corresponding components. Further products comprise optics, optical systems, opto-mechanics, infrared viewers and optical metrology.

TOPAG develops and manufactures diffractive beam splitters and Top Hat beam shaping optics for the optimization of laser processes. We support our customers with wave optical analysis, design of optical systems and laser application development.

NT260 – Tunable Nanosecond Laser for Photoacoustic Imaging and Spectroscopy

TOPAG is distributor of the Lithuanian manufacturer Ekspla for Germany and Austria. Recently introduced, we now offer NT260 nanosecond laser with tuning range from 210 nm to 2.6 µm. The system stands out by its high repetition rate of 10 kHz, small linewidth of <3 cm^{-1} and gapless tuning over the entire wavelength range with maximum output power of 700 mW at 450 nm. The integrated device consists of pump laser and OPO in a compact single housing. This ensures excellent energy and power stability as well as long-term reliability. Typical applications are fluorescence and pump-probe experiments. The system is also well suited for demanding applications like Raman spectroscopy, ion beam spectroscopy or photoacoustic imaging that require narrow linewidth excitation or fast, tunable pulse trains.

Q-Tune-HR – High Repetition Rate Tunable Nanosecond Optical Parametric Oscillator

- Up to 100 kHz @ 750-1800 nm tuning range, max pulse energy >50 µJ @ 1200 nm
- Up to 10 kHz @ 1600-3200 nm tuning range, max pulse energy >100 µJ @ 1650 nm
- Compact, air-cooled, easy control via computer
- Options: air purging for long lifetime of OPO optics, fiber coupling

MPL – Diode Pumped Sub-Nanosecond Lasers for Medical Treatment

- >2 mJ @ 1064 nm @ up to 100 Hz, optional harmonics
- Down to 350 ps pulse duration
- >3 GShot lifetime of pump diodes
- Applications; tattoo removal, pigmentation treatment, skin care

Laser Beam shaping – Top Hat Profiles and Beam Splitting for Efficient Laser Processing & Analytics

- FBS® Top Hat shapers for diffraction limited spots in µm range: square, round, line profiles
- GTH Top Hat shapers for spots in mm range: square, round, line profiles
- DBS Beam Splitters: 1- and 2-dimensional array of spots

tpm taberna pro medicum GmbH - is proud to be the global leader in digital high frequency and high resolution ultrasound for skin diagnostics in medicine, aesthetics and cosmetics. Everything from one source: development, production, maintenance, repair, sales and service made in Germany.

The family business was founded in 1978 after more than 8 years of experience in sales and service of medical ultrasound equipment for ophthalmology. Since 2012 the company is managed and further developed by Sven Scharenberg in second generation. Right from the start tpm has been an advanced, highly sophisticated technically oriented company.

After three years of intensive research and development, tpm was proud to introduce in 1986 the first commercially available A/B digital ultrasound system worldwide – the DUB20 with 20 MHz, designed especially for dermatology and cosmetic use.

Objective and quantitative noninvasive skin lesions assessment and differentiation are among the current trends in modern dermatology, oncodermatology and aesthetic medicine.

High frequency ultrasound with frequencies of more than 22 MHz for the examination of human skin is a fully developed technique offering a wide range of possibilities both clinically and experimentally. Ultrasonography with a frequency 22-33 MHz allows reliable imaging of cutaneous and superficial subcutaneous structures up to a depth of 12 mm, and valuable for the pathology visualization in the dermis and upper subcutaneous layers.

For the epidermis and papillary dermis, precise visualization and measurement frequencies of 50-75 MHz are preferable. High frequency ultrasound skin imaging is a valuable tool for skin tumors, inflammatory, sclerotic, productive and other skin lesions diagnosis and differentiation.

High frequency ultrasound is also reported as a noninvasive instrument for skin fillers detection and filler type recognition.

The best choice is the combination of two frequencies ranges 20 - 33 MHz and 50 - 75 MHz in one system the DUB – SkinScanner75, e.g. a melanocytic naevus with 75 MHz:

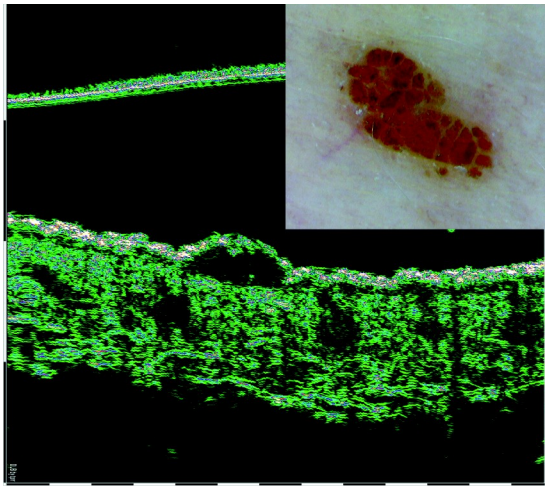

A - I

Fatima Alsamad


Emilia Alves


Wolfgang Becker


Hans Georg Breunig


Razvigor Darlenski


Maxim Darvin

Arnaud Dubois


Ana Evora


Joachim Fluhr


Tiago Folgosa Granja


Victor Infante

J - M


Lily Jiang


Aisada König


Karsten König

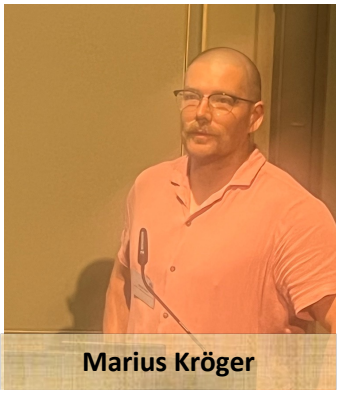
Marius Kröger

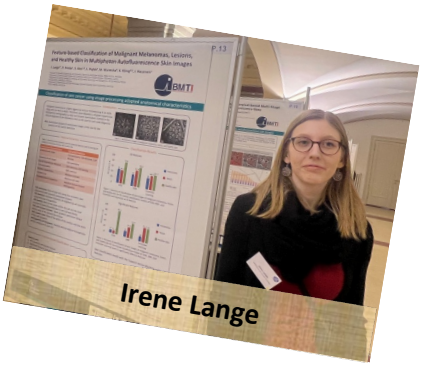
Irene Lange

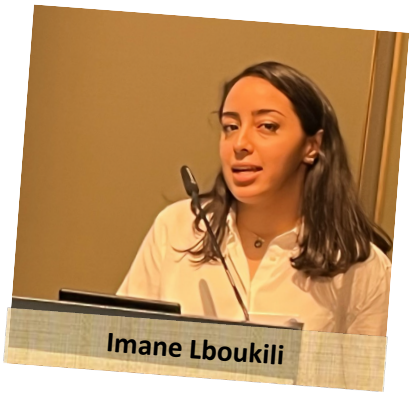
Imane Lboukili


Edoardo Mazza


Francis McGlone


Martina Meinke

Laurent Misery


Neelam Muizzuddin

N - S


Thomas Nappez


Dmitry Pankin


Gerwin Puppels

Na Qiao


Bernard Querleux


Carina Reble


Johannes Schleusener


Thomas Schnalke


Matthias Seise


Jorgen Serup

T - Z


Martha Tate


Phuong Thao Tran


Sijia Wang


Tracy Wang


Marek Warzecha


Ming Yang


Hassan Zahouani


Hamza Zaidi

Humboldt University

Charité

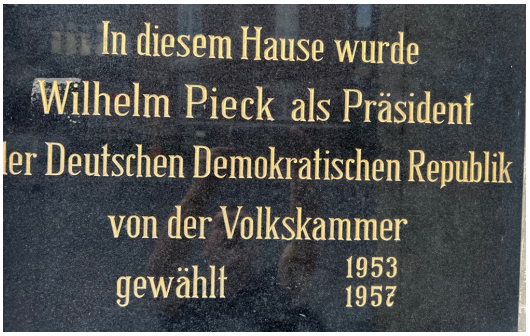

Langenbeck-Virchow-House